ISBN 978-82-326-6202-9 (printed ver.)
ISBN 978-82-326-6959-2 (electronic ver.)
ISSN 1503-8181 (printed ver.)
ISSN 2703-8084 (electronic ver.)

NTNU
Norwegian University of
Science and Technology

Doctoral theses at NTNU, 2022:33

Haoge Liu

Subsea Field Layout Optimization

minimizing overall development cost in early phase design

Haoge Liu
Doctoral thesis

Doctoral theses at NTNU, 2022:33

NTNU
Norwegian University of
Science and Technology
Thesis for the degree of
Philosophiae Doctor
Faculty of Engineering
Department of Geoscience and Petroleum

NTNU
Norwegian University of
Science and Technology

Haoge Liu

Subsea Field Layout Optimization

minimizing overall development cost in early phase design

Thesis for the degree of Philosophiae Doctor

Trondheim, February 2022

Norwegian University of Science and Technology
Faculty of Engineering
Department of Geoscience and Petroleum

NTNU
Norwegian University of
Science and Technology

NTNU
Norwegian University of Science and Technology

Thesis for the degree of Philosophiae Doctor

Faculty of Engineering
Department of Geoscience and Petroleum

ISBN 978-82-326-6202-9 (printed ver.)
ISBN 978-82-326-6959-2 (electronic ver.)
ISSN 1503-8181 (printed ver.)
ISSN 2703-8084 (electronic ver.)

Doctoral theses at NTNU, 2022:33

Printed by Skipnes Kommunikasjon AS

Abstract

This study focuses on building a systematic method for the subsea field layout optimization with the aim of minimizing the overall field development cost. The subsea field layout optimization is a very complex problem which mainly includes well trajectories, location-allocation of subsea facilities (mainly the manifolds), flowline and umbilical routing, and location-allocation of drilling sites. Because the function of flowline and umbilical is to connect the well heads and subsea facilities, we simplify the flowline and umbilical routing as a cost function into the location-allocation of subsea facilities. Hence the complex problem is divided into 3 sub-problems: the "1-site-n-wells" problem, the "location-allocation of manifolds" problem and the "k-sites-n-wells" problem.

We extend the original 2D Dubins Curve to the 3D drilling scenario to solve the "1-site-n-wells" problem where we can find the best drilling site location and the wellbore trajectories for multiple wells to be drilled from the same drilling site. A binary linear programming (BLP) method which guarantees the global optimum with extreme high efficiency is created to solve "location-allocation of manifolds" problem. The 3D Dubins Curve method and the BLP method are then systematically combined to solve the "k-sites-n-wells" problem. Thus, the systematic method for the subsea field layout optimization is built, and the method has the flexibility to handle various user-defined cost and constraints.

Abundant case studies and a real field data test provided by a SUBPRO industrial partner validate the correctness and the advantage of our method both in accuracy and efficiency.

We are confident that our method will benefit the petroleum industry in the future and the BLP method will have a wider application in various areas where the problems can be deduced as a size-constrained clustering problem.

Acknowledgement

This work was carried out as a part of SUBPRO, a Research-based Innovation Centre within Subsea Production and Processing. I gratefully acknowledge the project support from SUBPRO (grant number 237893), which is financed by the Research Council of Norway, major industry partners and NTNU.

Personally, I owe great thanks to my main supervisor Professor Tor Berge Gjersvik and co-supervisor Professor Audun Faanes. It was their professional knowledge that helped me understand the project thoroughly at the very beginning. It was their encouragement that made me feel confident while facing the technical issues. It was their trust that gave me the freedom to try my bold ideas and finally achieved the successful results, especially given that I was detained in China for more than 7 months due to COVID-19. It was their friendliness and humor that relieved my stress while pursuing for the PhD degree. Along with the academic supports, my main supervisor also helped me a lot for my personal life in Norway. As a Chinese student in Norway, I really feel warmed by my supervisor's support and my heart is full of gratitude to him. This is indeed as what the old Chinese proverb goes "love thy apprentice as thy son; respect thy teacher as thy father".

Besides, I shall thank all my referees who recommended me for this PhD position, especially Prof. Khaled ElBassioni and Prof. MD Motiur Rahman at Khalifa University of which I voluntarily dropped out after a year of PhD study. Now I can be proud with my PhD achievements to tell all my referees that I haven't failed them and thanks for their support during my bad days in UAE.

Additionally, thanks for the company of my friends, especially the company of my three roommates --- Xiyang Xie, Da Shuai, and Shuo Pang --- in the first year of my PhD. I also owe special thanks to Yurou Li and Gefei Kong who helped me a lot in correcting the format mistakes in this thesis.

At last, as a single child under the special Chinese "One-Child" policy, I am grateful to my parents for their understanding and mental support all these years when I have been far away from home since the year 2014. I hope in the future as they are aging, I can always be there with them when they need me.

Content

List of Figures

List of Tables

Chapter 1. Introduction

1.1 Background

Industry benchmarks show a significant increase in oil and gas field development cost over last decade. The cost challenge is much harsher in subsea field development. According to the report [1] released by Norway's Oil and Gas Technology Strategy for 21st Century (OG21), the subsea cost tripled from the year 2005 to 2013. Taking the low oil price and its volatility into account, it's crucial to cut the subsea field development cost to maintain the industry profitability.

Subsea field development involves quite a complicated procedure where the layout design plays one of the most important roles to cut the overall cost. From the reservoir to the topside facility, the subsea field layout design mainly includes well trajectories, location-allocation of subsea facilities (mainly the manifolds), flowline and umbilical routing, location-allocation of drilling sites, etc. Generally, the design starts from a set of completion intervals provided by geologists and reservoir engineers. We need optimize the number of drilling sites, economically determine which intervals should be drilled from the same drilling site and find the best locations for these drilling sites; meanwhile, for the subsea facilities on the seabed, we need optimize the number and the locations of manifolds and their connections to the wellheads to minimize the flowline/cable cost. To minimize the overall field development cost, we need not only a method to achieve the optimum in every single designing phase, but also to find the interrelationships of cost within all these phases.

Research on the related topic can date back to 1970s [2, 3], where the well construction cost was simplified as a function only related with horizontal distance. In the following decades, quite a few optimization models emerged with different conditions taken into consideration [4-12], and the scope of the optimization model has already reached so large that recent work [7-10] started to focus on maximizing net present value (NPV), rather than minimizing development cost. No matter how big the scope is, the layout optimization problem can be mathematically described as a mix-integer nonlinear problem (MINLP), but normally we can only get a local optimal solution of the MINLP model by heuristic algorithms within affordable time. Practically, engineers always reduce the problem to a mix-integer linear problem (MILP) or a mere integer linear problem (ILP) by giving some good options empirically. However, the reduced

MILP/ILP model based on experience cannot guarantee the global optimum, either. Based on data published by the Norwegian Petroleum Directorate [13], the annual sum of investments and exploration costs in Norway is around 200 billion NOK. Hence, there is no doubt that the gap between the global optimal layout and the current optimal layout our industry can achieve is very lucrative.

1.2 Objective

The objective of this study is to develop a systematic method for subsea layout optimization to minimize the overall cost. In details, once the completions intervals, cost items and engineering constraints are given, the following parameters need to be optimized:

1. number of drilling sites
2. location of drilling sites
3. allocation of drilling sites to completion intervals
4. well trajectories
5. number of manifolds
6. location of manifolds
7. allocation of manifolds to well heads.

As the cost of flowline and umbilical is almost determined once the locations of facilities and engineering requirements are given, this study does not involve detailed optimization for the routine of flowline and umbilical, the cost of flowline and umbilical treated as a user-defined cost function involved in the location-allocation problem of manifolds. The focus of this study is providing an efficient optimization method for the subsea field layout design. Many engineering details may be reasonably simplified for a better and clearer demonstration of the core ideas of the method.

1.3 Related Publications and Main Contributions

This research has generated a series of three papers titled as “subsea field layout optimization”[14-16], published with Open Access in the Journal of Petroleum Science and Engineering, which is the top-1 journal in petroleum engineering according to JCR™ (Journal Citation Reports). The main contribution is that it provides a systematic method with high efficiency to optimize the subsea field layout with the aim of minimizing the overall field development cost. In details, it provides much more efficient methods with

high accuracy for the two basic technical problems --- the well trajectory design and the continuous spaced location-allocation problem --- along with the process of combining the two methods to solve the practical subsea field layout optimization problem.

1.4 Thesis Structure

This is a paper-based thesis, the content of the following chapters is summarized as follows:

Chapter 2 introduces how the subsea field layout optimization problem is divided into sub-problems along with their backgrounds.

Chapter 3~5 introduce the technical details of solving the three sub-problems, along with case studies.

Chapter 6 introduces the real field test provided by Equinor.

Chapter 7 concludes this study with suggestions for future work.

Chapter 2. Problem Description and Breakdown

Even there are as many as 7 parameters need to be optimized, as listed in the Section 1.2, we can simply divide the problem into two parts: the location-allocation problem of drilling sites and the location-allocation problem of manifolds. As the cost of flowline and umbilical is simplified in this study, the location-allocation problem of manifolds just needs a good method for the continuous spaced location-allocation problem. The location-allocation problem of drilling sites will require the directional well trajectory planning in addition.

Therefore, the subsea layout optimization problem is broken down into the following three sub-problems:

2.1 Sub-problem 1: "1-site-n-wells"

The "1-site-n-wells" sub-problem can be summarized as follows: given several well completion intervals along with the engineering constraints such as the dogleg severity and drilling site location constraints, all wells are drilled from the same drilling site, find the optimal drilling site location so that the cost of all the wells is minimized.

If we peel off this sub-problem deeper, it will be "1-site-1-well" where we need to find the trajectory when the completion interval and the drilling site location are both given. This is essentially a directional well trajectory planning problem. Directional well trajectory planning is one of the most difficult tasks in field development because of too many different types of constraints and the unpredictable incurring cost. But statistically, the well drilling cost is almost linearly related with the trajectory length. The work of D. S. Amorim Jr. [17] reveals that the cost per meter always converges to a stable value as the well length increases, proving the statistically linear relationship between the drilling cost and the wellbore length. Based on the statistical result, the optimal trajectory can be considered as the shortest trajectory with curvature constraints. Even though, practically, the shortest trajectory may not be the optimal because of the complex downhole situations, it's still the design basis for well planning.

The curvature constrained method for well trajectory optimization dates back to the early 1970s[18, 19] when directional drilling technology started to develop. Since then, it has evolved several types of curves [20-27] for the well trajectory, including the circular arc, the polynomial spline, the catenary and the clothoid or the Euler spiral. However, all

these decades, the drilling industry seemed to overlook the Dubins Curve [28] which exactly gives the shortest curvature-constrained path between two directional points in 2D given that the moving direction is forward only.

Dubins concluded that the shortest path is made by joining circular arcs of maximum curvature and a straight line, which was later proved by Johnson [29] by using Pontryagin's maximum principle. In details, the Dubins Curve is comprised of two families which are the CCC and CSC, where “C” stands for circular arc, and “S” stands for straight line. The CCC family consists of RLR and LRL, where “R” stands for right turn, and “L” stands for left turn. The CSC family consist of RSR, RSL, LSR, LSL. The shortest path is one of the six patterns, as shown in Fig. 2.1. While extending the original 2D Dubins Curve into 3D, Sussman[30] pointed out a situation when the two points are too close, the optimal path should be helicoidal which can be regarded as a special CCC pattern. Till now, the Dubins Curve has already matured in the autopilot industry for path planning of cars, robots, UAVs, AUVs, etc [31-36].

The drilling process is almost the same as the piloting process, and the well trajectory planning is essentially a path planning. Obviously, CCC family is not suitable for drilling because of the large turning angle in the trajectory. Hence, here in this study, we will extend the CSC patterns of the original 2D Dubins Curves into 3D as the optimal well trajectory for well planning. The property of Dubins Curve not only guarantees the shortest path but also minimizes the length of curved section. Consequently, the straight section of Dubins Curve avoids higher inclination angles than necessary. All these features are beneficial for drilling.

By adopting the Dubins Curve for the optimal wellbore trajectory, we can then use gradient descent method to determine the optimal drilling site for a cluster of wells or to design a multilateral well to reach several completion intervals. In the Chapter 3, we will show the feasibility and efficiency of our well trajectory planning method which combines the Dubins Curve strategy and the gradient descent method in solving the “1-site-n-wells” problem. Wider application of the method will also be discussed after the Case Study.

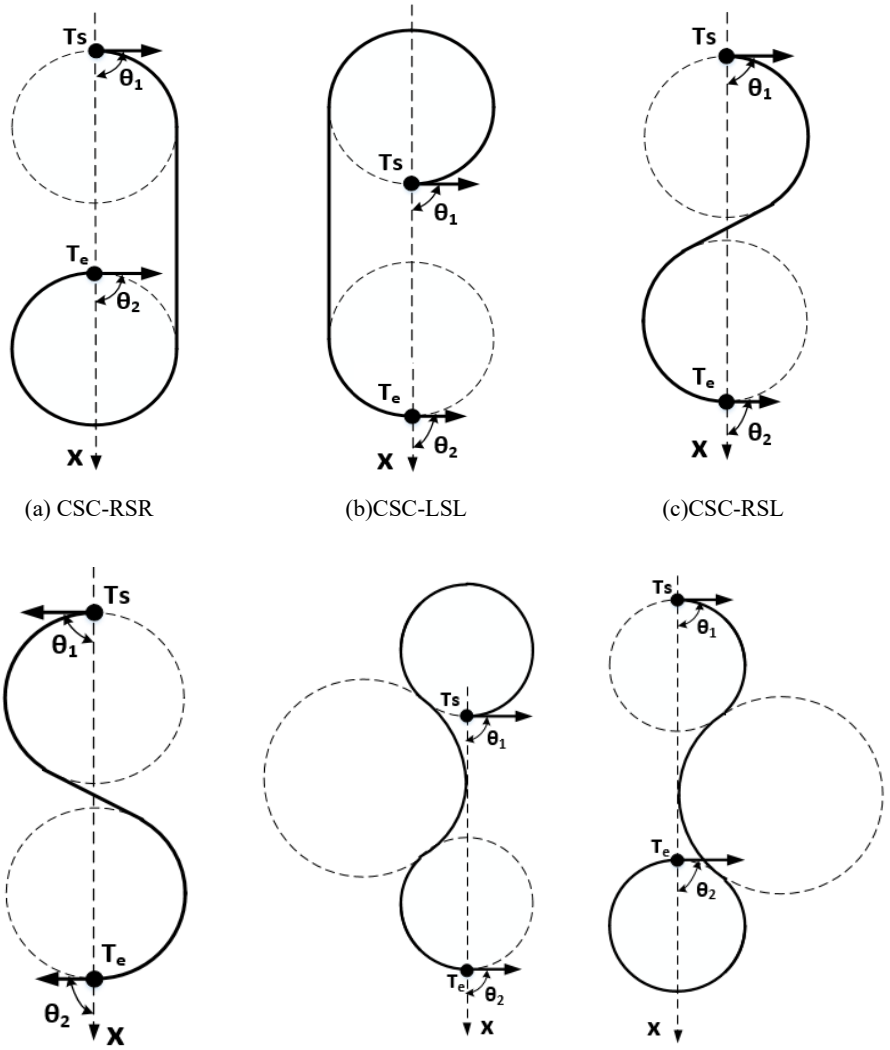

(a) CSC-RSR (b)CSC-LSL (c)CSC-RSL

(d) CSC-LSR (e)CCC-LRL (F)CCC-RLR

Fig. 2.1 Patterns of 2D Dubins Curve
(modified based on [36])

2.2 Sub-problem 2: location-allocation of manifolds

A manifold is a subsea facility like a hub used to collect the production from several different wells. Based on the number of connection slots on the manifold, there are many types such as: 2-slot, 4-slot and 6-slot, etc. The 4-slot manifold is the most widely used in Norway.

Given the locations of the wellheads on the seabed, we must optimize the locations of the manifolds and the connection relationship between manifolds and wells so that the tie-back flowline costs can be minimized. This is the meaning of the "location-allocation". More specifically, this sub-problem is a continuous spaced location-allocation problem as the manifold can be located anywhere rather than a set of location options.

The location-allocation problem of manifolds, which directly affects the flowline cost, has always been treated as a MINLP or an ILP when there are explicit location options for the facilities [37-44]. The MINLP is an easy way to describe the real-world problem in a mathematic language, however finding the global optimal solution to the model is an NP-Hard problem which can easily exceed the time we can afford. Hence, practically, engineers use heuristic algorithms [44], such as the simulated annealing (SA) algorithm [39] or the genetic algorithm [41], to search a good local optimum; or give several good location options for the manifolds based on their experience and knowledge, to reduce the MINLP model to an ILP model. Nevertheless, the global optimum can no longer be guaranteed.

As we want to achieve the minimum in flowline cost, it is easy to come to the classic Minimum Spanning Tree (MST) problem. Indeed, if we do not consider the influence of flowline maintenance on the production in the future, the classic MST algorithms [45, 46] or dynamic MST algorithms [47] can give us the optimum solution of the minimum cost. However, practically, we cannot afford to let too many wells depend on the same flowline in case of the production suspension due to maintenance or any emergency. Besides, different production fluids may not be suitable to be mixed and transported in the same flowline. Therefore, it is conventional in the industry to just connect several wells together to a manifold which is then connected to the topside facilities. A carefully designed MST algorithm with the practical issues taken into consideration may exist and completely break away from the industrial conventions, but it is outside of the scope of this study.

Considering the conventional layout, we propose to regard the location-allocation problem as a size-constrained clustering problem and solve it with the help of graphic theories. It should be noted that, changing the perspective on this layout optimization problem does not change the NP-hardness for finding the global optimum: the well-known K-Means algorithm [48, 49] for clustering problem cannot fulfill the size constraint, besides, it cannot guarantee the global optimum; the exact size-constrained 2-clustering [50, 51] algorithm is a very efficient algorithm which generates the global

optimum, however, it's only suitable for dividing data points into 2 clusters; Zhu's work [52] which converted the size-constrained clustering problem into a ILP model, actually revealed the hardness equivalence.

Even though this new perspective does not change the NP-hardness, the concept of clustering enlightened us to build a much more efficient algorithm to achieve the global optimum for this NP-hard problem, making it practically feasible to solve a much larger-scale problem. Briefly, our algorithm takes the advantage of Delaunay Triangulation to linearize the MINLP model into a binary linear problem (BLP) model without increasing the magnitude of variable number compared to the original MINLP's. In the Chapter 4, we elaborate our method for a simplified version of this NP-hard problem where there is only one type of manifold so that it will be easy for readers to understand our method completely. In the case study, the comprehensive comparison to the previously published methods and the commercial MINLP solver in LINGO, which has matured for about 40 years, shows the great advantage of our method. In the further discussion, we introduce how to use our method to deal with several types of manifolds and many other practical scenarios.

2.3 Sub-problem 3: "k-sites-n-wells"

When wells are drilled from the same drilling site, they are gathered by a template on the seabed. Otherwise, they are set as satellite wells. The conventional template specification based on the maximum number of connected wells includes 2-slot, 4-slot, and 6-slot. The slot of the template can be left vacant, for example, a 4-slot template can be used to connect 3 wells together. Normally, one m-slot template wellhead costs less than the sum of m satellite wellheads. The template specification of more slots is available but not popular because connecting too many wells together tends to make the increment of the drilling cost exceed the saved cost from less rig mobilization times and number of templates.

As the name indicates, the "k-sites-n-wells" problem requires us to determine the optimal number of drilling sites along with their locations and allocations to the given set of well completion intervals. Compared to the "1-site-n-wells" problem, this problem is much more complex because of the combinatory problem involved. Currently, there is no good solution to such a problem in the industry. Practically, engineers are required to

manually input the combinations filtered based on their experience to find out the best. Such a process is quite tedious, and it cannot guarantee the global optimum.

In this study, we have successfully developed a method which systematically combines the methods for solving the Sub-problem 1 and Sub-problem 2 for the complex "k-sites-n-wells" problem. Our method can guarantee the global optimum with extremely high efficiency. The details of our method are elaborated in Chapter 5, along with abundant case studies.

Chapter 3. Solution to Sub-problem 1: "1-site-n-wells"

3.1 Mathematical Description

Given k well completion intervals, $k \in Integer^{+}$, each completion interval is defined by its start point $P_{2,i} = \left(Px_{2,i}, Py_{2,i}, Pz_{2,i}\right)$ and the drilling direction vector $V_{2,i} = \left(Vx_{2,i}, Vy_{2,i}, Vz_{2,i}\right)$ where $Vz_{2,i} \le 0$ to ensure the direction is not upward; the highest allowed kickoff point $P_{1,i} = (Px_1, Py_1, Pz_{1,i})$ for every wellbore should be at the depth of Z_i m, i.e., $Pz_{1,i} = Z_i < 0$, $i \in \{1,\ 2,\ \ldots,\ k\}$. The drilling direction vector at every kickoff point is vertical downwards $V_{1,i} = (0, 0, -1)$. The maximum allowed turning rate/dogleg severity is κ°/30 m, i.e., minimum allowed turning rate radius is $r_{\min} = \dfrac{5400}{\pi\kappa}$ m. The cost of a wellbore trajectory can be a user-defined function related with the trajectory structure following the form as $COST = cstC\left(Lc\right) + cstS\left(Ls, \theta\right)$, where Lc is the length of non-straight section, Ls is the length of straight section, θ is the deviation angle of the straight section; $cstC\left(Lc\right)$ is the cost function of non-straight section which is continuous and positively correlated with Lc, i.e., $\dfrac{\partial cstC\left(Lc\right)}{\partial Lc} > 0$; $cstS\left(Ls, \theta\right)$ is the cost function of straight section which is continuous and positively correlated with Lc and θ, i.e., $\dfrac{\partial cstS\left(Ls, \theta\right)}{\partial Ls} > 0$ and $\dfrac{\partial cstS\left(Ls, \theta\right)}{\partial \theta} > 0$.

The objective is to find the optimal drilling site $D: (Px_1, Py_1, 0)$ to drill multiple wells from one drill site such that they can reach all completion intervals with the total cost of all trajectories minimized while fulfilling the dogleg severity constraint.

3.2 Basic Assumption and Simplification

1. The formation underground is drillable in all directions.

2. The surface for the drilling site is a horizontal plane $z = 0$.

3. Every completion interval is reasonable, so that it is easily reachable. For example, if the maximum allowed turning rate/dogleg severity is 1.5°/30 m, i.e., the minimum curvature radius is r = 1145.9 m, while the start point of the completion interval is too

shallow at $Pz_2 = -1000$ m, and the vector is required to be horizontal $V_2 = (-1, 0, 0)$, then such a completion interval is considered as unreasonable, because we cannot reach such a completion interval with an easy trajectory as we have to drill below the interval depth and then drill upwards even if the wellbore starts to kick off at the surface, unless we reduce the turning rate radius, i.e., increasing the dogleg severity. As shown in Fig. 3.1.

4. For wells drilled from one drilling site, the difference within the exact locations of wellheads is quite small, hence we can consider all wellheads' locations are the same as the drilling site location.

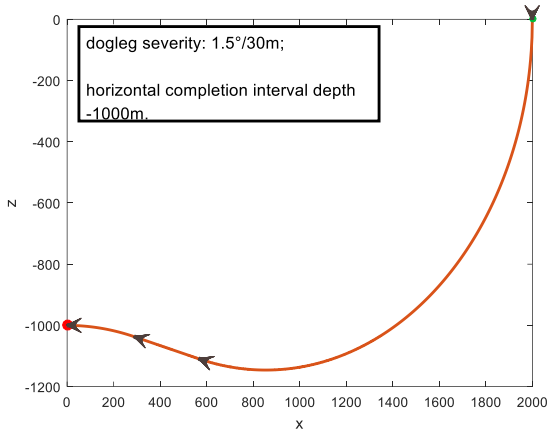

Fig. 3.1 Unreasonable Well Completion Interval for a Given Dogleg Severity

3.3 Method

3.3.1 Mathematical Model

This optimization problem can be divided into two levels. The first level is to find the optimal trajectory of minimum cost when the completion interval (P_2, V_2) and highest allowed kickoff point (P_1, V_1) are both given:

$$\begin{aligned} Obj. \quad & \min\left[COST\left(P_1, V_1, P_2, V_2, r\right)\right] \\ & = \min\left[cstC\left(Lc\right) + cstS\left(Ls, \theta\right)\right] \\ s.t. \quad & r \geq r_{\min} \end{aligned} \tag{3-1}$$

The Equation (3-1) cannot implicitly tell which parameters should be taken as the variables to be optimized to achieve the objective. Given $\frac{\partial cstC\left(Lc\right)}{\partial Lc} > 0$, $\frac{\partial cstS\left(Ls, \theta\right)}{\partial Ls} > 0$ and $\frac{\partial cstS\left(Ls, \theta\right)}{\partial \theta} > 0$, the objective can be converted into Equation

(3-2) if Lc, Ls and θ can reach minimum at the same time with the r constraint. It should be noted that Lc, Ls and θ are function of (P_1,V_1,P_2,V_2,r), for convenience, we just write as Lc, Ls and θ rather than $Lc(P_1,V_1,P_2,V_2,r)$, $Ls(P_1,V_1,P_2,V_2,r)$ and $\theta(P_1,V_1,P_2,V_2,r)$.

$$\begin{aligned} Obj.\quad & \min\left[cstC(Lc)+cstS(Ls,\theta)\right] \\ & = cstC\left(\min(Lc)\right)+cstS\left(\min(Ls),\min(\theta)\right) \\ s.t.\quad & r \geq r_{\min} \end{aligned} \tag{3-2}$$

The Dubins Curve which starts from the highest allowed kickoff point to the start point of completion interval just fulfills the Equation (3-2). Practically, the curved wellbore section is more costly than the straight section, i.e., $\frac{\partial cstC(Lc)}{\partial Lc} > \frac{\partial cstS(Ls,\theta)}{\partial Ls}$, hence minimizing the curved length is prior compared to minimizing the straight length in cutting the overall cost. While ensuring the curved length L_c to be minimum, the Dubins Curve also minimizes the total length of the curve $L_c + L_s$ between two directional points, i.e., L_s is minimized as well. What's more, Dubins Curve makes the straight section to be less inclined in our drilling scenario where $V_0 = [0,0,-1]$, which means θ is also minimized. Hence the solution of the first level optimization problem is to find the Dubins Curve, and the Equation (3-1) becomes equivalent to Equation (3-3). The Equation (3-3) is just to find out the Dubins Curve given (P_1,V_1,P_2,V_2,r). In Section 3.3.2, we will see that finding the Dubins Curve is solving a set of three transcendental equations.

$$\begin{aligned} Obj.\quad & \min\left[COST(P_1,V_1,P_2,V_2,r)\right] \\ & = cstC(Lc)+cstS(Ls,\theta) \\ s.t.\quad & r \geq r_{\min} \\ & Lc, Ls, \theta \in DubinsCurve \\ & Pz_1 = Z \end{aligned} \tag{3-3}$$

The second level is to find the optimal drilling site $D:(Px_1,Py_1,0)$ so that the total cost of all optimal lateral trajectories is minimum, given all the completion intervals($P_{2,i}$, $V_{2,i}$), the highest allowed kickoff points' depth $Pz_{1,i} = Z_i$ and their directions $V_{1,i}$. Compared with the first level problem, the x and y components of highest allowed

kickoff point (Px_1, Py_1) becomes the unknown variables that need to be optimized. As shown in Equation (3-4), the second level optimization is the model for solving the whole "1-site-n-wells" problem.

$$\begin{aligned} Obj. \quad & \min_{D:(Px_1,Py_1)} \sum_{i=1}^{k} COST\left(P_1,V_1,P_2,V_2,r\right)_i \\ & = \min_{D:(Px_1,Py_1)} \sum_{i=1}^{k} \left[cstC\left(Lc\right)_i + cstS\left(Ls,\theta\right)_i \right] \\ s.t. \quad & r_i \geq r_{\min} \\ & Lc_i, Ls_i, \theta_i \in DubinsCurve \\ & Pz_{1,i} = Z_i \end{aligned} \tag{3-4}$$

For each lateral trajectory $\forall i \in \{1,2,...,k\}$, once the drilling site $D:(Px_1, Py_1, 0)$ and the highest kickoff depth Z_i are given, we can obtain the minimum $COST\left(P_1,V_1,P_2,V_2,r\right)_i$ from the first level optimization whose constraints also fulfill the second level optimization. Hence by gradient descent, we can optimize the unknown variables (Px_1, Py_1) to achieve the objective, i.e., to find out the optimal drilling site to minimize the total cost. By using the MATLAB built-in function "fmincon", we can easily solve the model.

3.3.2 **3D Dubins Curve for Wellbore Trajectory**

The original Dubins Curve [28] only solves the 2D scenario, for the 3D well planning scenario, we can derive it as follows. Given the highest allowed kickoff position $P_1:(Px_1, Py_1, Pz_1)$ and direction vector $V_1 = (0,0,-1)$, the well completion interval $P_2:(Px_2, Py_2, Pz_2)$ and direction vector $V_{2,i} = \left(Vx_{2,i}, Vy_{2,i}, Vz_{2,i}\right)$, as shown in Fig. 3.2, C_1 is the end point of the first circular section, i.e., build-up section. C_2 is the start point of the second circular section which can be either the continued build-up section as shown in Fig. 3.2(a) or the drop-down section as shown in Fig. 3.2(b) and (c). In certain cases, C_1 can coincide with P_1, C_2 can coincide with P_2. Another property of Dubins Curve is that the minimum allowed curvature radius value is the radius value of both circles:

$$r = r_{\min} \tag{3-5}$$

Denote the straight section vector, which is unknown, as

$$T = \overline{C_1 C_2} = (Tx, Ty, Tz) \tag{3-6}$$

The unit vector of T is

$$t = \frac{T}{\|T\|} \tag{3-7}$$

The vector perpendicular to the first circular plane is

$$U_1 = T \times V_1 \tag{3-8}$$

The radius vector oriented from P_1 towards O_1 is

$$\Omega_1 = V_1 \times U_1 \tag{3-9}$$

The unit vector of Ω_1 is

$$\omega_1 = \frac{\Omega_1}{\|\Omega_1\|} \tag{3-10}$$

Hence the center of the first circle is

$$O_1 = P_1 + r \cdot \omega_1 \tag{3-11}$$

The radius vector oriented from C_1 towards O_1 is

$$\Phi_1 = T \times U_1 \tag{3-12}$$

The unit vector of Φ_1 is

$$\phi_1 = \frac{\Phi_1}{\|\Phi_1\|} \tag{3-13}$$

Therefore, the point C_1 can be expressed as

$$C_1 = O_1 - r \cdot \phi_1 \tag{3-14}$$

Similarly, we can get ω_2, O_2, ϕ_2, and then the point C_2

$$C_2 = O_2 - r \cdot \phi_2 \tag{3-15}$$

Use the definition of T to get the three unknown variables (Tx, Ty, Tz)

$$T = C_2 - C_1 \tag{3-16}$$

The Equation (3-16), where C_1 and C_2 are functions of T, is a set of 3 transcendental equations with 3 unknown variables (Tx, Ty, Tz). It is almost impossible to get the explicit analytical expression for (Tx, Ty, Tz) from these transcendental equations, but we can use gradient descent algorithm to obtain their values. This can be done by using the MATLAB built-in function "fsolve". After $T = (Tx, Ty, Tz)$ is calculated from Equation (3-16), we can calculate the other geometric parameters of the 3D Dubins Curve.

The turning angle on each circular plane

$$\gamma_1 = \angle P_1 O_1 C_1 = \arccos\left(\frac{V_1 \cdot T}{\|V_1\| \cdot \|T\|}\right) \tag{3-17}$$

$$\gamma_2 = \angle P_2 O_2 C_2 = \arccos\left(\frac{V_2 \cdot T}{\|V_2\| \cdot \|T\|}\right) \tag{3-18}$$

The length of each circular section

$$L_{c1} = \gamma_1 \cdot r \ ; \qquad L_{c2} = \gamma_2 \cdot r \tag{3-19}$$

The total curved length is the sum of two circular section

$$Lc = L_{c1} + L_{c2} \tag{3-20}$$

The length of the straight section

$$Ls = \|T\| \tag{3-21}$$

The calculation process not only gives us the optimal trajectory, but also tells if an assigned drilling site is suitable to drill to the completion interval. As shown in Fig. 3.2(c), when it requires the trajectory to turn around, i.e., γ_2 is bigger than 90°, we may consider that drilling site is not so suitable even it is feasible.

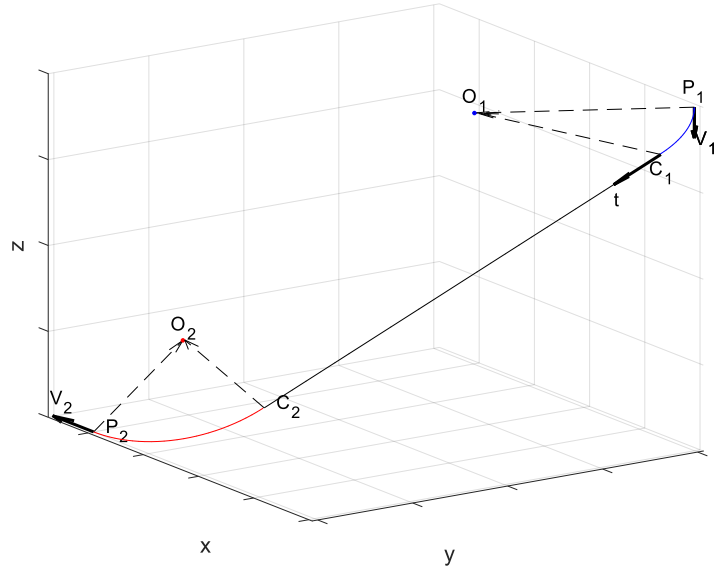

(a)

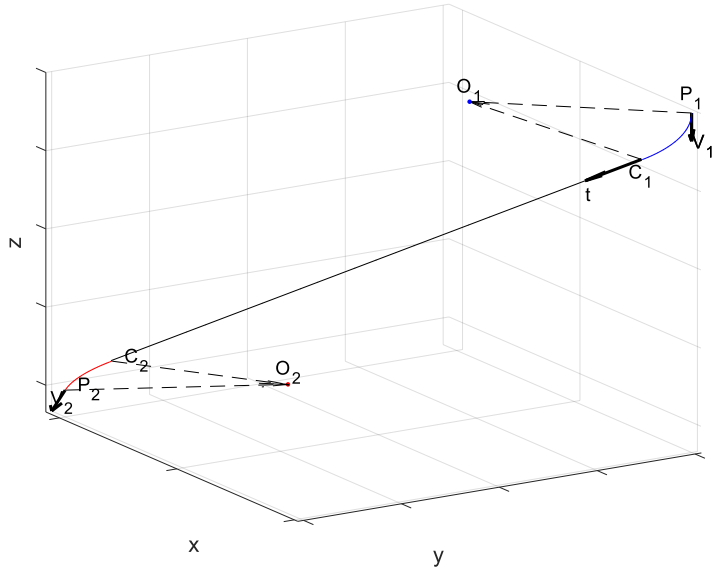

(b)

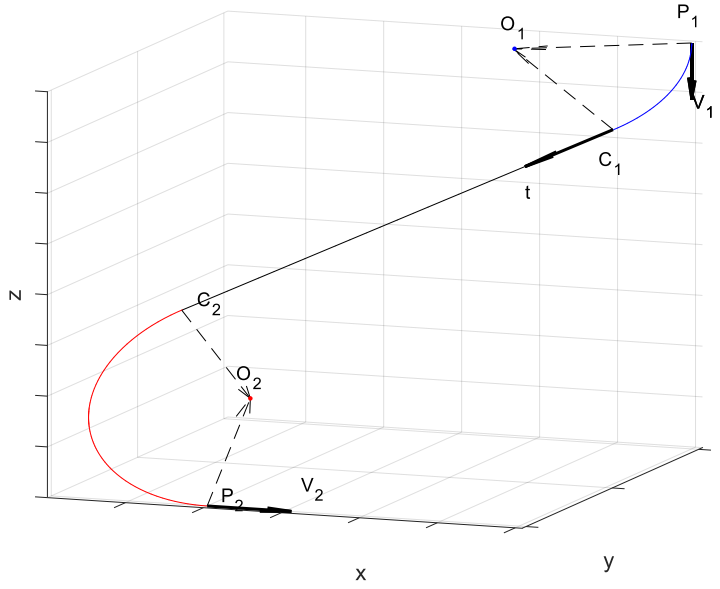

(c)

Fig. 3.2 3D Dubins Curve for Wellbore Trajectory

3.4 Case Study

In this section, we first test on some special cases where the human intuition can tell the correct results to validate our method. Then we demonstrate the results for more

complex general cases. For demonstration, assign the user-defined cost functions in a simple but reasonable form as follows:

$$cstC\left(Lc\right)=2Lc \tag{3-22}$$

$$cstS\left(Ls,\theta\right)=\left(1+\sin\theta\right)Ls \tag{3-23}$$

Such cost functions indicate that the circular well trajectory is more expensive than straight trajectory because $2\geq 1+\sin\theta$; besides, the vertically straight well trajectory is cheaper than the inclined trajectory because $1+\sin\theta\geq 1$, where $\theta\in\left[0,\frac{\pi}{2}\right]$. Of course, the users can assign their own cost functions as they like provided the functions are continuous and fulfill the requirements that $\frac{\partial cstC\left(Lc\right)}{\partial Lc}>0$, $\frac{\partial cstS\left(Ls,\theta\right)}{\partial Ls}>0$ and $\frac{\partial cstS\left(Ls,\theta\right)}{\partial\theta}>0$.

As for the computational time, it will be trivial to report the exact time for each case, because it only takes several seconds for a case without plotting the optimal cost distribution figure, coded by MATLAB, and conducted on an Intel i5-4210U CPU. Such a short time on such an old CPU bespeaks the efficiency of the method, and we believe there is still space for improvement in algorithms and codes.

3.4.1 **Case 1: validation cases**

In the validation cases, we assign representative values for the input parameters so that it's more convenient for us to have the correct intuition results and then to compare with the numerical results generated by our method. The initialization of the drilling site location for the gradient descent algorithm is set as (1, 1) for all the following validation cases.

Case 1.1

For a single well completion interval, the best drilling site should be vertically above the point where the tangent vector of the circle tangential to the completion interval is straight upwards. In such a case, the optimal trajectory is a 2D curve, and there is only one curved section, i.e., P_1 and C_1 coincide. As shown in Table. 3-1 and Fig. 3.3. The tiny numerical error is induced by the gradient descent computation.

Table. 3-1 Case 1.1

Case	Input Parameters				Optimal Drilling Site (Px_1, Py_1)	
	P_2	V_2	Pz_1	$r_{\min}$	Intuition	Numerical
(a)	(0, 0, -4)	(-1, 0, 0)	-1	1	(1, 0)	$(1.0000,\ -9.3944\times10^{-10})$
(b)	(0, 0, -3.5)	(-1, -1, 0)	-1	1	$\left(\frac{1}{\sqrt{2}}, \frac{1}{\sqrt{2}}\right)$	$(0.7071,\ 0.7071)$
(c)	(0, 0, -4)	$\left(-1,\ 0,\ -\frac{1}{\sqrt{3}}\right)$	-1	1	(0.5, 0)	$(0.5000,\ -6.9746\times10^{-9})$

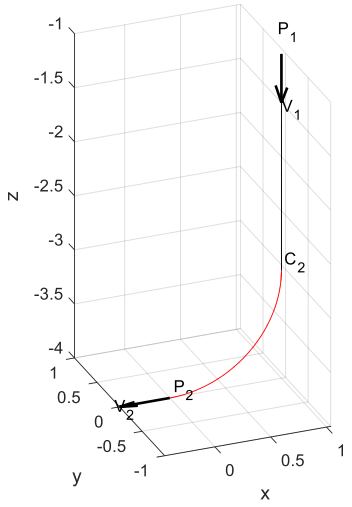

(a)

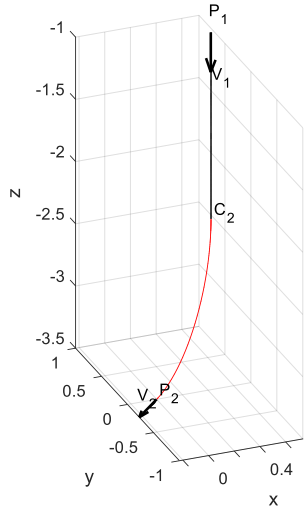

(b)

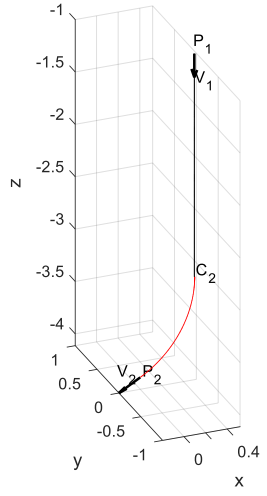

(c)

Fig. 3.3 Optimal Drilling Site and Well Trajectory for Case 1.1

The optimal cost distribution of a drilling site where $Px_1, Py_1 \in [-2, 2]$ is shown in Fig. 3.4. The position resolution of the figure is 0.1. The blank area, as shown in Fig.

3.4(b), indicates that if the drilling site is located there, then the completion interval cannot be reached easily at the given turning rate constraint. In other words, a CCC family of Dubins Curve is required. From the figures we can see how the well completion interval affects the cost distribution.

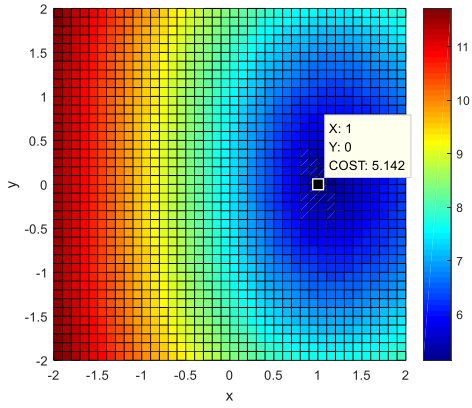

(a)

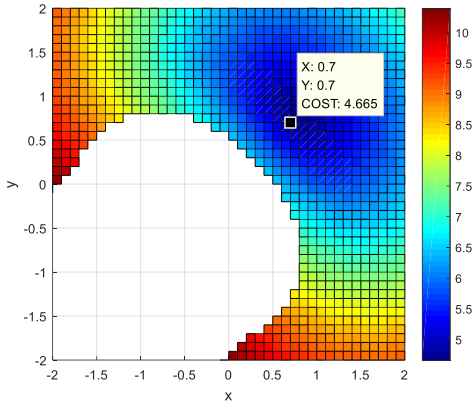

(b)

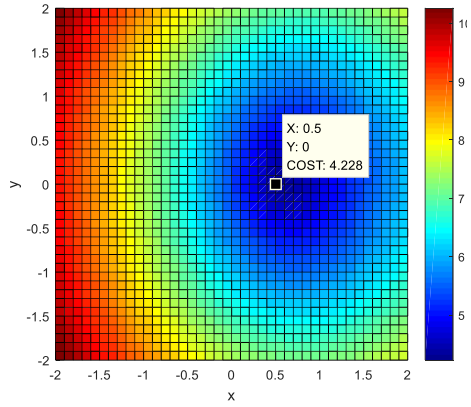

(c)

Fig. 3.4 Optimal Cost Distribution for Case 1.1

Case 1.2

For an even number of well completion intervals distributed symmetrically to a vertical line, the best drilling site is the cross point of the vertical line and the surface plane. As shown in Table. 3-2 and Fig. 3.5.

The optimal cost distribution of a drilling site where $Px_1, Py_1 \in [-2, 2]$ with the position resolution of 0.1 is shown in Fig. 3.6. From the figure, we can see the symmetrical property of the cost distribution corresponding to the symmetry of the well completion intervals. The case 1.2(a) is not just axis symmetric, but also symmetric to x-

plane and y-plane, hence the cost distribution is not just an odd function, but also an even function. While the case 1.2(b) is only axis symmetric, hence the cost distribution for case 1.2(b) is just an odd function.

Table. 3-2 Case 1.2

Case	Input Parameters				Optimal Drilling Site (Px_1, Py_1)	
	$P_{2,i}$	$V_{2,i}$	$Pz_{1,i}$	r_{min}	Intuition	Numerical
(a)	(2, 0, -4)	(1, 0, 0)	-1	1	(0, 0)	(0.0000, 0.0000)
	(-2, 0, -4)	(-1, 0, 0)	-1	1		
(b)	(2, 0, -4)	(1, 0, 0)	-1	1	(0, 0)	$(-1.8422\times10^{-17},\ 3.0342\times10^{-16})$
	(-2, 0, -4)	(-1, 0, 0)	-1	1		
	(1.5, 1 , -7)	(0, 1, 0)	-1.5	1.5		
	(-1.5, -1 , -7)	(0, -1, 0)	-1.5	1.5		

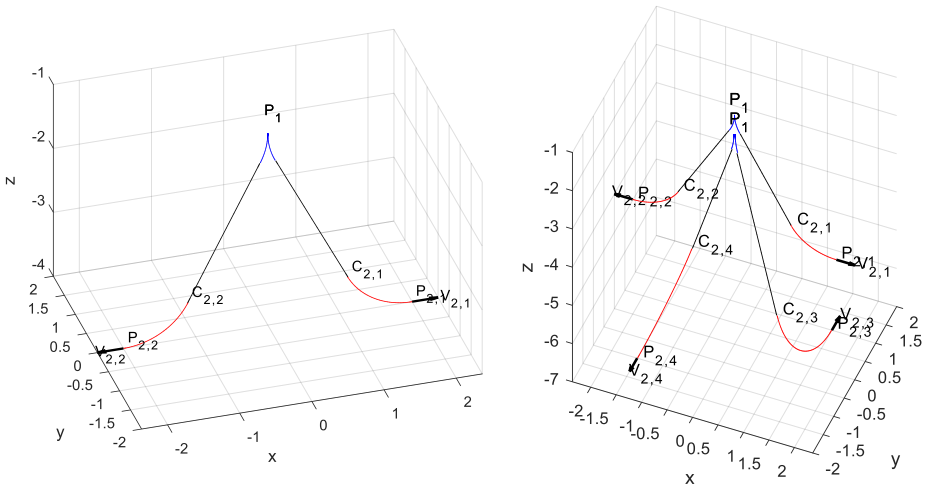

(a) (b)

Fig. 3.5 Optimal Drilling Site and Well Trajectories for Case 1.2

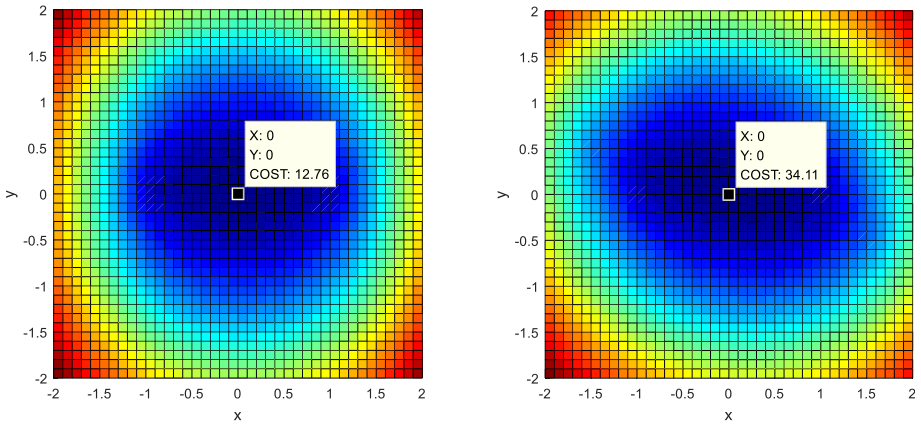

(a) (b)

Fig. 3.6 Optimal Cost Distribution for Case 1.2

3.4.2 **Case 2: general cases**

In the general cases, we use a more realistic set of completion intervals, generated by manipulating data from a real field as shown in Table. 3-3. Highest kickoff point for all laterals is $Z_i = -300$ m.

Table. 3-3 Completion Intervals in Case 2

Interval No.	Start Point $P_{2,i}$ of Interval	End Point of Interval	Direction Vector $V_{2,i}$
1	(410.90, 209.89, -3850.27)	(413.54, 211.37, -3879.12)	(2.64, 1.48, -28.85)
2	(3011.47, 2098.01, -4368.09)	(2995.05, 2087.54, -4376.20)	(-16.42, -10.47, -8.11)
3	(1784.37, 763.80, -4179.39)	(1789.20, 767.85, -4207.38)	(4.83, 4.05, -27.99)
4	(1475.43, 789.75, -2066.32)	(1482.84, 793.68, -2071.76)	(7.41, 3.93, -5.44)

Case 2.1

If the maximum allowed turning rate/dogleg severity is only 2°/30 m, i.e., minimum allowed turning rate radius is $r_{\min} = 859.4$ m. The optimal drilling site and well trajectories for the 4 well completion intervals in Table. 3-3 is shown in Fig. 3.7. The optimal cost distribution of a drilling site where $Px_1 \in [400, 3200]$, $Py_1 \in [200, 2100]$ with the resolution of 50 is shown in Fig. 3.8. The blank area indicates that if the drilling site is located there, then there is at least one completion interval that cannot be reached. The data mark indicates the optimal drilling site of the lowest total cost based on the discretized values at the mesh nodes. The exact optimal drilling site location is $(Px_1, Py_1) = (1129.33, 606.19)$, and the corresponding optimal cost is 22878.0.

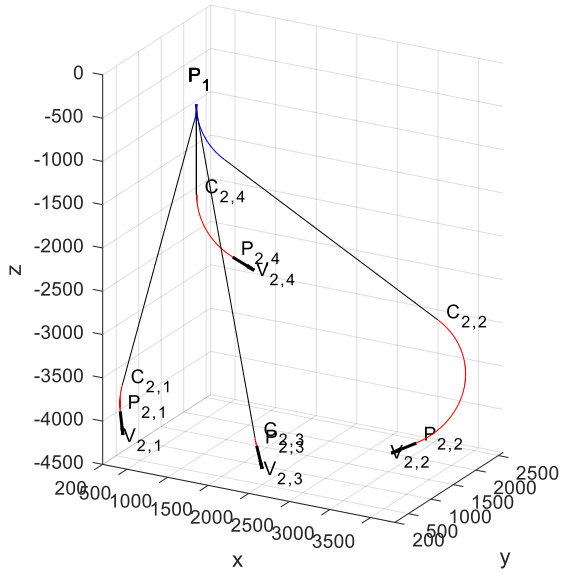

Fig. 3.7 Optimal Drilling Site and Well Trajectories for Case 2.1

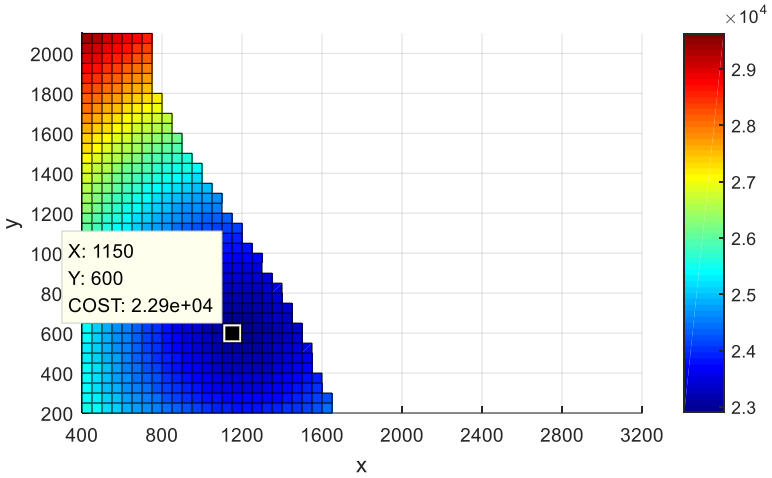

Fig. 3.8 Optimal Cost Distribution for Case 2.1

Case 2.2

From Case 2.1, we can easily tell that it is the 4th well completion interval which is relatively shallow that causes the unreachable situation, i.e., the blank area in Fig. 3.8. If we do not consider the 4th well completion interval, the solution is as follows.

The optimal drilling site and well trajectories for the first 3 well completion intervals in Table. 3-3 are shown in Fig. 3.9. The optimal cost distribution of a drilling site where

$Px_1 \in [400, 3200]$, $Py_1 \in [200, 2100]$ with the resolution of 50 is shown in Fig. 3.10. The data mark indicates the optimal drilling site of the lowest total cost based on the discretized values at the mesh nodes. The exact optimal drilling site location is $(Px_1, Py_1) = (1768.28, 750.31)$, and the corresponding optimal cost is 19367.4. As we are not considering the 4th well completion interval, there is no more blank area in Fig. 3.10.

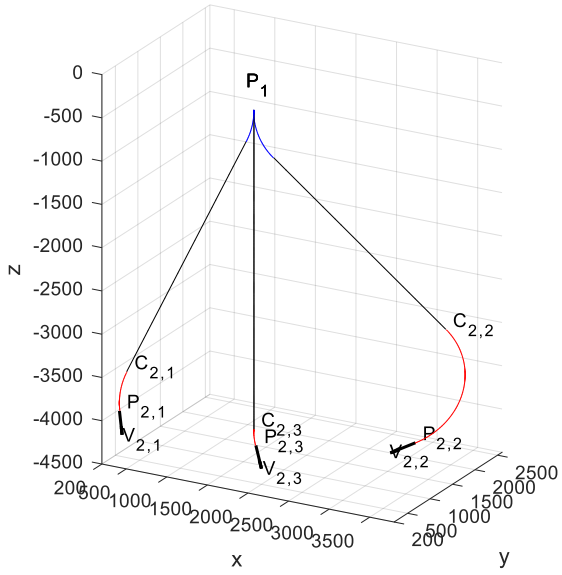

Fig. 3.9 Optimal Drilling Site and Well Trajectories for Case 2.2

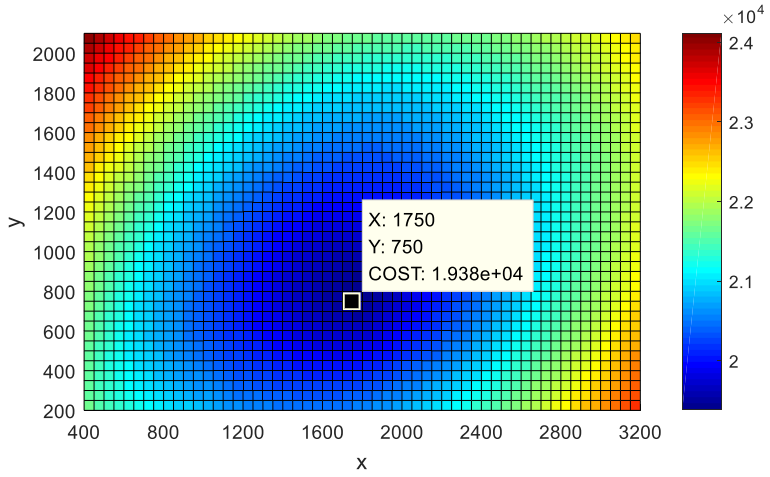

Fig. 3.10 Optimal Cost Distribution for Case 2.2

Case 2.3

From Case 2.1, we can see that the 2nd well completion interval is not so suitable to be drilled from the same drilling site as the other 3 intervals, because it requires a big turn in the trajectory. It may be better to leave the 2nd well completion interval as a satellite well or consider it with the possible well intervals in the future development.

The optimal drilling site and well trajectories for the well completion intervals NO.1, NO.2 and NO.4 in Table. 3-3 is shown in Fig. 3.11. The optimal cost distribution of a drilling site where $Px_1 \in [400, 3200]$, $Py_1 \in [200, 2100]$ with the resolution of 50 is shown in Fig. 3.12. The blank area indicates that if the drilling site is located there, then there is at least one completion interval that cannot be reached. The data mark indicates the optimal drilling site of the lowest total cost based on the discretized values at the mesh nodes. The exact optimal drilling site location is $(Px_1, Py_1) = (1129.33, 606.19)$, and the corresponding optimal cost is 12518.4. Comparing to the result in Case 2.1, we can see that the 2nd well completion interval almost does not affect the optimal drilling site location. The slight effect of the 2nd well completion interval on the cost distribution can be seen from the data marks in Fig. 3.8 and Fig. 3.12.

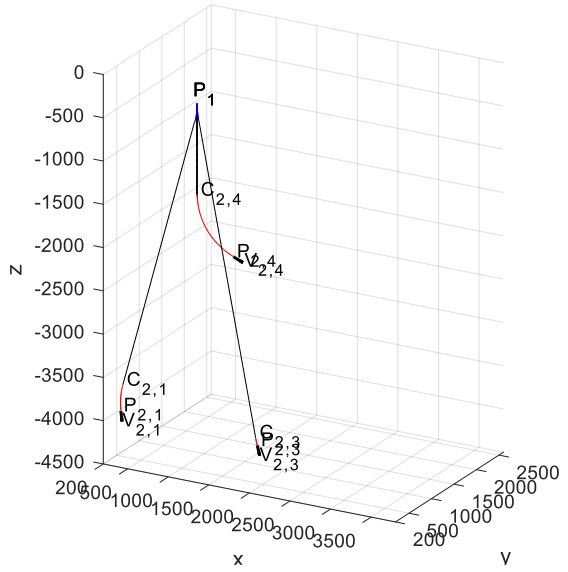

Fig. 3.11 Optimal Drilling Site and Well Trajectories for Case 2.3

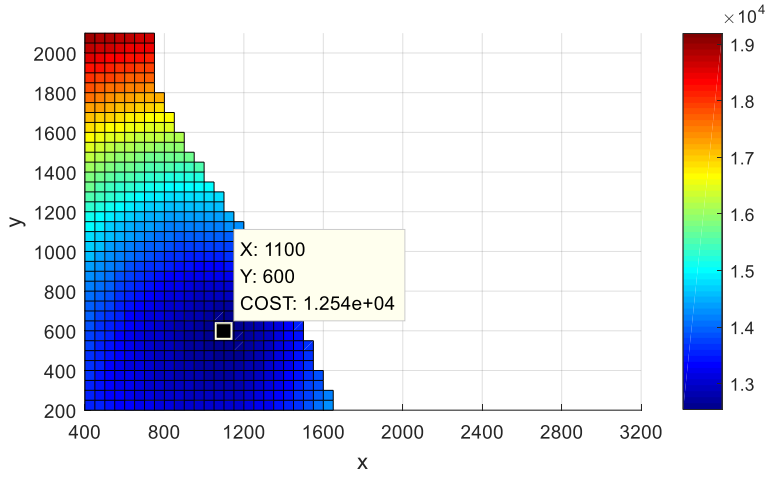

Fig. 3.12 Optimal Cost Distribution for Case 2.3

Case 2.4

If the maximum allowed turning rate/dogleg severity is increased to 4°/30 m, i.e., minimum allowed turning rate radius is $r_{\min} = 429.7$ m. The optimal drilling site and well trajectories for the 4 well completion intervals in Table. 3-3 is shown in Fig. 3.13. The optimal cost distribution of a drilling site where $Px_1 \in [400, 3200]$, $Py_1 \in [200, 2100]$ with the resolution of 50 is shown in Fig. 3.14. Where we can see there is no more blank area in Fig. 3.14 compared to the Fig. 3.4. The data mark indicates the optimal drilling site of the lowest total cost based on the discretized values at the mesh nodes. The exact optimal drilling site location is $(Px_1, Py_1) = (1302.38, 697.97)$, and the corresponding optimal cost is 20048.1.

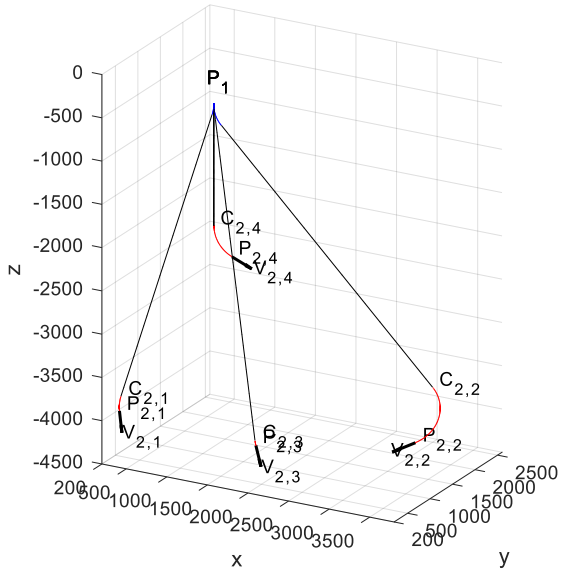

Fig. 3.13 Optimal Drilling Site and Well Trajectories for Case 2.4

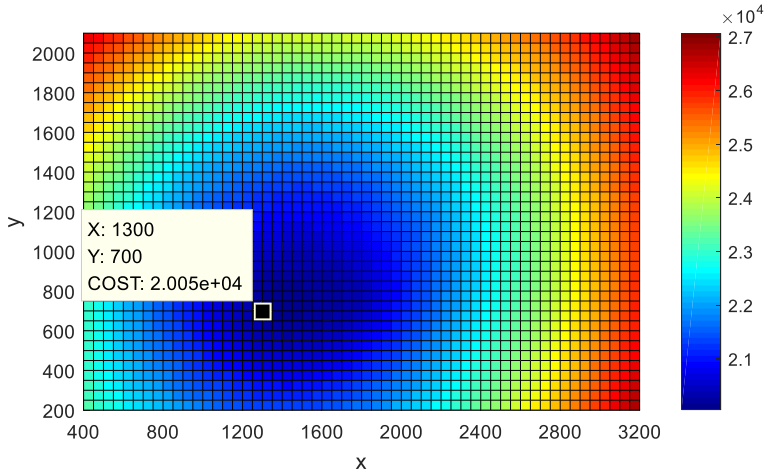

Fig. 3.14 Optimal Cost Distribution for Case 2.4

3.5 Further Discussion

1. When there is a turning around in the trajectory, such as the 2nd trajectory in Case 2.2 and we want to avoid such a risk, we can do the following:

   a. Firstly, we can add one more nonlinear constraint Equation (3-24) into our model Equation (3-4) . Fig. 3.15 and Fig. 3.16 show the result of Case 2.2 with Equation (3-24) added as a constraint. The Equation (3-24) limits the turning angle between the straight section and the second curved section to be no larger than

90°. The optimal drilling site location is $(Px_1, Py_1) = (2570.53, 1504.94)$, and the corresponding optimal cost is 21011.91.

$$\gamma_2 = \arccos\left(\frac{V_2 \cdot T}{\|V_2\| \cdot \|T\|}\right) \le \frac{\pi}{2} \quad \Leftrightarrow \quad T \cdot V_2 \ge 0 \tag{3-24}$$

b. If the result from step a. is not favorable, then discuss with the geological engineers and reservoir engineers to check if it is possible to modify the completion interval so that the turning around does not happen.

c. If modification is also impossible, we should consider two drilling sites for the given intervals. Then the problem will include another challenge problem of finding the best combination of intervals for the drilling sites, which is beyond our study here. Of course, for a small-scale problem, a compromised solution can be that we separate the unwanted interval for a satellite well. And then compare the total cost with the result from step a. As for the challenging "k-sites-n-wells" problem, kindly refer to our following two papers in the series where we provide an unparalleled efficient method.

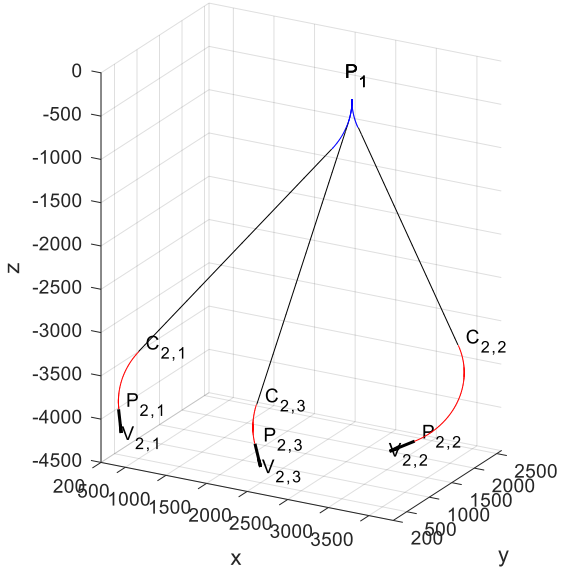

Fig. 3.15 Optimal Drilling Site and Well Trajectories for Case 2.2 with Turning Angle ≤90°

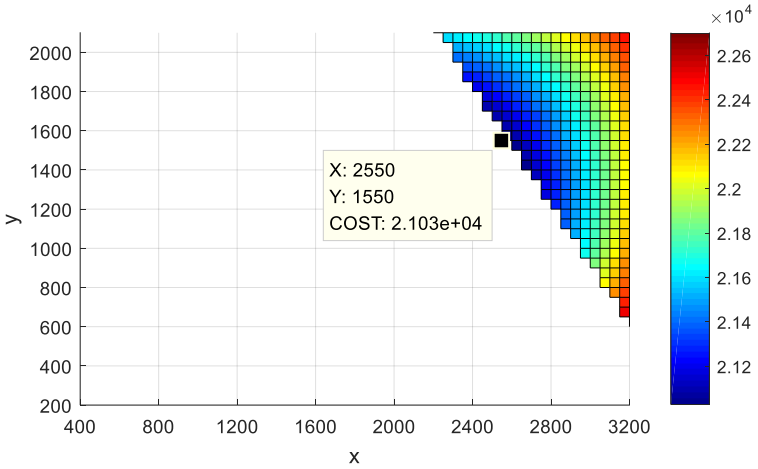

Fig. 3.16 Optimal Cost Distribution for Case 2.2 with Turning Angle≤90°

2. We can also easily include the constraint for the drilling site location. For example, if the well location has a limit $Py_1 \le 1300$ along with the nonlinear constraint Equation (3-24), we will get the optimal drilling site location at $(Px_1, Py_1) = (2704.44, 1300.00)$ with the cost of 21100.20.

3. We can also include the formation information into the cost function. But the original Dubins Curve trajectory no longer guarantees to be the optimal. In order to get the accurate optimized result, we will firstly need to discretize the formation according to the heterogeneity, then optimize all the intermediate nodes between the kickoff point and the well completion interval point. This process is of course much more complicated, but the optimization idea of using the Dubins Curve and gradient descent method remains the same. This is a good start point for our future work to make drilling cost estimation more accurate.

4. If we want to find the exact locations of all wellheads $D_i : (Px_{1,i}, Py_{1,i}, 0)$ in one drilling site $D_0 : (Px_1, Py_1, 0)$, we can continue to do a similar optimization process with the all wellheads' locations D_i in the vicinity of the optimized drilling site D_0. Of course, there can be various definition of vicinity, here gives a simple case where D_i are in the radius of Q centered at D_0:

$$
\begin{aligned}
Obj. \quad & \min_{D_i:(Px_1,Py_1)_i} \sum_{i=1}^{k} COST\left(P_1,V_1,P_2,V_2,r\right)_i \\
& = \min_{D_i:(Px_1,Py_1)_i} \sum_{i=1}^{k} \left[cstC\left(Lc\right)_i + cstS\left(Ls,\theta\right)_i \right] \\
s.t. \quad & r_i \geq r_{\min} \\
& Lc_i, Ls_i, \theta_i \in DubinsCurve \\
& Pz_{1,i} = Z_i \\
& \left\| D_i - D_0 \right\|_2 \leq Q
\end{aligned}
\tag{3-25}
$$

5. At last, we can also combine this optimization process with the seabed facility layout to obtain the overall optimized subsea field development plan. Of course, we should firstly solve the combinatorial problem just discussed in 1.c.

3.6 Summary

This chapter introduces the concept of Dubins Curve for well trajectory planning. Based on the CSC family of 2D Dubins Curve, we have proposed an efficient generic 3D well trajectory optimization method which can be a good way to optimize the drilling site location and the wellbore trajectories to reach multiple completion intervals. It provides a tool for drilling cost estimation at the early phase of the field development. What is more, this method has very good potential to be more accurate and to be embedded into a systematical method for the overall field layout optimization.

Chapter 4. Solution to Sub-problem 2: location-allocation of manifolds

4.1 Mathematical Description

Given n wells to tie back to k manifolds on the seabed, all wellheads' locations are known, then find the optimal manifold location so that it can minimize the tie-back flowline cost, where $m, k \in Integer^{+}$; m is the cluster size, i.e., the number of connected wells to a manifold, it is also the number of slots on the manifold if there is no vacant slot unconnected. Practically, there are manifolds of several different slot-sizes, normally including 2-slot, 4-slot, and 6-slot. For an easy understanding of our method, we firstly simplify the problem as there is only one type of manifold, i.e., $m = 4$. Therefore, the total number of wells is $n = m \cdot k$ which is a multiple of m.

As for more general problems where the number of wells is not a multiple of m, or when we want to use several types of manifolds, or even when the basic assumptions no longer exist, they will all be discussed in Section 4.5. After we introduce our method in Section 4.3 and Section 4.4, you will find it easy to solve these general problems as well once you grasp the core idea of our method.

4.2 Basic Assumption and Simplification

We adopt the same assumptions used in the previously published case study [37] with which we are going to compare:

1. the seabed is simplified as a continuous 2D-plane;

2. the flowline cost is proportional to the square of distance, i.e., squared Euclidean distance.

4.3 Method

4.3.1 Brief Analysis

As the name suggests, the location-allocation problem of manifolds includes two parts: the location of manifolds, and the allocation relation between wells and manifolds. The allocation part can be regarded as a clustering problem. The second assumption, which assumes the cost to be proportional to the square of the distance, makes it quite easy to locate the manifold once the wells are clustered: the location of a manifold is the geometric mean position of the wells allocated to the manifold, i.e., the wells in the same

cluster. This can be easily derived by partial differentiation, refer to the Section 3.4 in Wang's work [37] for the derivation details. Hence, given the positions of m wellheads in a cluster $\mathbf{p}_i:(x_i,\ y_i)$, $i=1,\ 2,\ \ldots,\ m$, the position $\mathbf{p}_M:(X,Y)$ of the manifold that connects these m wells can be easily calculated as Equation (4-1) shows:

$$X=\frac{\sum_{i=1}^{m}x_i}{m},\quad Y=\frac{\sum_{i=1}^{m}y_i}{m} \tag{4-1}$$

The number of all clusters is easily obtained by the combination formula shown in Equation (4-2).

$$C_n^m=C_{mk}^m=\frac{n!}{m!(n-m)!}=\frac{(mk)!}{m!\left[m(k-1)\right]!} \tag{4-2}$$

When m is small, the number of all clusters is still growing relatively slow as the problem scale n grows. But the combinations of the clusters still increase sharply. The number of combinations is given in Equation (4-3). Nowadays, the computational limit of the prevalent CPUs is around 1×10^{12} $FLOPS$. Given $m=4$, $k=5$, i.e., to allocate $n=20$ wells to 5 manifolds, the number of all combinations is around 2.546×10^{9}, which is still within the computational ability. If k just increases a bit to $k=10$, i.e., $n=40$, the number will become around 3.546×10^{27} which is beyond of the computational ability.

$$\frac{C_{mk}^m\cdot C_{m(k-1)}^m\cdot C_{m(k-2)}^m\ldots C_m^m}{k!}=\frac{\prod_{i=0}^{k-1}C_{m(k-i)}^m}{k!}=\frac{\prod_{i=0}^{k-1}\frac{\left[m(k-i)\right]!}{m!\left[m(k-i-1)\right]!}}{k!}=\frac{(mk)!}{(m!)^k\times k!} \tag{4-3}$$

However, the wells in an optimal cluster are adjacent and that makes most of the clusters impossible to be optimal. We regard the clusters where the wells are adjacent as useful clusters. Compared to the number of all clusters, the number of useful clusters is much smaller, resulting in a much smaller number of useful combinations. This is the key idea to solve the problem efficiently. A useful combination consists of k useful clusters of size m. As shown in Fig. 4.1, the cluster {1,2,3,14} is a useful cluster, while the cluster {1,2,9,10} is obviously not.

As for the number of useful clusters, we cannot give an explicit expression to calculate this because it depends on how the wells are distributed, and how we define the adjacent relationship. But we will show how small it is in the following case studies in Section 4.4.

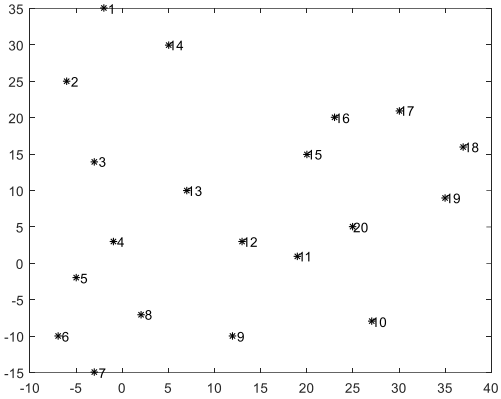

Fig. 4.1 Example of Wellheads' Positions in 2D

4.3.2 **Mathematical Model: from MINLP to BLP**

Based on the previous methods, such as Wang's work [37], the problem can be directly interpreted as a MINLP model:

$$\min_{\mathbf{C},\boldsymbol{\delta}} \mathbf{C}.*\boldsymbol{\delta} = \min_{\mathbf{C},\boldsymbol{\delta}} \sum_{i=1}^{k}\sum_{j=1}^{n} c_{i,j}\delta_{i,j} \tag{4-4}$$

$$s.t. \quad \sum_{j=1}^{n} \delta_{i,j} = m, \forall i \in \{1,\ 2, 3 \ldots k\}$$

$$\sum_{i=1}^{k} \delta_{i,j} = 1, \forall j \in \{1,\ 2,\ 3 \ldots n\}$$

Where $\boldsymbol{\delta}$ is the binary variable matrix whose dimension is $k \times n$, as shown in Equation (4-5), $\delta_{i,j} = 1$ means the j well is connected to the i manifold. $\boldsymbol{\delta}$ indicates the allocation between the manifolds and wells. k is the number of manifolds/clusters, n is the number of wells. $\mathbf{C}$ is the continuous variable matrix of flowline cost dependent on $\boldsymbol{\delta}$ and it has the same dimension as $\boldsymbol{\delta}$. $c_{i,j}$ is the nonlinear term of the flowline cost of connecting the j well to the i manifold. Therefore, the total number of MINLP variables is $2kn$. ".*" is element-wise multiplication operator. The first constraint ensures that each manifold connects to m wells, and the second ensures that each well is only connected to one manifold.

$$\boldsymbol{\delta} = \begin{bmatrix} \delta_{1,1} & \delta_{1,2} & \dots & \delta_{1,n} \\ \delta_{2,1} & \delta_{2,2} & \dots & \delta_{2,n} \\ . & . & . & . \\ . & . & . & . \\ . & . & . & . \\ \delta_{k,1} & \delta_{k,2} & \dots & \delta_{k,n} \end{bmatrix} \tag{4-5}$$

The formulation is very easy, but it is very hard to find the global optimum for such a MINLP model. In Wang's work [37], he could only use a heuristic method to get an approximation. In industry, engineers usually provide several candidate positions for the manifolds based on their knowledge and experience, so that $\mathbf{C}$ can be pre-calculated to be a coefficient matrix, rather than a continuous variable matrix, therefore reducing the MINLP model into an ILP model. The industrial method is also a compromised method to achieve a good approximation rather than the global optimum, unless the global optimal locations are exactly included in the candidate locations.

We can eliminate the continuous variables in the MINLP model, making it a nonlinear integer programming (NIP) problem, as shown below:

$$\begin{aligned} &\min_{\boldsymbol{\delta} \in Binary} \ \mathrm{Cost}\left(\boldsymbol{\delta}, m, \mathbf{p}\right) \\ &= \min_{\boldsymbol{\delta} \in Binary} \sum_{i=1}^{k} \left(\sum_{j=1}^{n} \left(\delta_{i,j} \left(x_j - X_i \right)^2 + \delta_{i,j} \left(y_j - Y_i \right)^2 \right) \right) \\ &s.t. \quad \sum_{j=1}^{n} \delta_{i,j} = m, \forall i \in \{1,\ 2, 3 \dots k\} \\ &\qquad \sum_{i=1}^{k} \delta_{i,j} = 1, \forall j \in \{1,\ 2,\ 3 \dots n\} \end{aligned} \tag{4-6}$$

Where $\mathbf{p}$ is the well position matrix comprised of well position vector $\mathbf{p}_i : \left(x_i,\ \mathrm{y}_i\right)$, $i \in \{1,\ 2,\ 3 \dots n\}$. $\left(X_i, Y_i\right)$ is the position coordinate of the i manifold, shown in Equation (4-7), which is actually equivalent to Equation (4-1).

$$X_i = \frac{\sum_{jj=1}^{n} \delta_{i,jj} x_{jj}}{m}, \qquad Y_i = \frac{\sum_{jj=1}^{n} \delta_{i,jj} y_{jj}}{m} \tag{4-7}$$

Even though there is no more continuous variable, and the number of the NIP variables is half of the MINLP's, i.e., kn, the computational complexity of the NIP is completely equivalent to the MINLP, because the nonlinear term of the cost is still in the objective function, making it practically infeasible for a MINLP/NIP solver to find the

global optimum of this specific model with only 40 wells. The Equation (4-3) shows the difficulty of finding the global optimum for the model. The infeasibility will also be shown in the following case study in Section 4.4.

But an insight into the Equation (4-6) reveals that one important cause of the inefficiency is repeatedly computing $k \times n$ times for the same position of the i manifold, i.e., $\left(X_i, Y_i\right)$. If we just compute this manifold position term only once, and store it as a coefficient, then the Equation (4-6) will become a simple linear equation. A naive idea of enumerating all possible clusters, which avoids from this redundant computation, leads to the following BLP model:

$$\min_{\boldsymbol{\gamma} \in Binary} \sum_{j=1}^{N} \gamma_j \cdot \text{cost}\left(\mathbf{A}, m, \mathbf{p}\right)_j \tag{4-8}$$

$$s.t. \quad \mathbf{A}_{n \times N} \boldsymbol{\gamma}_{N \times 1} = \mathbf{1}_{n \times 1}$$
$$\mathbf{A} \in Binary$$

Where $N = C_n^m$ is the number of all possible clusters of size m, it is also the number of variables in this BLP model. $\boldsymbol{\gamma}$ is the binary variable vector whose dimension is $N \times 1$, $\gamma_j = 1$ means the j cluster is selected for the optimal combination. $\boldsymbol{\gamma}$ indicates the selection of clusters. $\mathbf{A}$ is the coefficient matrix of dimension $n \times N$, as shown below, $a_{i,j} = 1$ means the i well is in the j cluster. From MINLP/NIP to BLP, the allocation relationship between manifolds and wells, i.e., $\boldsymbol{\delta}$, is equivalently converted to the selection of clusters, i.e., $\boldsymbol{\gamma}$.

$$\mathbf{A} = \begin{bmatrix} a_{1,1} & a_{1,2} & \dots & a_{1,N} \\ a_{2,1} & a_{2,2} & \dots & a_{2,N} \\ \cdot & \cdot & \cdot & \cdot \\ \cdot & \cdot & \cdot & \cdot \\ \cdot & \cdot & \cdot & \cdot \\ a_{n,1} & a_{n,2} & \dots & a_{n,N} \end{bmatrix}, \quad where \sum_{i=1}^{n} a_{i,j} = m, \forall j = \{1,\ 2,\ 3 \dots N\} \tag{4-9}$$

Different from the dependent relationship between the $\mathbf{C}$ and $\boldsymbol{\delta}$ in the MINLP model in Equation (4-4). The $\text{cost}\left(\mathbf{A}, m, \mathbf{p}\right)_j$ is a function independent of the variables $\boldsymbol{\gamma}$, hence it is still a coefficient rather than a variable. This coefficient can be calculated as shown below.

$$\text{cost}\left(\mathbf{A},m,\mathbf{p}\right)_j=\sum_{i=1}^{n}\left(a_{i,j}\left(x_i-\frac{\sum_{ii=1}^{n}a_{ii,j}x_j}{m}\right)^2+a_{i,j}\left(y_i-\frac{\sum_{ii=1}^{n}a_{ii,j}y_j}{m}\right)^2\right) \tag{4-10}$$

Compared with the MINLP model, the corresponding BLP model has a larger number of variables. Ostensibly, more variables mean computationally harder. However, it simplifies the computational complexity drastically because it is linear, therefore, we can use relaxation strategy along with branch and cut algorithm to solve the BLP model much faster. As for solving the BLP model, we can directly use the ILP/BLP solvers provided by IBM CPLEX, LINGO, GUROBI, TOMLAB, or just use the build-in function "intlinprog" in MATLAB Optimization Toolbox, etc.

Nevertheless, the number of all possible clusters still grows too fast as $N=C_n^m=O(n^m)$, even for $m=4$. It can easily run of the memory. Hence, as discussed in Section 4.3.1, we can make N to be the number of useful clusters rather than the number of all possible clusters to make it much more efficient.

4.3.3 **Find the useful clusters**

Obviously, the points in a useful cluster are close to each other. To build the adjacent relationship, we use the Delaunay Triangulation to build an undirected adjacent graph first. Delaunay Triangulation connects points in a nearest-neighbor manner as it maximizes the minimum angle in all triangles. The algorithm to construct Delaunay Triangulation has been well developed since it was proposed by Delaunay in 1934. Lawson's [53] and Bowyer-Watson's [54, 55] are the two classic algorithms for Delaunay Triangulation. The time complexity of the most efficient Delaunay Triangulation algorithm can be bounded as $O(n\log n)$ [56], where n is the number of points. As for the coding implementation in MATLAB, we can directly use the build-in function "delaunay".

Delaunay Triangulation also bears a convex hull property which makes the adjacency on the boundaries unwanted, as shown in Fig. 4.2. For example, the Point 7 and Point 10 in Fig. 4.2 are quite far apart, and the adjacent relation between these two points is obviously unwanted. To handle this trivial issue, we can use the following strategy to eliminate the unwanted adjacent relation on boundaries:

1. Add 8 ward points outside of the convex hull, and do Delaunay Triangulation for all the points, as shown in Fig. 4.3, the ward points are marked as black dots. The number of ward points can increase a bit as the problem scale grows large.

2. Delete the ward points and their connected edges, as shown in Fig. 4.4. Then, we get a non-convex Delaunay Triangulation graph which shows a better adjacent relationship on boundaries.

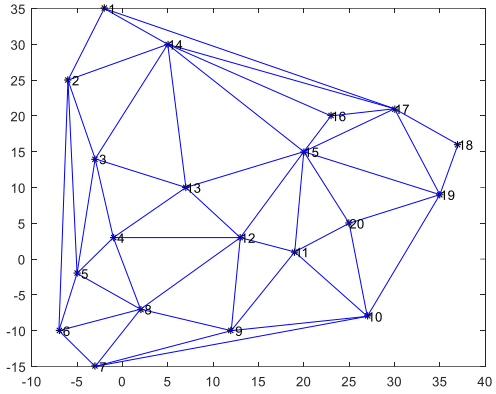

Fig. 4.2 Delaunay Triangulation of Original Points

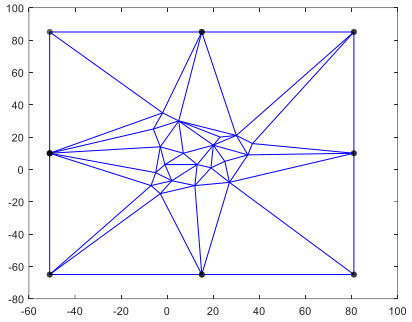

Fig. 4.3 Delaunay Triangulation with Ward Points

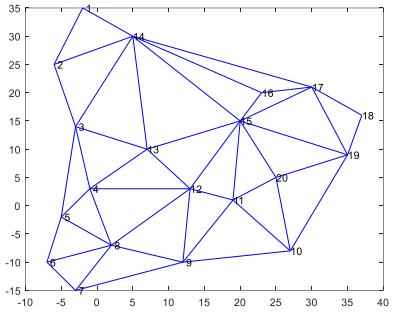

Fig. 4.4 Non-convex Delaunay Triangulation

After we get the adjacent graph, as shown in Fig. 4.4, we mark all the edges as distance 1, and build up the adjacent matrix of this undirected graph. The distance matrix of the undirected graph in Fig. 4.4 is given in Appendix IV. The conventional adjacency matrix only indicates the relationship of distance ≤ 1, denoting such an adjacent relationship as adjacent-1. To prove that the adjacent-1 relationship contains all the global optimal clusters, we can either enumerate all the clusters when the problem scale is not too large or modify the adjacency matrix to indicate the relationship of distance ≤ 2, i.e., to use the adjacent-2 relationship to find the useful clusters. Both the adjacent-1 matrix

and the adjacent-2 matrix of the undirected graph in Fig. 4.4 are given in Appendix IV as well. No doubt, the adjacent-2 matrix will introduce more useful clusters into the BLP model resulting in a longer computational time. We use the adjacent-2 relationship as a backup proof of the correctness of the adjacent-1 when it is infeasible to enumerate all clusters.

Then, the basic criterion to pick out the useful cluster from the adjacent relationship is that the selected points can form a tree in the adjacent graph, for example, {1, 2, 3, 5} is a useful cluster, but {1, 2, 5, 13} is not in the adjacent-1 relationship because this cluster cannot form a tree as the shortest distance from point 13 to any other point in the cluster is larger than 1, however, {1, 2, 5, 13} will become a useful cluster in the adjacent-2 relationship. We provide our algorithm for finding all the useful clusters with the basic criterion in Appendix III.

More strictly, a useful cluster should never isolate any points, for example, {2, 14, 16, 17} fulfills the basic criterion, but it is not a strictly useful cluster because it isolates the point 1. Obviously, the strict criterion will give us less useful clusters which means more efficiency in solving the BLP model. However, we find that for most problems of various scales, applying the strict criterion decreases the overall efficiency if we use a good BLP solver such as the IBM CPLEX. Hence, here we do not recommend the strict criterion for finding useful clusters. Or maybe it is just because our algorithm for strict criterion is not good enough.

At last, it should be noted that the algorithm of finding useful clusters presented in the Appendix III is not efficient enough to deal with clusters of large sizes. But fortunately, in the location-allocation problem of manifolds, we barely need to deal with clusters of size larger than 8. As for a very special case where the points are only divided into two clusters, we recommend the 2RCC algorithm [50, 51] which can directly generate the two global optimal clusters.

4.4 Case Study

We tested our BLP method on different cases to show its efficiency and robustness. We also compared our BLP method with the previous MINLP/NIP method solved by LINGO. Among the commercial solvers mentioned in Section 4.3.2, LINGO is the only one which provides nonlinear solvers without limitation in the problem scale under an academic license. In order not to bias the comparison, the following results of LINGO are

based on the original codes provided by LINDO technical support. The computational time is generated from a laptop Dell Inspiron 15-7537 (Intel Core i5-4210U, 12 GB DDR3 1600MHz). Besides, we also invited Dr. Hong Chen to use his SA algorithm[39] to compute the 100 points problem in Case 2 for comparison.

As we coded in MATLAB to implement our method, we used IBM CPLEX API, which is very MATLAB-user-friendly, to solve the BLP model. It should be noted that LINGO can also solve the BLP efficiently, however, their API for MATLAB is not so friendly as IBM's.

4.4.1 **Case 1: test on a published case**

The first case is exactly the same as that in Wang's work [37]. The positions of the 20 wells are given in Table. 4-1, also shown in Fig. 4.1 ~ Fig. 4.6:

Table. 4-1 Positions of 20 Wells

Well No.	1	2	3	4	5	6	7	8	9	10
x	-2	-6	-3	-1	-5	-7	-3	2	12	27
y	35	25	14	3	-2	-10	-15	-7	-10	-8

Table. 4-1 Positions of 20 Wells (Continued)

Well No.	11	12	13	14	15	16	17	18	19	20
x	19	13	7	5	20	23	30	37	35	25
y	1	3	10	30	15	20	21	16	9	5

Compared with Wang's CPU (Intel Core Duo P8700), Intel Core i5-4210U has a superior performance in parallel computation but inferior computational ability for a single core/thread, as shown in Table. 4-2, based on Whetstone benchmarks conducted by the Asteroids@home project [57]. Hence, to have a better comparison, we implemented our method in serial computation. Note that the data provided by the Asteroids@home changes slightly as the project goes on.

Table. 4-2 Comparison of CPU performance [57]

CPU model	cores/computer	GFLOPS/core	GFLOPS/computer
Intel Core 2 Duo CPU P8700 @ 2.53GHz	2	2.96	5.92
Intel Core i5-4210U CPU @ 1.70GHz	4	2.59	10.32

The result comparison of five 4-slot manifold layout is given in Table. 4-3 and Fig. 4.5. It seems that there is not too much improvement compared with Wang's result. However, if we take the two 10-slot manifold layout for comparison, as shown in Table. 4-4 and Fig. 4.6, the big gap in the optimal cost in Wang's method becomes unacceptable.

For this specific problem which only divides the points into two clusters, we directly use the 2RCC algorithm.

It should be noted that it is meaningless to strictly compare the computational time with Wang's because of the difference between global optimum and local optimum. The improvement of computational time of achieving the global optimum is huge by comparing LINGO's result and ours.

Compared to the large number of all clusters, it is easy to see the efficiency of our method lies on the small number of useful clusters. In this case, the number of useful clusters, i.e., the number of clusters under the "adjacent-1" relationship is only 373, which is also the number of BLP variables. While the number of MINLP variables is 200, which has the same magnitude as the BLP variable number. The "adjacent-2" is also conducted in case that the computation for all clusters runs out of memory.

Table. 4-3 Comparison of Five 4-slot Manifold Layout

	Wang [37]	LINGO (MINLP/NIP)		Our Method (BLP)		
		local	global	adjacent-1	adjacent-2	all
Optimal Cost	1278.75	1261.25	1261.25	1261.25	1261.25	1261.25
Global Optimal(Y/N)	N	Y	Y	Y	Y	Y
Computational Time	0.156s	62s~73s	>4000s	0.08~0.17s	0.15~0.26s	0.21~0.43s
Number of Clusters				373	3171	4845

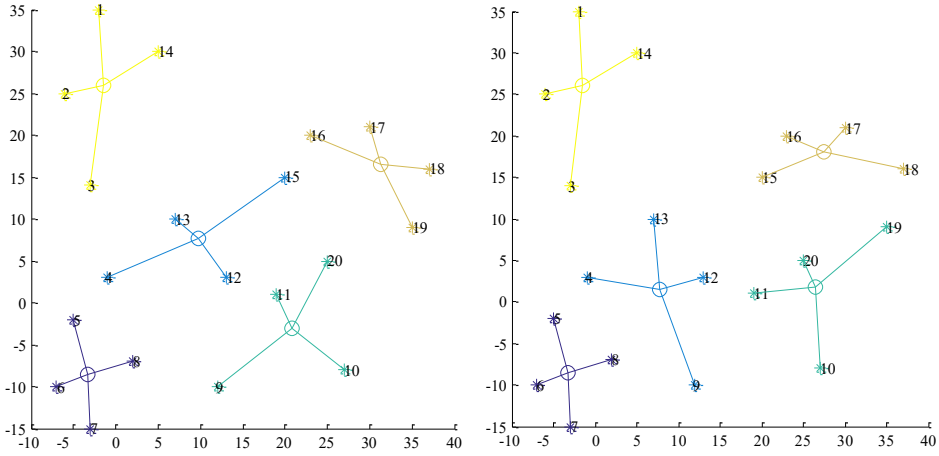

(a) Result by Wang [37] (b) Result by LINGO/Our Method

Fig. 4.5 Comparison of Five 4-slot Manifold Layout

Table. 4-4 Comparison of Two 10-slot Manifold Layout

	Wang [37]	LINGO/local	LINGO/global	2RCC
Optimal Cost	5724.9	4664.7	4664.7	4664.7
Global Optimal(Y/N)	N	Y	Y	Y
Computational Time	0.156s	18s~35s	>20s	0.10s~0.13s

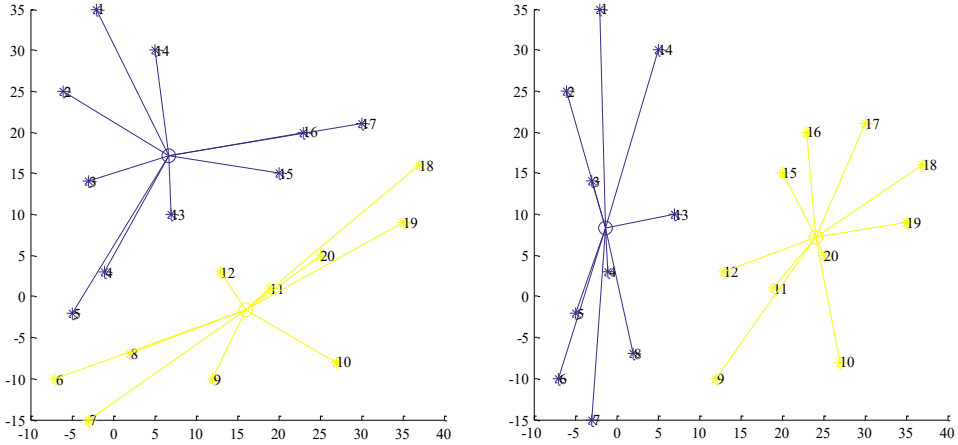

(a) Result by Wang [37] (b) Result by LINGO/2RCC

Fig. 4.6 Comparison of Two 10-slot Manifold Layout

4.4.2 **Case 2: test on larger-scale cases**

It is quite tricky that when the number of wells is just doubled, the problem would become almost infeasible for a global solver. Refer to the analysis in Section 4.3.1. Expectedly, we could not find any published work that has a case of more than 20 wells. We randomly generated 100 points, shown in Appendix II. Firstly, we used the first 40 points to test, and the results are shown in Table. 4-5 and Fig. 4.7. The result of LINGO local solver is the best it achieved in 20 trials, and each trial takes more than 10 minutes. The LINGO global solver cannot get the result even after 8 hours. Our method can easily get the global optimum. In this 40-point case, the number of useful clusters generated by our method is 1088, which is less than 3 times of the number in the 20-point case. While the number of MINLP variables is 800, which is 4 times of the number in the 20-point case.

Table. 4-5 Comparison of Ten 4-slot Manifold Layout

	LINGO (MINLP/NIP)		Our Method (BLP)		
	local	global	adjacent-1	adjacent-2	all
Optimal Cost	1020.51	Infeasible	1010.96	1010.96	1010.96
Global Optimal(Y/N)	N	Infeasible	Y	Y	Y
Computational Time	751~850s	>8h	0.23~0.35s	0.97~1.21s	3.34~4.41s
Number of Clusters			1088	17261	91390

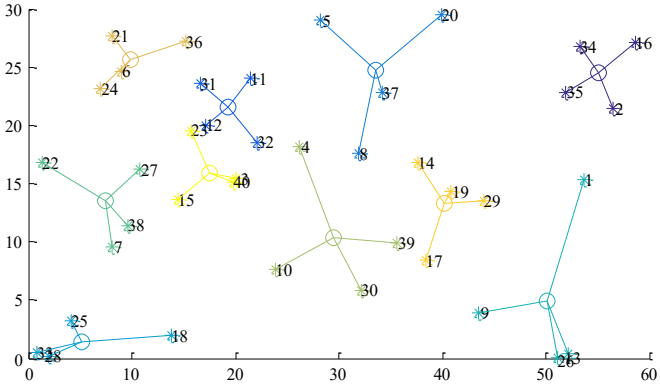

(a) Result by LINGO

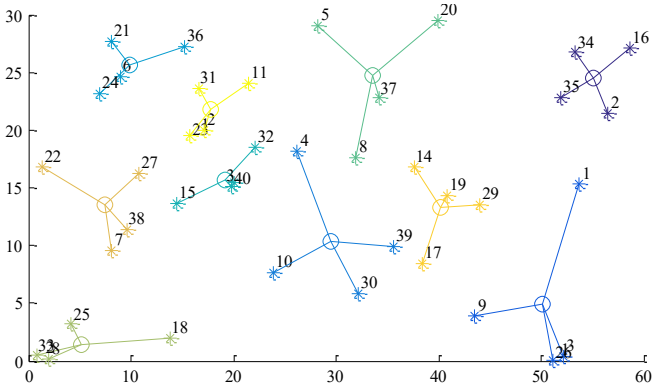

(b) Result by Our Method

Fig. 4.7 Comparison of Ten 4-slot Manifold Layout

Till now, we have already seen the advantage of our method. It is already meaningless to compare for a larger-scale problem, but we provide our results in Table. 4-6 and Fig. 4.8 for reference. Besides, we also invited Dr. Hong Chen to try his SA method [39] on the 100-point problem for comparison. His method always converges at the optimal cost around 970, which is just a local optimum, with the time cost of more than half an hour. By comparing to the MINLP or NIP variable number, we can see a much slower growing trend of the BLP variable number, which indicates its efficiency for large scale problem. As for a larger problem where there are 500 randomly distributed points with $m = 4$, it can be solved by our method within 3 minutes.

Table. 4-6 Comparison on Larger-scale Problems

		Optimal Cost	Computational Time	Number of Clusters (BLP Variable Number)	MINLP Variable Number	NIP Variable Number
first 60 points	adjacent-1	983.40	0.43~0.57s	1928	1800	900
	adjacent-2	983.40	3.13~3.96s	35420		
	all	983.40	33.11~35.43s	487635		
first 80 points	adjacent-1	855.62	0.44~0.57s	2872	3200	1600
	adjacent-2	855.62	6.43~7.47s	59840		
	all	Infeasible (out of memory)		1581580		
100 points	adjacent-1	858.96	0.73~0.81s	3820	5000	2500
	adjacent-2	858.96	8.66~9.32s	86867		
	all	Infeasible (out of memory)		3921225		
SA method[39] for 100 points		≈970	≈35mins			

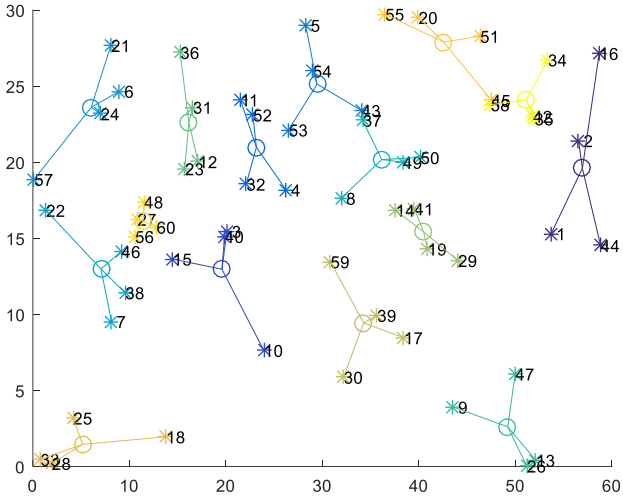

(a) Result of the First 60 Random Points

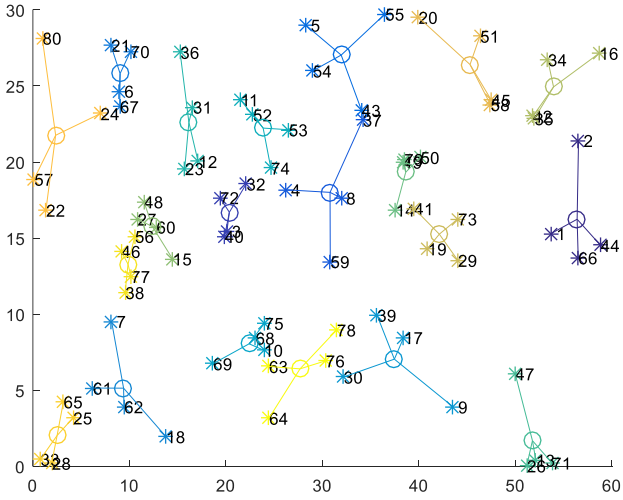

(b) Result of the First 80 Random Points

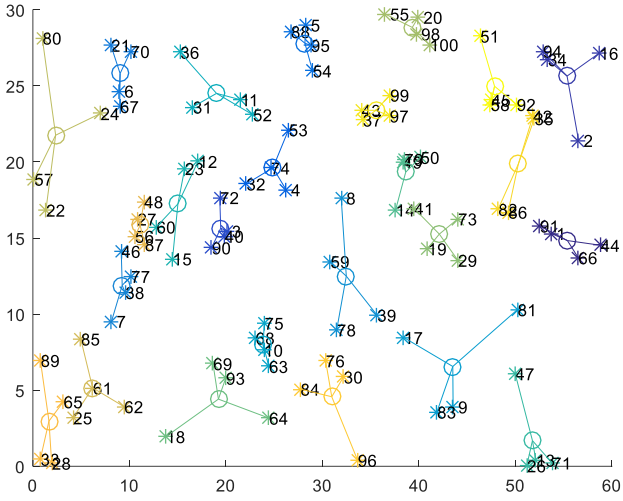

(c) Result of the 100 Random Points

Fig. 4.8 Results of Larger-scale Problem by Our Method

4.4.3 **Case 3: test on highly ill-conditioned cases**

We intentionally generated two sets of points distributed orthogonally. Such a distribution pattern is highly ill-conditioned because there are too many combinations (local optimal solution) of the same total cost in the orthogonal distribution so that it can easily trap a local/heuristic solver at a bad local optimum or at least increase the

computational time of the local/heuristic solver to converge to a good local optimum. It should be noted that, the follow result of LINGO/local is the best result from 20 trials, whereas most of the time, it cannot converge to the global optimum. The computational time of LINGO/local is the time of the trial which reaches the global optimum. Our method is deterministic.

Table. 4-7 Comparison of a 20-Point Highly Ill-conditioned Case

	LINGO/local	Our Method
Computational Time	92s~145s	0.09s~0.19s

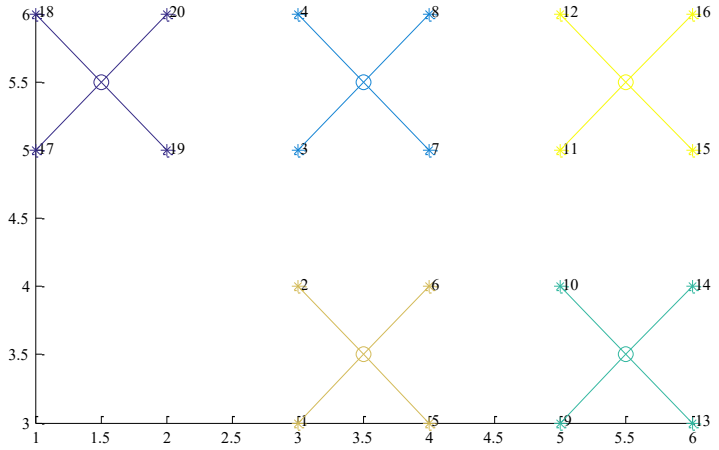

Fig. 4.9 Result of a 20-Point Highly Ill-conditioned Case

Table. 4-8 Comparison of a 36-Point Highly Ill-conditioned Case

	LINGO/local	Our Method
Computational Time	565s~662s	0.21s~0.35s

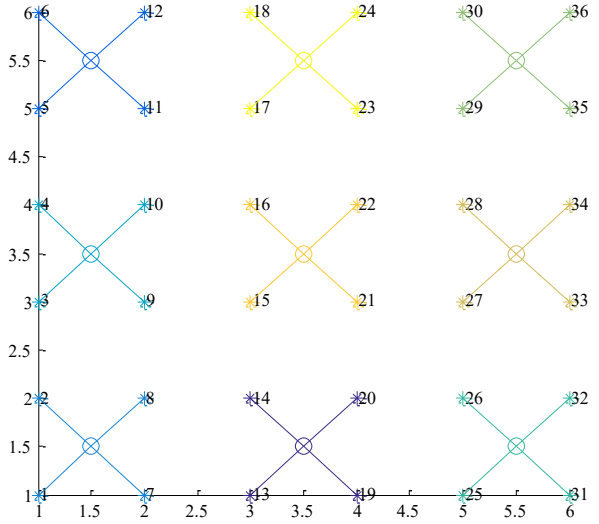

Fig. 4.10 Result of a 36-Point Highly Ill-conditioned Case

As we increase the number of points, the LINGO/local solver can no longer converge to the global optimum within 20 trials. While our method can get the global optimum for such a problem of 100 points with the time around 0.61s ~ 0.78s.

4.5 Further Discussion

Now consider for a more general problem where the number of wells n is not a multiple of m, i.e., $n = m \cdot k + h$, $h \in \{1, 2, ..., m-1\}$. Because $h < m$, we can directly get the useful clusters of size h while we are finding the useful clusters of size m by the algorithm provided in Appendix III. Then use the method proposed in Section 4.3.2 to build the BLP model. The only difference is that N now becomes the total number of useful clusters of both size m and size h, denoted as N_m and N_h ,respectively. $\mathbf{A}$ and $\boldsymbol{\gamma}$ also need to include clusters of both sizes, as shown in Equation (4-12) below. In this case, it is solving a problem where there are manifolds of two different slot sizes. More generally, it can also handle the problem where there are manifolds of more than 2 different slots. For example, if we have manifolds of $m_1, m_2, ..., m_t$ slots, the model can be built as Equation (4-13). For more details about the application in the clustering problem of more than one size, we will introduce them in the following Chapter 5.

$$\min_{\boldsymbol{\gamma} \in Binary} \sum_{j=1}^{N_m+N_h} \gamma_j \cdot \text{cost}\left(\mathbf{A}, m, h, \mathbf{p}\right)_j \tag{4-11}$$

$$\begin{aligned} s.t. \quad & \mathbf{A}_{n\times(N_m+N_h)} \boldsymbol{\gamma}_{(N_m+N_h)\times 1} = \mathbf{1}_{n\times 1} \\ & \mathbf{A} \in Binary \\ & \sum_{i=1}^{n} a_{i,j} = m, \forall j = \{1,\ 2,\ 3\ ...\ N_m\} \\ & \sum_{i=1}^{n} a_{i,j} = h, \forall j = \{N_m+1,\ N_m+2,\ N_m+3\ ...\ N_m+N_h\} \end{aligned}$$

$$\mathbf{A} = \begin{bmatrix} a_{1,1} & a_{1,2} & ... & a_{1,N_m} & a_{1,N_m+1} & a_{1,N_m+2} & ... & a_{1,N_m+N_h} \\ a_{2,1} & a_{2,2} & ... & a_{2,N_m} & a_{2,N_m+1} & a_{2,N_m+2} & ... & a_{2,N_m+N_h} \\ . & . & . & . & . & . & . & . \\ . & . & . & . & . & . & . & . \\ . & . & . & . & . & . & . & . \\ a_{n,1} & a_{n,2} & ... & a_{n,N_m} & a_{n,N_m+1} & a_{n,N_m+2} & ... & a_{n,N_m+N_h} \end{bmatrix} \tag{4-12}$$

$$\min_{\boldsymbol{\gamma}\in Binary} \sum_{j=1}^{\sum_{l=1}^{t} N_{m_l}} \gamma_j \cdot \mathrm{cost}\left(\mathbf{A}, m, h, \mathbf{p}\right)_j \tag{4-13}$$

$$s.t. \quad \mathbf{A}_{n\times\left(\sum_{l=1}^{t} N_{m_l}\right)} \boldsymbol{\gamma}_{\left(\sum_{l=1}^{t} N_{m_l}\right)\times 1} = \mathbf{1}_{n\times 1}$$

$$\mathbf{A} \in Binary$$

$$\sum_{i=1}^{n} a_{i,j} = m_1, \forall j = \{1,\ 2,\ \ldots,\ N_{m_1}\}$$

$$\sum_{i=1}^{n} a_{i,j} = m_2, \forall j = \{N_{m_1}+1, N_{m_1}+2,\ \ldots,\ N_{m_1}+N_{m_2}\}$$

$$\vdots$$

$$\sum_{i=1}^{n} a_{i,j} = m_l, \forall j = \{\sum_{l=1}^{t-1} N_{m_l}+1, \sum_{l=1}^{t-1} N_{m_l}+2,\ \ldots,\ \sum_{l=1}^{t} N_{m_l}\}$$

When there are barriers on the seabed, as it was discussed in [39, 42], we can just delete the useful clusters which intersect with the barriers. The time complexity of checking intersection of N clusters with a barrier is linear to N, i.e., $T = O\left(N\right)$; while solving a BLP model of N variables has a higher order of N, i.e., $T = O\left(N^c\right), c > 1$. Hence, we can expect the efficiency to be the same or even higher because of less useful clusters.

When we consider the seabed as a 3D, i.e., the first basic assumption no longer exists, we can firstly project the well positions onto 2D to find the useful clusters, then the difference is the cost function of each cluster, i.e., Equation (4-10).

When the cost function is not proportional to the squared Euclidean distance, i.e., the geometric mean position is no longer the manifold's optimal location, we just replace the Equation (4-10) with the given cost function, and then calculate the optimal manifold location by gradient descent or any viable method and the cost for each cluster based on the given cost function. For example, when the cost is proportional to the Euclidean distance, then the manifold's optimal location is the geometric median of the connected wells. The difference in computational complexity is completely dependent on the difference in the complexity of the cost function. The effect of the complexity of the cost function of a cluster on the whole problem is just linear. The NP-hardness lies in the combinatory problem, not the computation for cost.

It should be noted that there are different methods to define the adjacent relationship for finding the useful clusters. The method for reducing all clusters to useful clusters is

problem (cost function) dependent. The Delaunay Triangulation method is not a universal method for all scenarios. The method for finding useful clusters directly affects the efficiency and accuracy. For example, if we simply define the adjacent relationship by Euclidean distance, it will be hard to determine the proper distance radius for defining a useful cluster. As shown in Fig. 4.7, some clusters extend in a relatively large distance, while others are quite confined in a small radius. If the distance radius is set too small, we will miss the optimal clusters and cannot obtain the global optimum, i.e., accuracy is affected; if it is too large, it will lead to a large number of useful clusters, i.e., efficiency is affected. In Chapter 5 where the scenario is much more practical and more complex, we will propose another method which superposes the "economic zones" to find the useful clusters.

At last, if you have doubt in the global optimality for the adjacent-1 result, you can use adjacent-2 result to check if enumerating all clusters is impossible.

4.6 Summary

This chapter introduces a brand-new method to deal with the location-allocation problem of manifolds in subsea field layout optimization. With the help of graphic theories, our method reduces the traditional MINLP model into a significantly more efficient BLP model leading to a breakthrough in both accuracy and efficiency. The two core ideas of our method are the conversion from the allocation relationship between manifolds and wells to the selection of clusters of wells and the reduction from all clusters to useful clusters. The advantage of our method is well demonstrated in the case studies. Our efficient method makes the global optimal solution to the problem of a much larger scale feasible. Besides, it is not limited in subsea field layout optimization, it is actually a specific MINLP solver for any optimization problem which can be regarded as a location-allocation problem, or equivalently, a size-constrained clustering problem where the global optimal solution is the combination of clusters of adjacent points. As for other patterns of global optimal solutions, for example we want the minimum cost of all clusters to be maximized, we need carefully design a proper algorithm to reduce all clusters to useful clusters. However, it will be another problem whether there is such a proper algorithm for a specific pattern.

Chapter 5. Solution to Sub-problem 3: "k-sites-n-wells"

5.1 Mathematical Description

Given n well completion intervals, $n \in Integer^{+}$, each completion interval is defined by its start point $P_{2,i} = \left(Px_{2,i}, Py_{2,i}, Pz_{2,i}\right)$ and the end point of the first segment of the completion interval $P_{3,i} = \left(Px_{3,i}, Py_{3,i}, Pz_{3,i}\right)$, such as the dataset in Appendix II. Thus, the drilling direction vector $V_{2,i} = \left(Vx_{2,i}, Vy_{2,i}, Vz_{2,i}\right)$ is determined, where normally $Vz_{2,i} \le 0$ so that the direction is not upward. The highest allowed kickoff point $P_{1,i} = (Px_{1,i}, Py_{1,i}, Pz_{1,i})$ for every wellbore should be at the depth of Z_i m, i.e., $Pz_{1,i} = Z_i < 0$, $i \in \{1,\ 2,\ \ldots,\ n\}$. Obviously, the drilling direction vector at every kickoff point is vertical downwards $V_{1,i} = (0, 0, -1)$. The maximum allowed turning rate/dogleg severity is κ°/30 m, i.e., minimum allowed turning rate radius is $r_{\min} = \dfrac{5400}{\pi\kappa}$ m.

The preparation cost (e.g., rig re-location) for one drilling site is cst_{site}. $cst_{SF,1}$ is the cost of the subsea facilities for a satellite well. Similarly, $cst_{SF,2}$ is for a 2-slot template, $cst_{SF,4}$ is for a 4-slot template, and $cst_{SF,6}$ is for a 6-slot template. The wellbore cost can be a user-defined function related with the trajectory structure following the form as $cst_{Traj} = cstC\left(Lc\right) + cstS\left(Ls, \theta\right)$, where Lc is the length of non-straight section, Ls is the length of straight section, θ is the inclination angle of the straight section; $cstC\left(Lc\right)$ is the cost function of non-straight section which is continuous and positively correlated with Lc, i.e., $\dfrac{\partial cstC\left(Lc\right)}{\partial Lc} > 0$; $cstS\left(Ls, \theta\right)$ is the cost function of straight section which is continuous and positively correlated with Lc and θ, i.e., $\dfrac{\partial cstS\left(Ls, \theta\right)}{\partial Ls} > 0$ and $\dfrac{\partial cstS\left(Ls, \theta\right)}{\partial \theta} > 0$.

The objective is to find the optimal combination of these completion intervals so that the overall cost, i.e., the sum of site preparation cost, subsea facility cost and wellbore cost, is minimized. In details, we need determine the allocation relationship between

drilling sites and completion intervals; the number of the subsea facilities of different specifications, denoted as $n_{SF,m}$, specifically, $n_{SF,1}$, $n_{SF,2}$, $n_{SF,4}$ and $n_{SF,6}$ are the needed number of subsea facilities for satellite, 2-slot template, 4-slot template and 6-slot template, respectively; the number of the drilling sites n_{site}; and the drilling site location $P_{0,s}=\left(Px_{0,s},Py_{0,s},0\right)$, $s\in\{1,2,...,n_{site}\}$, which is vertically above the corresponding kickoff point(s).

5.2 Method

5.2.1 Mathematical Model and Main Process

This optimization problem can be written as Equation (3-3). The unknown variables that need to be optimized in the model include the number of drilling sites n_{site}, the number of subsea facilities of different specifications n_{SF}, and the positions P_0 of the n_{site} drilling sites.

$$\begin{aligned} Obj.\quad & \min_{n_{site},n_{SF},P_0}\left[COST\left(P_1,V_1,P_2,V_2,r,n_{site},n_{SF},cst_{site},cst_{SF}\right)\right] \\ & =\min_{n_{site},n_{SF},P_0}\left[n_{site}cst_{site}+\sum_{j=\{1,2,4,6\}}n_{SF,m}cst_{SF,m}+\sum_{i=1}^{n}cst_{Traj,i}\right] \\ s.t.\quad & r\geq r_{\min} \\ & Traj\in Dubins\,Curve \\ & Pz_1=Z \\ & n_{site}=\sum_{m=\{1,2,4,6\}}n_{SF,m} \end{aligned} \tag{5-1}$$

This problem can be decomposed into two problems: the optimal trajectory problem and the location-allocation problem. We have introduced our efficient and global optimal methods for solving these two types of problems in Chapter 3 and Chapter 4, respectively. Here we need systematically combine these two methods. Briefly, the main process is as follows:

Step 1. Use the 3D Dubins Curve method to calculate the optimal drilling site $P_{0,j}$ and the related trajectory cost $cst_{Traj,i}$ for each cluster of wells. Here $j\in\{1,2,...,\sum_{m=\{1,2,4,6\}}N_m\}$ is the index of clusters of wells; $i\in Cluster\ j$; N_m is the number of clusters of size m, designated $m\in\{1,2,4,6\}$. The total cost of each cluster $cstT_j$, as

Equations (5-2) shows, includes the cost of all trajectories in the cluster $\sum_{i\in Cluster\ j} cst_{Traj,i}$, the cost of drilling site preparation cst_{site} and the subsea facility cost for the cluster $cst_{SF,m}$, where m is the size of *Cluster* j. For example, if *Cluster* 100 is {5, 8, 15, 20}, it means the *Cluster* 100 is formed by the well #5, #8, #15, and #20, and the cluster size is 4.

$$cstT_j = \left(\sum_{i\in Cluster\ j} cst_{Traj,i} \right) + cst_{site} + cst_{SF,m}, \quad m = \text{size of } Cluster\ j \tag{5-2}$$

Step 2. Solve the BLP problem shown in Equation (5-3) to find the best clusters. The summation of N_m is the number of variables in this BLP problem. $\boldsymbol{\gamma}$ is the variable vector whose dimension is $\sum_{m=\{1,2,4,6\}} N_m \times 1$. $\gamma_j = 1$ means the j cluster is picked for the optimal combination. $\mathbf{A}$ is the binary coefficient matrix of dimension $n \times \sum_{m=\{1,2,4,6\}} N_m$, $a_{i,j} = 1$ means the i completion interval is allocated to the j cluster. If we do not want to use 6-slot templates, we can conveniently set cst_{SF6} a dummy value which is much larger than other subsea facility cost. But the better way is to delete the parameters related 6-slot in Equation (5-3) so that the computation for irrelevant terms can be avoided.

$$\begin{aligned}
Obj.\ & \min_{\boldsymbol{\gamma}\in Binary} \sum_{j=1}^{N_1+N_2+N_4+N_6} \gamma_j \cdot cstT_j \\
s.t.\ & \mathbf{A}_{n\times(N_1+N_2+N_4+N_6)} \boldsymbol{\gamma}_{(N_1+N_2+N_4+N_6)\times 1} = \mathbf{1}_{n\times 1} \\
& \sum_{i=1}^{n} a_{i,j} = 1,\ \forall j = \{1,\ 2,\ldots,\ N_1\} \\
& \sum_{i=1}^{n} a_{i,j} = 2,\ \forall j = \{N_1+1,\ N_1+2,\ldots,\ N_1+N_2\} \\
& \sum_{i=1}^{n} a_{i,j} = 4,\ \forall j = \{N_1+N_2+1,\ N_1+N_2+2,\ldots,\ N_1+N_2+N_4\} \\
& \sum_{i=1}^{n} a_{i,j} = 6,\ \forall j = \{\sum_{m=\{1,2,4\}} N_m + 1,\ \sum_{m=\{1,2,4\}} N_m + 2,\ldots,\ \sum_{m=\{1,2,4\}} N_m + N_6\} \\
& \mathbf{A} \in Binary
\end{aligned} \tag{5-3}$$

$$\mathbf{A}=\begin{bmatrix} a_{1,1} & a_{1,2} & \cdots & a_{1,N_1} & a_{1,N_1+1} & a_{1,N_1+2} & \cdots & a_{1,N_1+N_2} & \cdots & \cdots & a_{1,N_1+N_2+N_4+N_6} \\ a_{2,1} & a_{2,2} & \cdots & a_{2,N_1} & a_{2,N_1+1} & a_{2,N_1+2} & \cdots & a_{2,N_1+N_2} & \cdots & \cdots & a_{2,N_1+N_2+N_4+N_6} \\ \cdot & \cdot & \cdot & \cdot & \cdot & \cdot & \cdot & \cdot & \cdots & \cdots & \cdot \\ \cdot & \cdot & \cdot & \cdot & \cdot & \cdot & \cdot & \cdot & \cdots & \cdots & \cdot \\ \cdot & \cdot & \cdot & \cdot & \cdot & \cdot & \cdot & \cdot & \cdots & \cdots & \cdot \\ a_{n,1} & a_{n,2} & \cdots & a_{n,N_1} & a_{n,N_1+1} & a_{n,N_1+2} & \cdots & a_{n,N_1+N_2} & \cdots & \cdots & a_{n,N_1+N_2+N_4+N_6} \end{bmatrix}$$

Step 3. Count out $n_{SF,m}$ and n_{site} based on the obtained optimal $\boldsymbol{\gamma}$ from Step 2. The objective function of Equation (5-3) is the same as the objective function of Equation (3-3). Besides, the drilling sites' positions have already been calculated for all clusters including the optimal ones in Step 1. Hence, Equation (3-3) is solved.

However, there is a big issue in the process above: if we simply enumerate all the clusters, i.e., $\sum N_m = \sum C_n^m$, the huge number of all possible clusters can easily make the computation in Step 1 infeasible. We need some pre-processing to reduce all the possible clusters to useful clusters.

5.2.2 **Pre-process for Reducing Possible Clusters**

In Chapter 4, we introduced Delaunay Triangulation to reduce all possible clusters to only useful clusters by using the adjacency. In this problem the completion interval is not just a point but with a vector. The adjacency we need to find is not within the completion intervals, but within their wellhead locations. However, the wellhead location of a given completion interval is not fixed. We should firstly find the optimal wellhead location for each completion interval individually, then use the Delaunay Triangulation on the wellhead locations. Nevertheless, in this particular type of problems, we have a better way to define the adjacency to limit the useful clusters to a much smaller number.

Pre-Step 1. Assume all the wells to be satellite wells and find the optimal location for each satellite well, as shown in Fig. 5.1. In Fig. 5.1(a), the magenta line indicates the completion interval, the black line indicates the straight section, the blue line indicates the curved section. In Fig. 5.1(b), the diamond shape indicates the satellite wellhead position, the dashed line indicates the curved section of the well, and the different colors indicate different wells.

Meanwhile, we get the optimal cost distribution for each completion intervals within the field by using 3D Dubins Curve method. The optimal cost distribution reveals how the well trajectory cost changes as the satellite drilling site changes. Fig. 5.2 shows an

example of the optimal cost distribution of #1 interval where the trajectory cost is simply defined as the length of the trajectory. The position of minimum cost is the best satellite drilling site. It should be noted that the position/grid resolution of Fig. 5.2 is only 200×200, therefore there is error between the exact minimum value and the minimum value given in the figure. If we set the resolution higher, we can directly use the discretized value in the cost distribution contour to find the optimal drilling site $P_{0,j}$ and total cost $cstT_j$ of each cluster so that we can avoid from conducting the computationally costly 3D Dubins Curve method in the Step 1 of main process. Even though the computational time for pre-process increases if the resolution is set higher, but it is worthwhile to increase the resolution to some extent especially when we are dealing with a large number of wells or with various user-defined cost items.

Pre-Step 2. Set a threshold for the cost distribution of each completion interval to define an economic zone, as shown in Fig. 5.3. The economic zone is just a clip of the cost distribution contour. The threshold is based on the cost of subsea facilities for a satellite well $cst_{SF,1}$ and the cost of drilling site preparation cst_{site}, as shown in Equation (5-4). $\min(cst_{Traj,i})$ is the minimum of the cost distribution, such as the data cursor shows in Fig. 5.2 and Fig. 5.3(a); the corresponding position of $\min(cst_{Traj,i})$ is the best drilling site as a satellite for that #i well interval. The *factor* is used to control the possible numerical error in the discretized grid value so that we will not miss any optimal cluster. However, setting *factor* too large will introduce more useless clusters as useful clusters. We can roughly set it between 1 and 1.2 based on the resolution of the cost distribution. The logic of the threshold Equation (5-4) is that if the well is drilled as a template well and the drilling site is outside the economic zone, then the trajectory cost will exceed the saved cost from less drilling sites and less subsea facilities, which means it is better to drill the well as a satellite well rather than a template well. In other words, it is economic only if the template drilling site for the well is within its economic zone. Hence, in the Pre-Step 1 we do not need to compute the cost distribution on the whole field for a given well interval, we just need to compute from the assumed satellite wellhead position to the economic zone boundary.

$$threshold_i = \min(cst_{Traj,i}) + \left(cst_{site} + cst_{SF,1}\right) \times factor \tag{5-4}$$

Pre-Step 3. Superpose the economic zones to find the useful clusters. If n wells should be drilled as template wells from one drilling site, then the economic zones of the n wells must have a common overlapped zone. As Fig. 5.3 shows, wells #1, #2, #3 and #4 have a common overlapped zone around (6000, 6000), therefore these four wells can form a useful cluster of size 4 to be drilled as a 4-slot template. Of course, any two of these four wells can form a useful cluster of size 2 to be drilled as a 2-slot template. While well #29 has no overlapped zone with these four wells, therefore, none of these four wells can form a cluster with the well #29. With such a strategy, the number of the useful clusters we need to compute in the main process will be very small.

It should be noted that the economic zone of well #4 shown in Fig. 5.3(d) is not as regular as the others, because there is a blank area in its optimal cost distribution, i.e., if the drilling site is located in the blank area, the well completion interval #4 cannot be reached. The reason is that the interval #4 is relatively shallow as shown in Fig. 5.1(a).

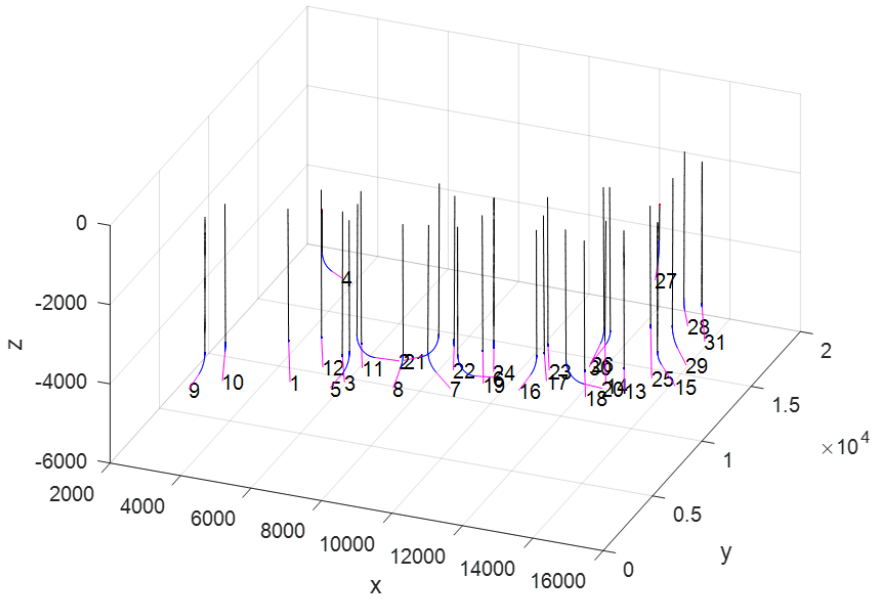

(a) 3D View of Satellite Wells for Dataset 2

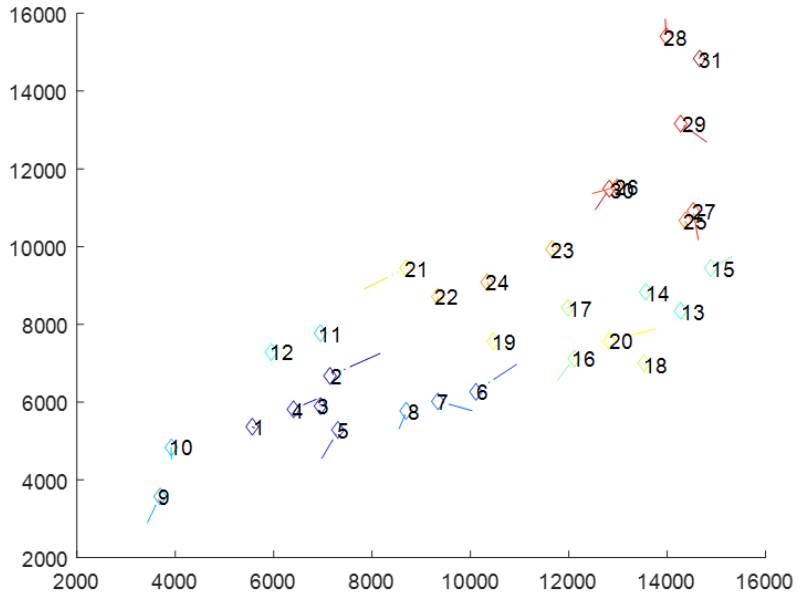

(b) 2D View of Satellite Sells for Dataset 2
Fig. 5.1 Satellite Wells (dogleg severity = 3°/30 m)

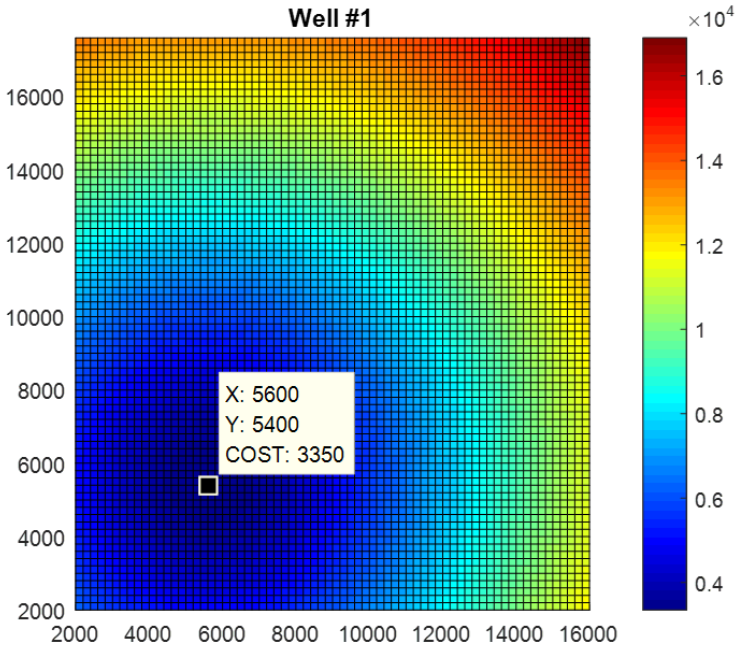

Fig. 5.2 Optimal Cost Distribution of Well #1

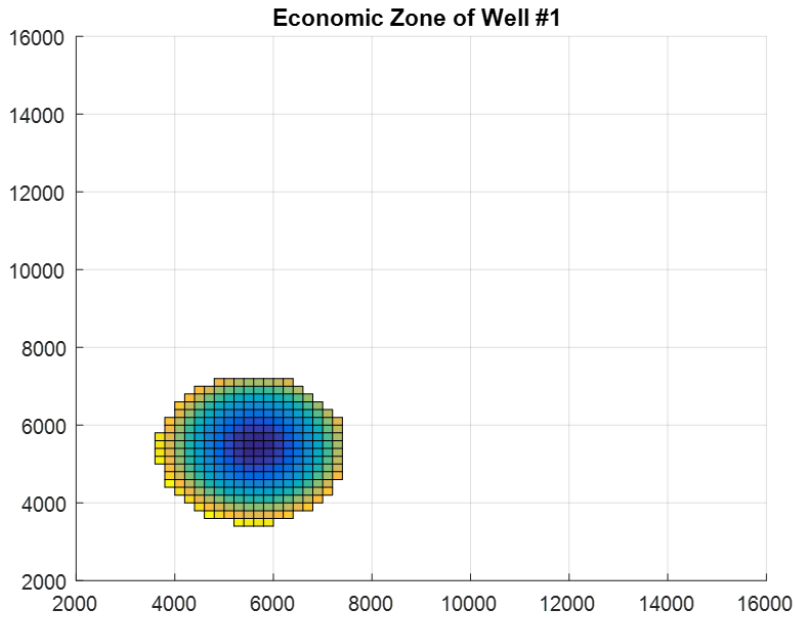

(a) Economic Zone of Well #1

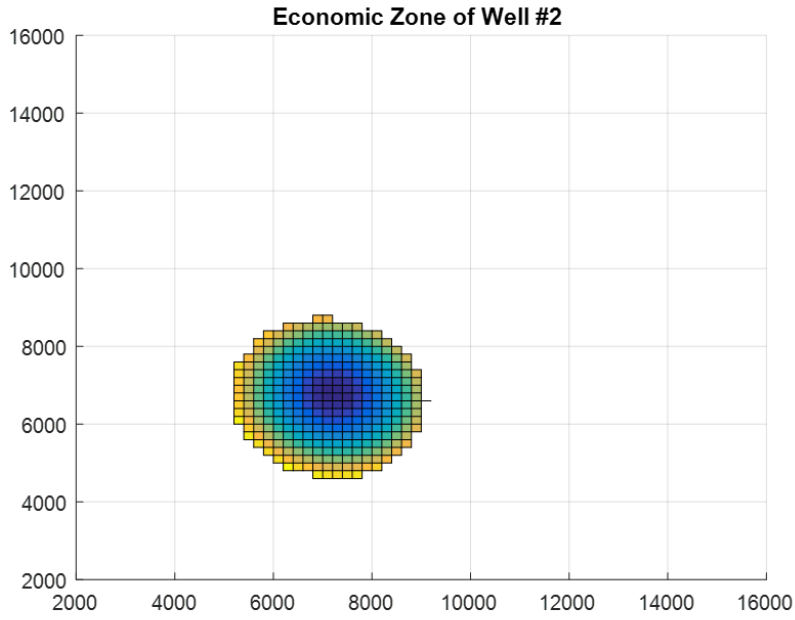

(b) Economic Zone of Well #2

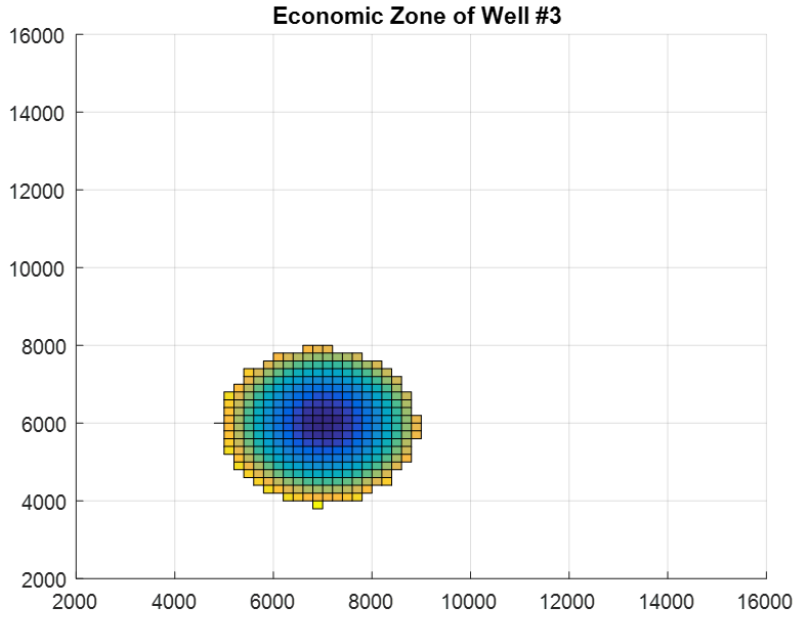

(c) Economic Zone of Well #3

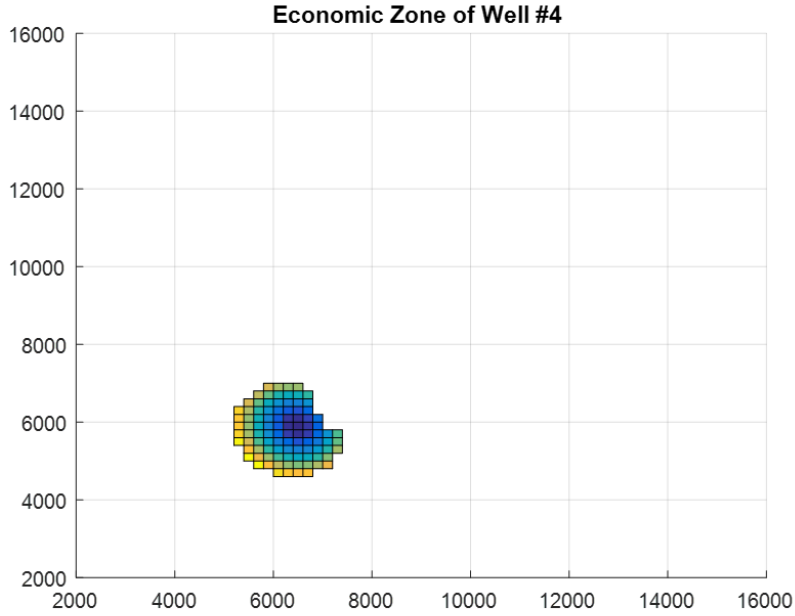

(d) Economic Zone of Well #4

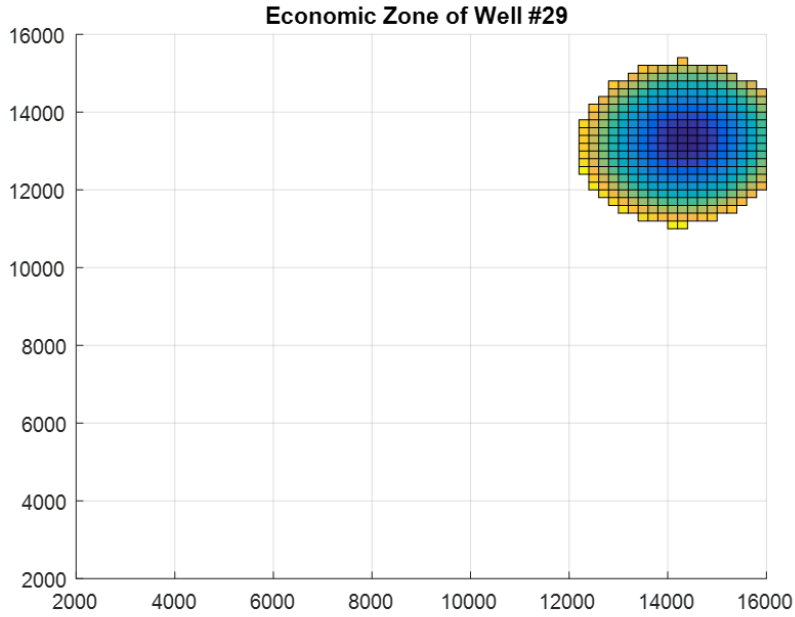

(e) Economic Zone of Well #29

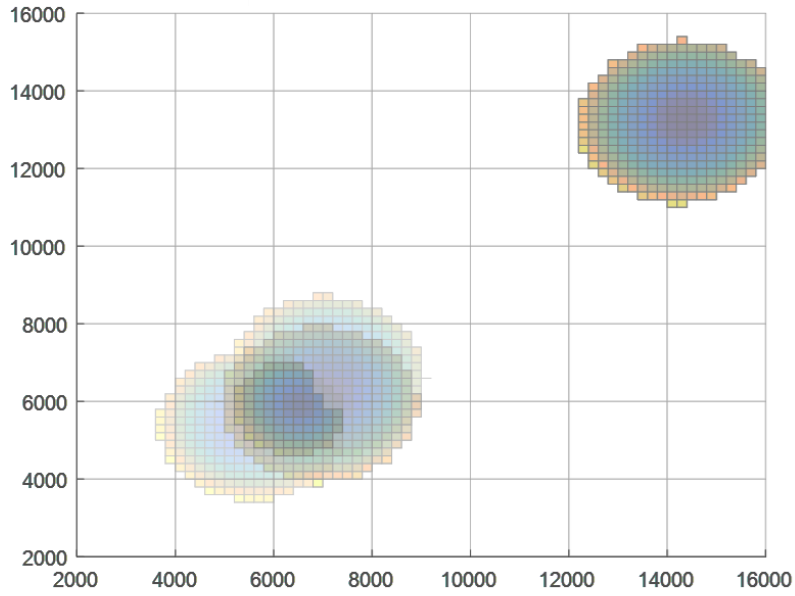

(f) Superposition of Economic Zones of Well #1, #2, #3, #4 and #29

Fig. 5.3 Example of Economic Zone ($cst_{site} = 500, cst_{SF1} = 20$)

5.2.3 **Flowchart of Full Process**

A flowchart of the full process is shown in Fig. 5.4 for a better understanding of our method. It should be noted that the most time-consuming part in the process is the 3D Dubins Curve method in Pre-Step 1 and main Step 1. Hence, we provide two choices for the workflow indicated by red lines and blue lines in the flowchart.

As the red lines indicate, if the grid resolution in Pre-Step 1 is fine enough, we can safely use the information calculated based on the grid values to save some computational time in main Step 1 by avoiding doing 3D Dubins Curve method to calculate the accurate information of useful clusters; otherwise, as the blue lines indicate, we must use the 3D Dubins Curve method again to refine the information of useful clusters. You may have doubt that the calculation based on grid values will not provide the global optimal solution. Indeed, if the grid is coarse, it may not even provide the optimal layout, as shown in Table. 5-8. But once the grid is fine, the error becomes small enough to become acceptable, as shown in Table. 5-9. The strategy for the grid resolution is further discussed in Section 5.4. In Step 2, feed the information of useful clusters into the BLP method to find out the optimal clusters and the corresponding minimum cost. With the optimal clusters obtained, we can gather the information with some basic calculations to get the final solution in Step 3.

5.3 Case Study

The data used in Lillevik’s work [58] is given in the Appendix V. The Dataset 1 is an intentionally forged dataset where all the completion intervals are horizontal and located at the same depth. The Dataset 2 is real field data. In this Section, we just use the Dataset 2. Dataset 1 will be used for further discussion in the next Section.

For comparison, we fully adopt Lillevik’s parameters: depth of kick off point is 500 m, i.e., $Pz_{1,i} = -500$; the maximum allowed turning rate is 3°/30 m. As Lillevik’s aim is the minimum total length of all wells, therefore we set the cost function of well trajectory to be the trajectory length, i.e., $cst_{Traj} = cstC\left(Lc\right) + cstS\left(Ls, \theta\right) = Lc + Ls$. Lillevik’s work cannot take other factors into consideration, but ours can involve the site preparation cost and subsea facility cost. Even though the objectives are different, we can still have a comparison on the total length of the wells. As for the other user-defined costs, we will manipulate them in the following cases to see how they affect the optimal field layout.

The cost and the length calculated by our method in the following case study are all based on the discretized/grid values of the optimal cost distribution, i.e., the output of Pre-Step 1 indicated by the red lines in Fig. 5.4, with the grid resolution of 50mx50m. Beside, set $factor = 1.2$ in Equation (5-4) for the case study here. The values for user-defined cost are dimensionless corresponding to the length of the wellbore trajectory. Practically, you can simply take in the real cost functions for wellbore trajectories and the real values for cost items.

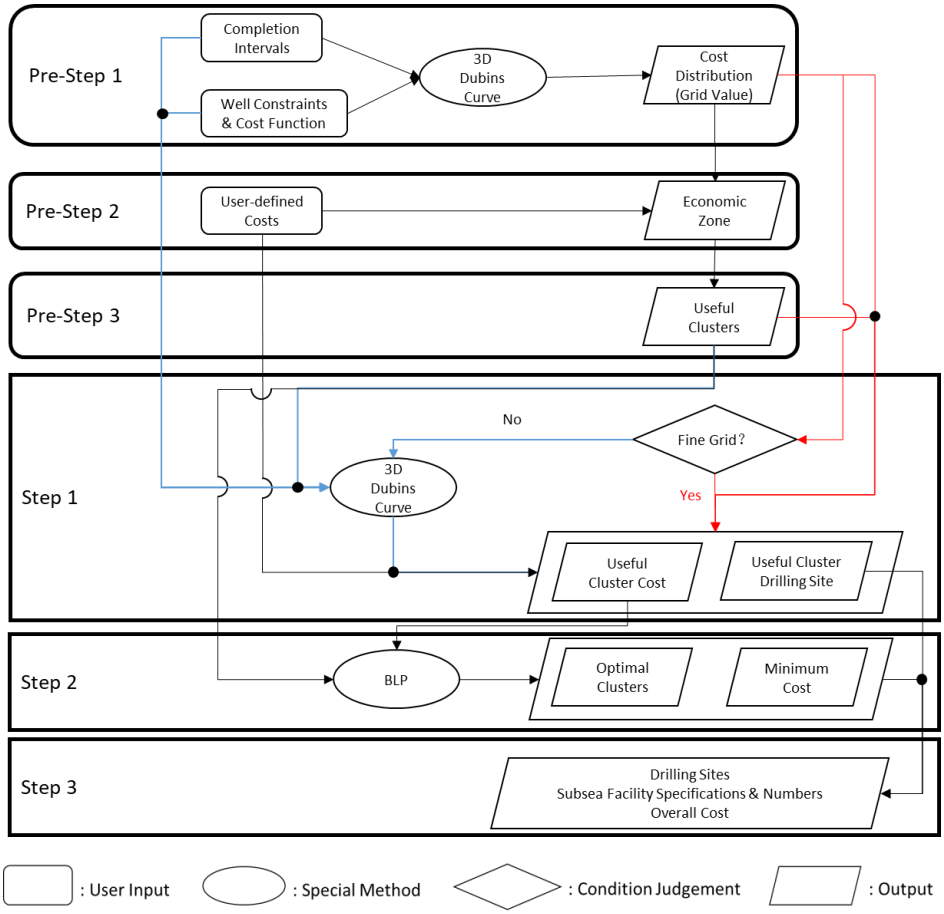

Fig. 5.4 Flowchart of Full Process

5.3.1 **Case 1: satellite only**

We intentionally make a case where $cst_{site} = 0$, $cst_{SF,i} = 0, i \in \{1,2,4,6\}$. This case guarantees the optimal layout to be all satellite wells. Because $cst_{site} = 0$ means that we

can move the rig and prepare the drilling site arbitrarily without considering the cost; $cst_{SF,i} = 0$ means that the template does not save any money. This case can be a validation for the correctness of our optimization method. Results are shown in Table. 5-1. The drilling site position for each completion interval is shown in Appendix VI. Because all the wells are satellite, the accurate value of each site position obtained in Pre-Step 1 is also provided.

$\sum_{j=1}^{N} \gamma_j \cdot cstT_j$ is the result from Equation (5-3), which counts the total cost from the kickoff point to the start point of completion interval for all wells. The overall cost need add the total cost above the kickoff point for all wells which is 15500 and the total cost of the completion intervals for all wells is 20271.03. As we set $cst_{site} = 0$ and $cst_{SF,i} = 0$, the overall cost is just the total length of all wells.

Table. 5-1 Result for the Layout of Satellites Only

Method	User-defined Cost	Layout	$\sum_{j=1}^{N} \gamma_j \cdot cstT_j$	Overall Cost	Total Length of all Wellbores (m)
Lillevik's		Satellite Only			147.95×10^3
Ours	$cst_{site} = 0$ $cst_{SF,1} = 0$ $cst_{SF,2} = 0$ $cst_{SF,4} = 0$ $cst_{SF,6} = 0$	Satellite Only	112180.80	147951.83	147.95×10^3

5.3.2 **Case 2: satellite and 2-slot mixed**

Now consider there are only satellite wells and 2-slot templates. We simply delete the parameters related with 4-slot and 6-slot in Equation (5-3). Change the user-defined cost, and we will see different optimal layout generated by our method. Results are shown in Table. 5-2. By comparing the total length, we can see that Lillevik's work is just a suboptimal solution. Comparing the optimal layouts of the Cases, it tells that the optimal layout tends to have more satellites if the cost of site preparation is less, which matches with the engineering intuition. Fig. 5.5 and Fig. 5.6 show the optimal layout for Case 2.1 and Case 2.2, respectively. The magenta line indicates the completion interval, the black line indicates the straight section, the blue line or the red line indicates the curved section. The drilling site position for each completion interval is shown in Appendix VI. The number of useful clusters is shown in Table. 5-3.

It should be noted that, the overall cost includes the site cost and the subsea facility cost which are now not 0, we need deduct the cost of rigs and wellheads from the overall cost to obtain the total length of all wellbores. Take the Case 2.1 for example, the optimal layout tells there are 14 2-slot templates and 3 satellites, incurring the site cost 14+3=17 times, hence the difference between the value of overall cost and the value of the total length of all wellbores is $17cst_{site}+14cst_{SF,2}+3cst_{SF,1}=5580$.

Table. 5-2 Result for the Layout of Satellites and 2-slot Mixed

Method	User-defined Cost	Layout	$\sum_{j=1}^{N}\gamma_j \cdot cstT_j$	Overall Cost	Total Length of all Wellbores (m)
Lillevik's [58]		{2,5} {3,11} {4,12} {6,8} {7,19} {13,20} {14,18} {15,27} {21,22} {24,30} {25,31} {26,28}; {1} {9} {10} {16} {17} {23} {29}			155.99×10^3
Ours (Case 2.1)	$cst_{site}=300$ $cst_{SF,1}=20$ $cst_{SF,2}=30$	{1,4} {2,11} {3,5} {6,19} {7,8} {9,10} {13,14} {16,17} {18,20} {21,22} {23,24} {25,27} {26,30} {28,31}; {12} {15} {29}	118794.29	154565.32	148.99×10^3
Ours (Case 2.2)	$cst_{site}=100$ $cst_{SF,1}=20$ $cst_{SF,2}=30$	{1,4} {2,11} {3,5} {7,8} {13,14} {16,20} {21,22} {25,27} {26,30} {28,31}; {6} {9} {10} {12} {15} {17} {18} {19} {23} {24} {29}	115286.94	151057.97	148.44×10^3

Table. 5-3 Number of Useful Clusters (Satellites and 2-slot Mixed)

	Number of Useful Clusters of Size m	
	$m=2$	$m=1$
Case 2.1	133	31
Case 2.2	58	

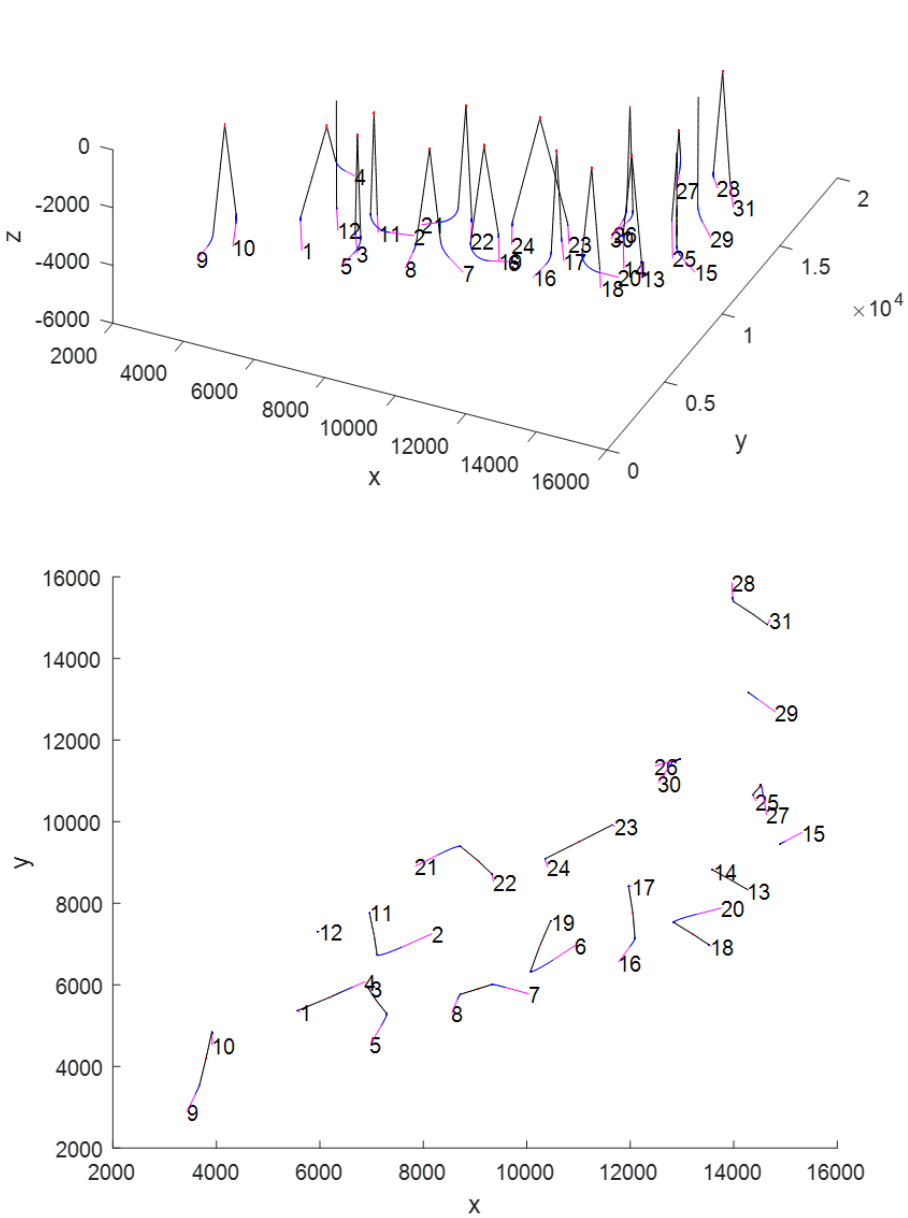

Fig. 5.5 Optimal Layout for Case 2.1

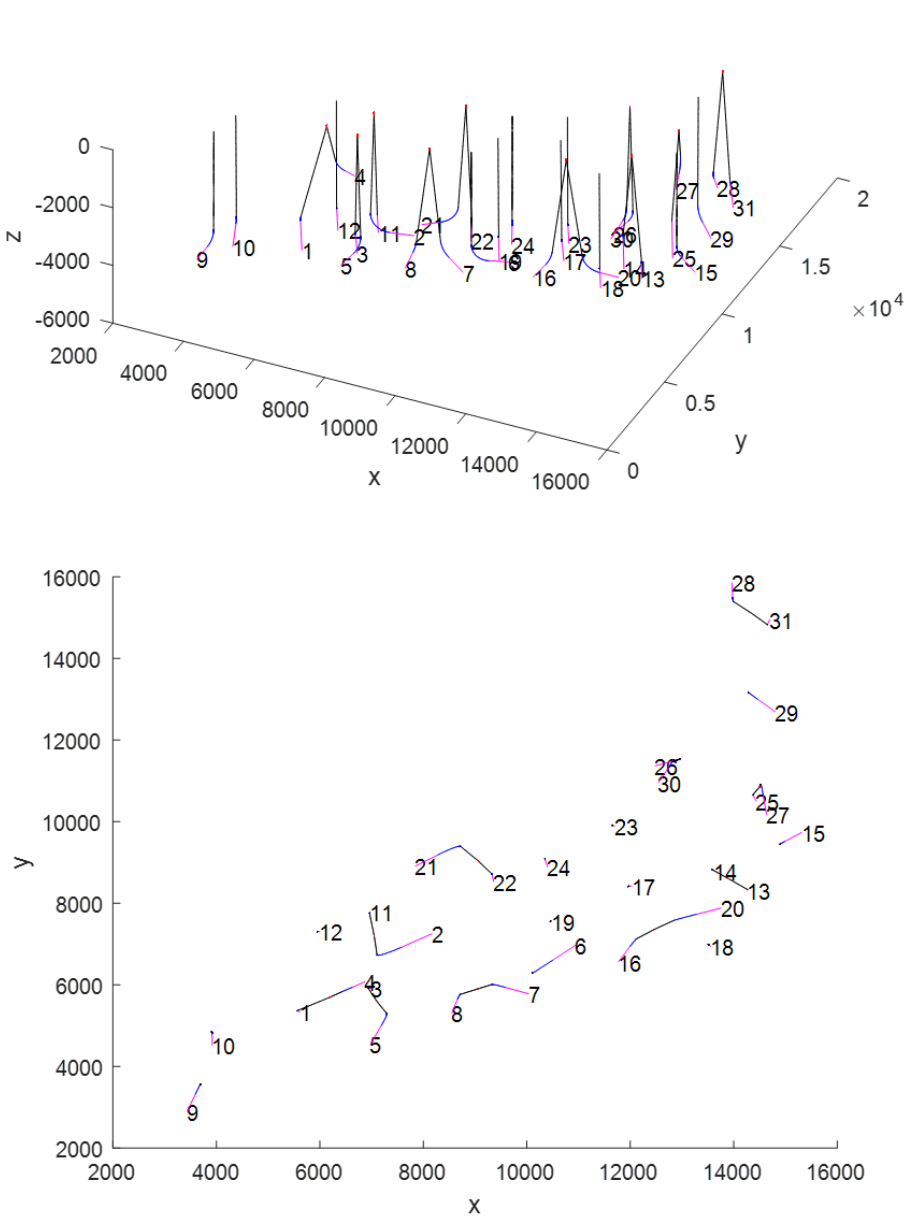

Fig. 5.6 Optimal Layout for Case 2.2

5.3.3 **Case 3: satellite, 2-slot and 4-slot mixed**

Lillevik's work did not provide the layout with more than 2 types of manifolds. For comparison, we set a dummy value for cst_{WH2} to find the optimal layout of satellite and 4-slot mixed. Change the user-defined cost, and we will see different optimal layout generated by our method. Results are shown in Table. 5-4. Fig. 5.7, Fig. 5.8 and Fig. 5.9 show the optimal layout for Case 3.1, Case 3.2, and Case 3.3, respectively. The drilling site position for each completion interval is shown in Appendix VI. The number of useful clusters is show in Table. 5-5.

Table. 5-4 Result for the Layout of Satellite, 2-slot and 4-slot Mixed

Method	User-defined Cost	Layout	$\sum_{j=1}^{N} \gamma_j \cdot cstT_j$	Overall Cost	Total Length of all Wellbores (m)
Lillevik's [58]		{1,4,11,12} {2,3,5,8} {6,7,22,24} {13,16,17,19} {14,15,18,20} {25,26,27,30}; {9} {10} {21} {23} {28} {29} {31}			157.47×10^3
Ours (Case 3.1)	$cst_{site} = 300$ $cst_{SF,1} = 20$ $cst_{SF,2} = 1e6$ $cst_{SF,4} = 50$	{1,2,3,4} {5,6,7,8} {16,17,18,20} {19,21,22,24} {25,26,27,30}; {9} {10} {11} {12} {13} {14} {15} {23} {28} {29} {31}	119999.13	155770.16	150.50×10^3
Ours (Case 3.2)	$cst_{site} = 300$ $cst_{SF,1} = 20$ $cst_{SF,2} = 30$ $cst_{SF,4} = 50$	{2,3,4,5} {16,17,18,20}; {6,19} {7,8} {9,10} {11,12} {13,14} {21,22} {23,24} {25,27} {26,30} {28,31}; {1} {15} {29}	118542.95	154313.98	149.35×10^3
Ours (Case 3.3)	$cst_{site} = 100$ $cst_{SF,1} = 20$ $cst_{SF,2} = 30$ $cst_{SF,4} = 50$	{1,4} {2,11} {3,5} {7,8} {13,14} {16,20} {21,22} {25,27} {26,30} {28,31}; {6} {9} {10} {12} {15} {17} {18} {19} {23} {24} {29}	115286.94	151057.97	148.44×10^3

Table. 5-5 Number of Useful Clusters (Satellites, 2-slot and 4-slot Mixed)

	Number of Useful Clusters of Size k		
	$k = 4$	$k = 2$	$k = 1$
Case 3.1	213	133	31
Case 3.2			
Case 3.3	6	58	

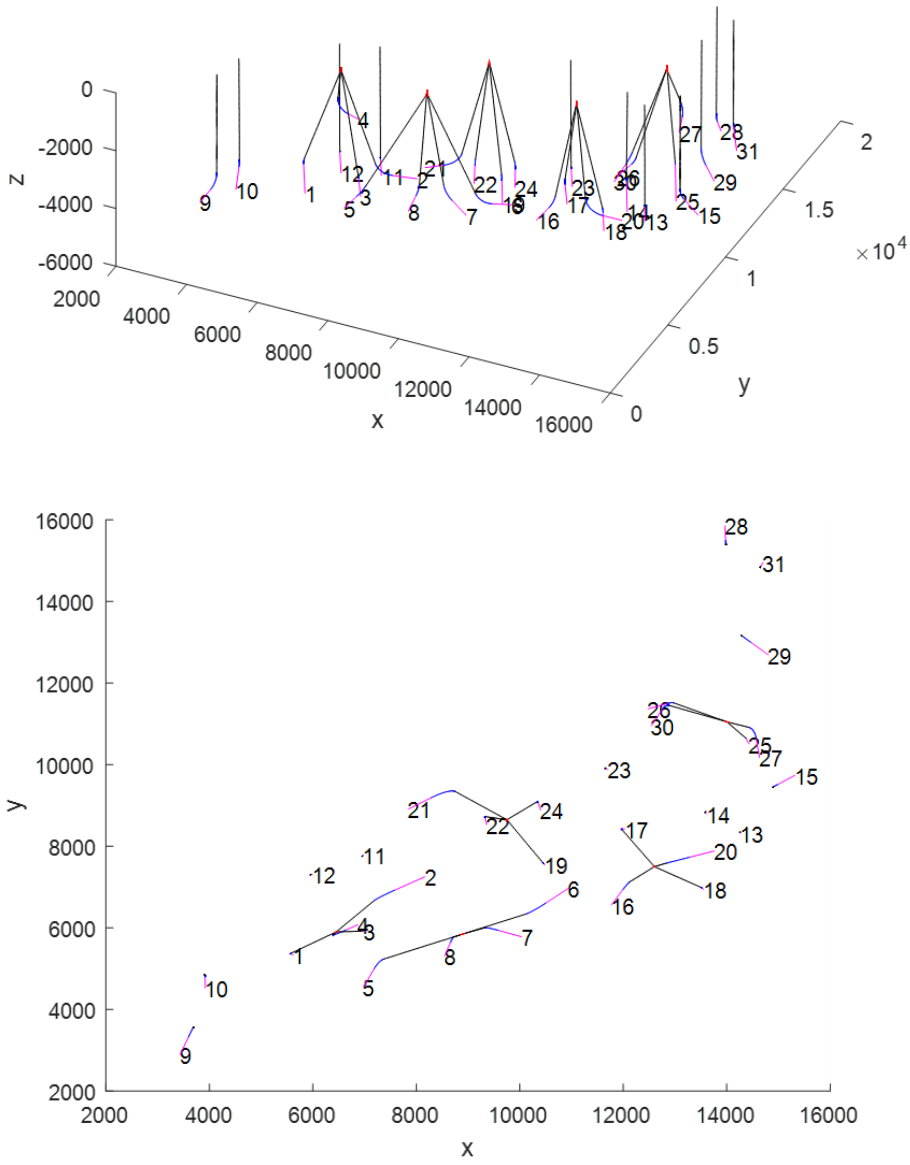

Fig. 5.7 Optimal Layout for Case 3.1

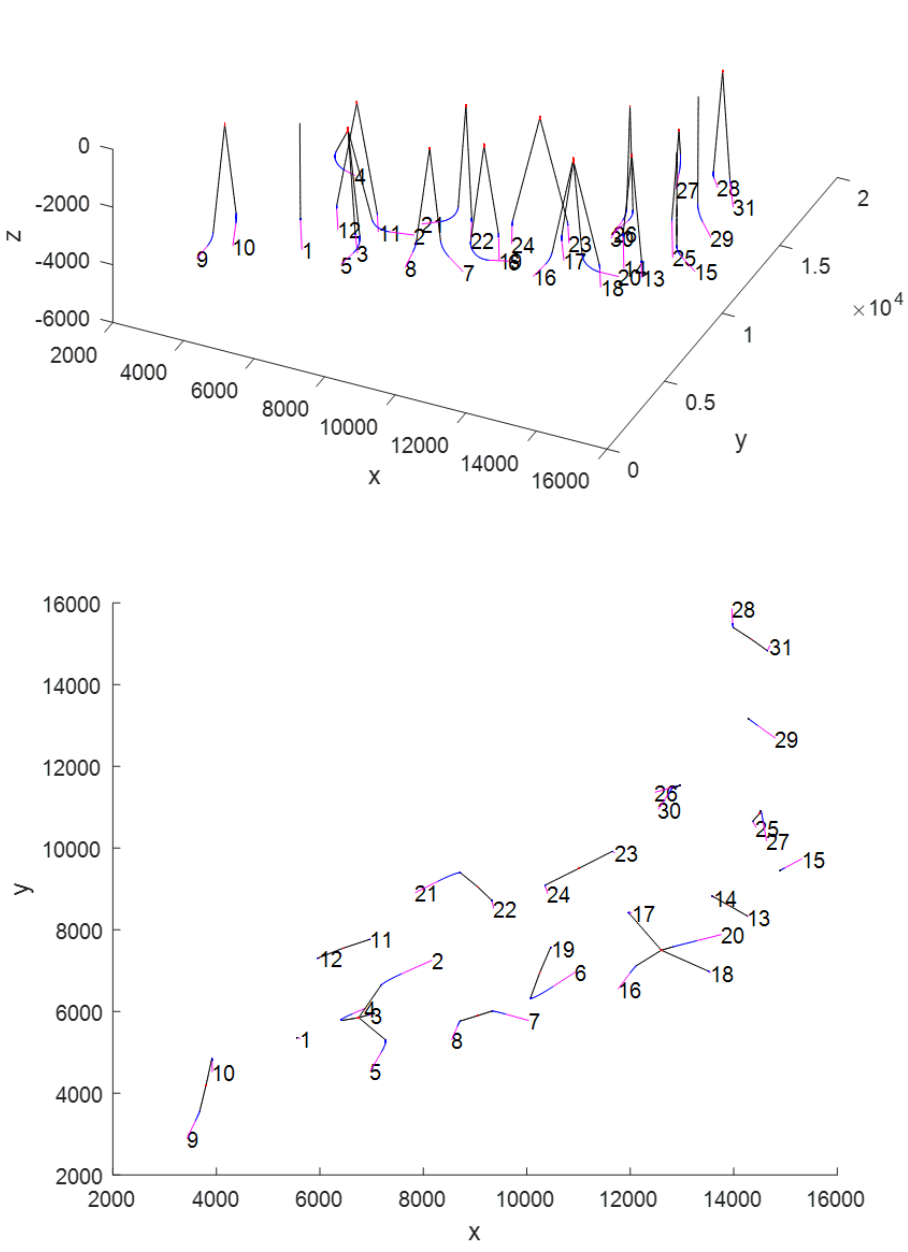

Fig. 5.8 Optimal Layout for Case 3.2

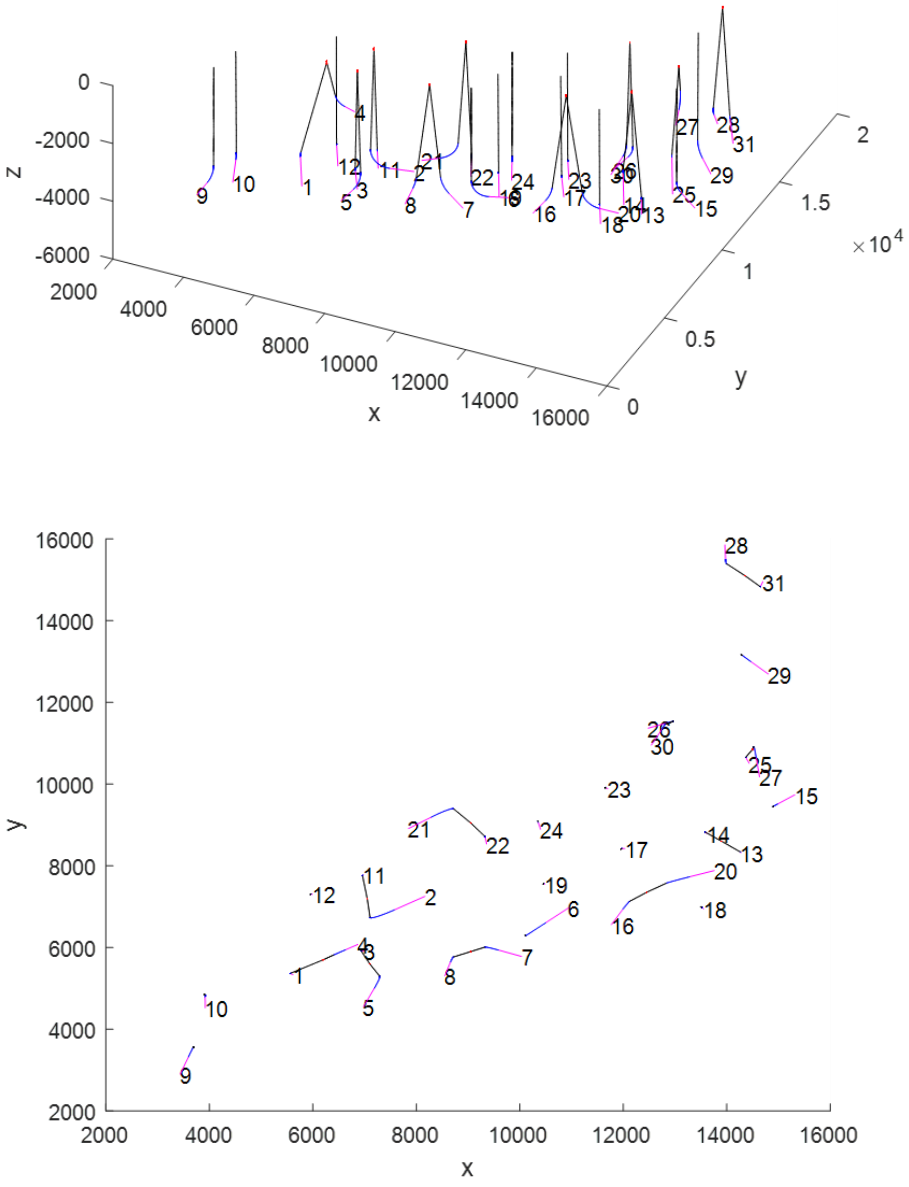

Fig. 5.9 Optimal Layout for Case 3.3

5.3.4 **Case 4: vacant slot allowed**

The cases above have demonstrated the feasibility and advantage of our method, especially comparing to the existing work, and it will be quite meaningless to show more cases of the layout of mixing satellite, 2-slot, 4-slot, 6-slot, etc.

Practically, the *m*-slot template may not be fully occupied, for example, one 4-slot template only connects 3 wells with 1 slot left vacant. To deal with such a scenario, we can simply add the cluster of size 3 into Equation (5-3) and set $cst_{SF,3} = cst_{SF,4}$. Take the Case 3.2 for comparison. Results are shown in Table. 5-4. Compared to the Case 3.2, we can see that with vacant slot allowed, the overall cost is reduced because of less clusters of small sizes, while the total length of all wellbores is increased.

Table. 5-6 Result for the Layout of with Vacant Slot Allowed

	User-defined Cost	Layout	$\sum_{j=1}^{N} \gamma_j \cdot cstT_j$	Overall Cost	Total Length of all Wellbores (m)
Case 4	$cst_{site} = 300$ $cst_{SF,1} = 20$ $cst_{SF,2} = 30$ $cst_{SF,3} = 50$ $cst_{SF,4} = 50$	{1,3,4,5}; {2,11,12} {13,14,15} {16,18,20} {21,22,24}; {6,19} {7,8} {9,10} {17,23} {25,27} {26,30} {28,31}; {29}	118192.40	153963.43	149.58×10^3

Table. 5-7 Number of Useful Clusters (vacant slot allowed)

	Number of Useful Clusters of Size k			
	$k = 4$	$k = 3$	$k = 2$	$k = 1$
Case 4	213	237	133	31

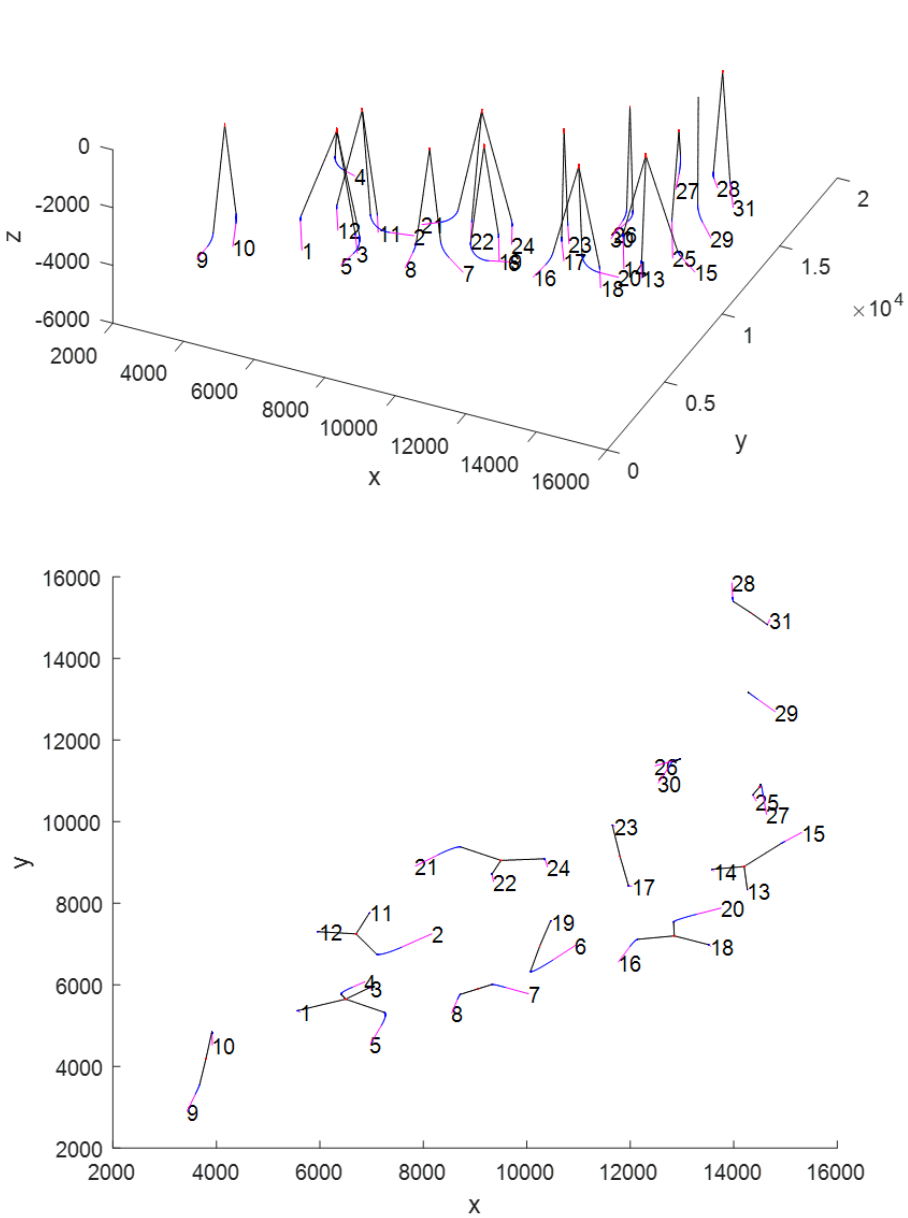

Fig. 5.10 Optimal Layout for Case 3.1

5.4 Further Discussion

5.4.1 Variable Water Depth

For simplicity of the Case Study above, we made the Basic Assumption 2 where the water depth is assumed to be constant across the field, resulting in the cost above kickoff point as an invariant for a given set of user-defined cost once the kickoff depth is fixed. However practically, the depth of the water can change over the lateral extent of the field, resulting in large difference in the cost above kickoff point, where the cost above kickoff point can no longer be treated as invariant. For such a scenario, the solution is quite easy: modify the Equation (5-2) to let the total cost of a cluster $cstT_j$ include the cost above the kickoff of the cluster.

5.4.2 Involving the Cost of Flowlines on Seabed

If we want to involve the cost of flowlines on seabed into the overall cost, we can firstly use the method introduced in this study to obtain the global optimal layout of wellheads, i.e., the wellheads' positions, which will then be used as the input for the BLP method introduced in Chapter 4 to obtain the global optimum for flowlines. This workflow cannot guarantee the global optimum for the overall cost because the cost of flowlines directly depends on the layout of wellheads, but not the layout of completion intervals. Nevertheless, as the cost for wellbores is much higher than the cost for flowlines, we can safely regard the sum of these two correlated global optimal results as an extremely good optimum which is very likely to be the global optimum.

Strictly, to ensure the global optimum, we should enumerate the layouts of wellheads from the minimum cost to a higher cost where the gap between the higher cost and the minimum cost is enough to cover the cost of flowlines.

5.4.3 Strategy for Grid Resolution

Table. 5-8 shows an example where the coarse resolution cannot obtain global optimal layout: for Dataset 1, set the cost of drilling site preparation and subsea facilities to be 0, then the layout result should be satellites only, just as the Case 1 for Dataset 2. However, the result based on the grid value with the resolution of 200m×200m turns out that there are two 2-slot templates in the optimal layout. Improving the resolution is the logical solution, but it takes much longer time for pre-process. For example, the pre-process time for the resolution of 50m×50m is 16 times that of the resolution of 200m×200m.

Table. 5-8 Coarse Resolution Fails to Obtain Global Optimal Layout

Resolution (m×m)	User-defined Cost	Layout	$\sum_{j=1}^{N} \gamma_j \cdot cstT_j$	Overall Cost	Total Length of all Wellbores (m)
200×200	$cst_{site} = 0$ $cst_{SF,1} = 0$ $cst_{SF,2} = 0$ $cst_{SF,4} = 0$ $cst_{SF,6} = 0$	{10,13} {11,21} Satellite for the others	69860.33	112394.39	112394.39
50×50		Satellite only	69814.39	112348.44	112348.44

Alternatively, we can use the 3D Dubins Curve method to refine the information of useful clusters based on coarse grid values, i.e., to accurately calculate the optimal drilling site $P_{0,j}$ and trajectory cost $cst_{Traj,i}$ for each useful cluster of wells, and then obtain the $cstT_j$. Come back to the real field Dataset 2 and take the Case 3.3 for example. If we set a coarse grid in Pre-Step 1 and then use 3D Dubins Curve method in main Step 1, we will still get the accurate values. The results are shown in Table. 5-9 and Appendix VI. We can see that there is no difference in the optimal layout, and the difference in the cost value is so small that we can safely ignore it. The additional computational time for using 3D Dubins Curve in main Step 1 is around 77 seconds, conducted on an Intel Core i7-10750H CPU. The time of Pre-Step 1 under parallel computation of 4 workers is around 118 seconds for the resolution of 200m×200m and 1776 seconds for 50m×50m.

We can see that for the computation of a single case, it costs less time to use a coarse grid and then use 3D Dubins Curve method in main Step 1. However, do not forget that the result from Pre-Step 1 can be reused for other cases of different user-defined subsea facility costs and site preparation costs. We can imagine that if the coarse grid values cannot be used in main Step 1 and we must refine the information of useful clusters, then after several computations of different cases, the sum of the additional time we spend on main Step 1 in these different cases can easily exceeds the time saved by a coarse resolution for pre-process.

Therefore, the strategy for grid solution is as follows:

1. If every cost function is well defined, practically it means that we have confirmed the facility providers and service providers for the field development, and we just need to find the optimal solution for one case, then we shall use coarse grid in Pre-Step 1, followed by 3D Dubins Curve method in main Step 1.

2. Otherwise, use a moderately fine resolution, but no need to be extremely fine. Then only if we are not satisfied or have doubt in the results based on grid values, use 3D Dubins Curve method in main Step 1 to refine the information of useful clusters.

Table. 5-9 Comparison between Grid Value and Accurate Value for Case 3.3

Method	User-defined Cost	Layout	$\sum_{j=1}^{N} \gamma_j \cdot cstT_j$	Overall Cost	Total Length of all Wellbores (m)
Case 3.3 (50×50)	$cst_{site} = 100$ $cst_{SF,1} = 20$ $cst_{SF,2} = 30$ $cst_{SF,4} = 50$	{1,4} {2,11} {3,5} {7,8} {13,14} {16,20} {21,22} {25,27} {26,30} {28,31}; {6} {9} {10} {12} {15} {17} {18} {19} {23} {24} {29}	115286.94	151057.97	148437.96
Case 3.3 (200×200 & refinement by 3D Dubins method)		{1,4} {2,11} {3,5} {7,8} {13,14} {16,20} {21,22} {25,27} {26,30} {28,31}; {6} {9} {10} {12} {15} {17} {18} {19} {23} {24} {29}	115284.97	151056.00	148436.00

5.5 Summary

Based on the two methods introduced in Chapter 3 and Chapter 4, we build an efficient global-optimal method to deal with the location-allocation problem of drilling sites to optimize the subsea field layout with the aim of minimizing the overall field development cost. A flowchart which clearly shows the full process of our method is created. Case studies show how the cost items affect the optimal layout. The correctness and the flexibility of our method to solve the comprehensive and practical subfield optimization problems are well demonstrated. Besides, the strategy for grid resolution is also discussed. We are confidently expecting that significant amount of money can be saved by the global optimal solution provided by our method in the field development.

Chapter 6. Industrial Application

One of the SUBPRO industrial partners --- Equinor --- provided us some valuable real field data as shown in Appendix VII. The dataset provides the trajectories of 19 wells drilled from 4 templates or drilling sites. The target is to minimize the total wellbore length.

6.1 Preprocessing of the Given Data

From the given data, we can easily plot the trajectories as Fig. 6.1 shows. The positive Y direction is towards the north. The total length of all 19 wellbores is 91685m. There are three special wells --- #2d (#8), #2e (#9) and #3d (#13) --- which have three turns in their angle, as the red arrows indicate in Fig. 6.1.

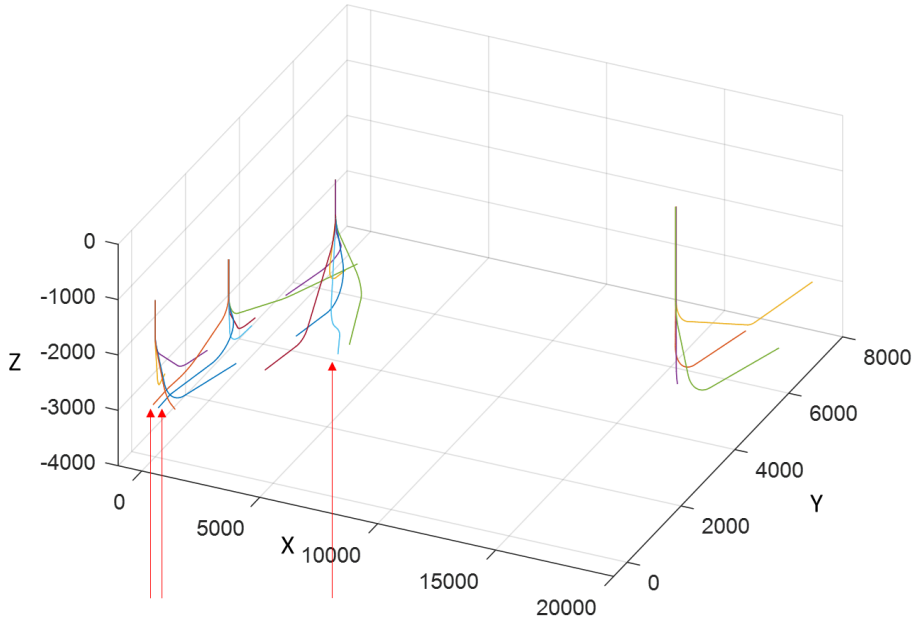

Fig. 6.1 Given Trajectories

For instance, zoom into the Well #3d, as shown in Fig. 6.2. Obviously, the engineers wanted to avoid something in the formation. However, the industrial partner did not provide us the formation details. For a fair comparison, we should eliminate the effect

these three special wells, otherwise, our 3D Dubins Curve method will definitely get much shorter length than the given data.

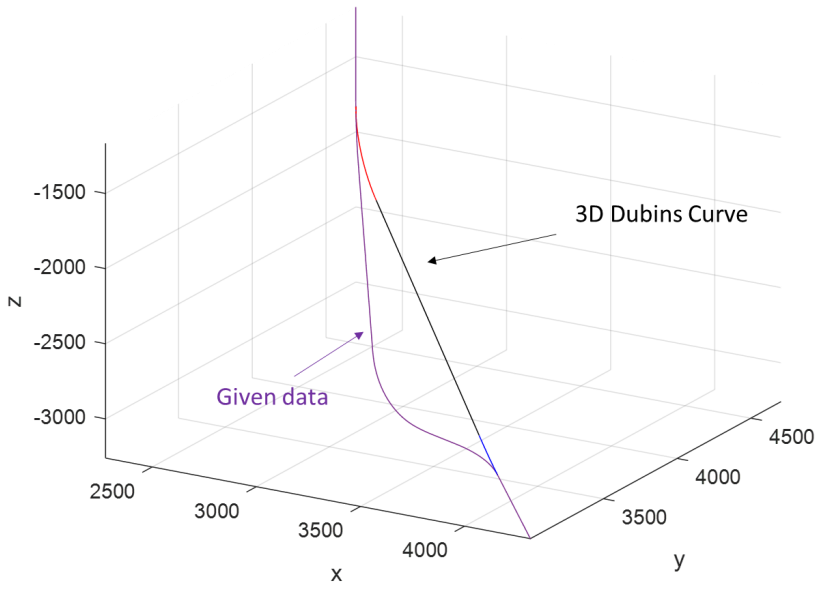

Fig. 6.2 Trajectory Comparison of the Well #3d

6.2 Results Comparison

6.2.1 **Same Allocation, Same Template Location**

Firstly, we use the same template location and same allocation as the given data and get the result as shown in Fig. 6.3. The wellbore length comparison is shown in Table. 6-1 where the three special wells are marked in red. We can see that except the three special wells, the wellbore length differences are very small. Actually, they are the same except some numerical errors caused by survey method in the given data. For example, the trajectory comparison of Well #5 which has the biggest difference is shown in Fig. 6.4, where (a) is the 3D view, (b) and (c) are the projected 2D view. We can clearly see that the given trajectory is making a sharper turn at the end of the build-up section, making the wellbore length a bit shorter than the 3D Dubins Curve which strictly fulfills the dogleg severity constraint. A sharper turn means the given trajectory exceeds the dogleg severity slightly. This comparison validates the correctness of our 3D Dubins Curve method and reveals that our method can mitigate the numerical error compared to the method used by Equinor.

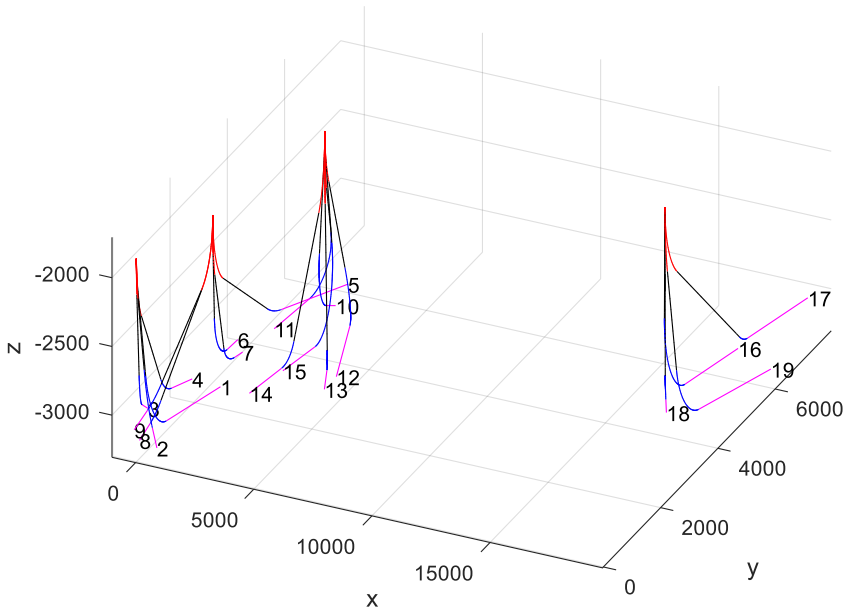

Fig. 6.3 Trajectories Based on 3D Dubins Curve Method

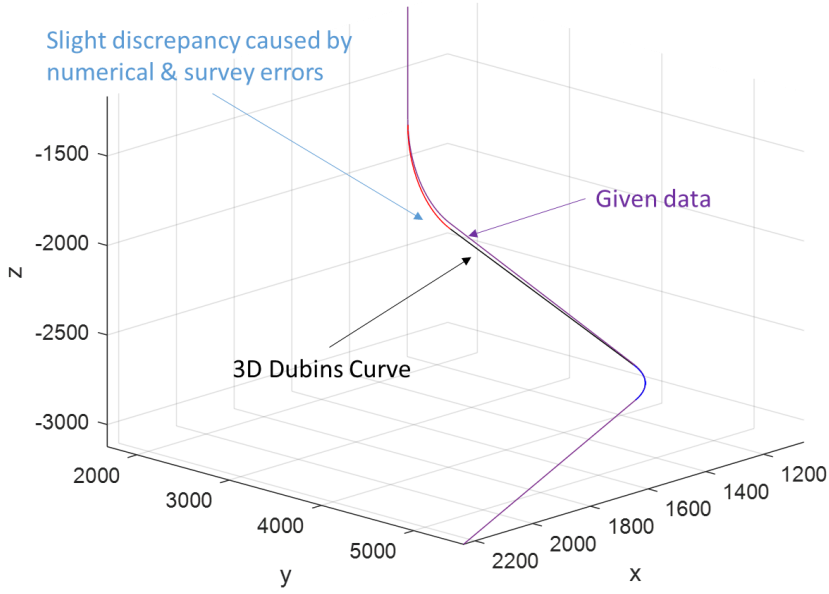

(a)

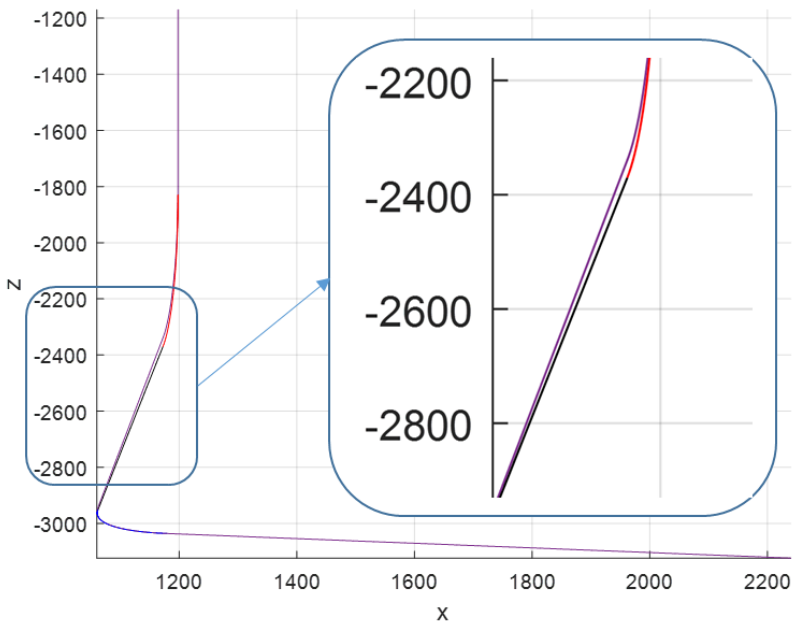

(b)

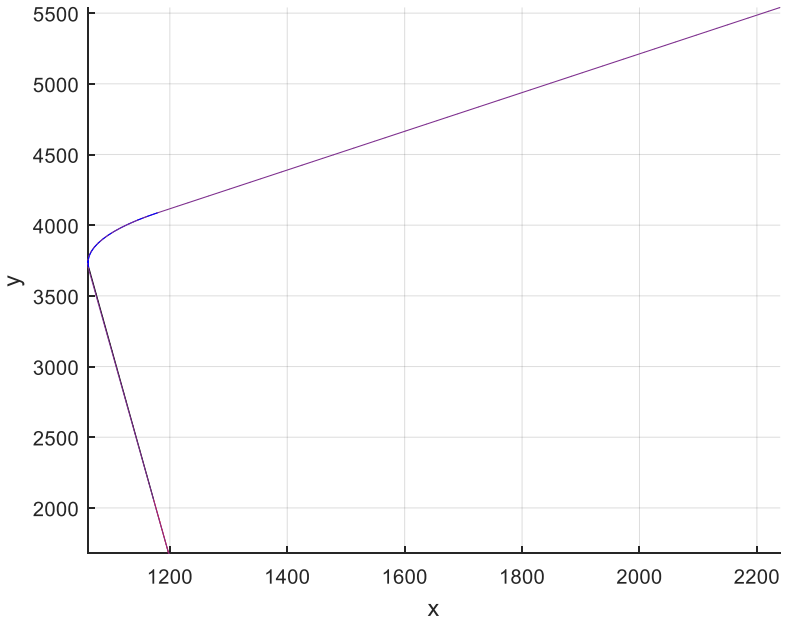

(c)

Fig. 6.4 Trajectory Comparison of Well #5

Table. 6-1 Wellbore Length (m) Comparison

Index	Given data	Same allocation & location		Same allocation & optimized location		
		Calculated	Difference	Calculated	Difference	Difference per Template(cluster)
#1	4958.99	4960.976	1.99	4958.658	-0.33	-167.98
#2	3471.67	3475.495	3.82	3505.883	34.21	
#3	4147.22	4150.76	3.54	4113.395	-33.82	
#4	4553.71	4566.191	12.48	4385.672	-168.04	
#5	6483.78	6503.577	19.80	6370.956	-112.82	-1868.42
#6	3789.73	3793.807	4.08	3719.092	-70.64	
#7	4588.19	4601.823	13.63	4154.734	-433.46	
#8	5143.43	4370.384	-773.05	4236.991	-906.44	
#9	4647.63	4500.181	-147.45	4302.567	-345.06	
#10	3922.29	3923.924	1.63	4098.363	176.07	-393.10
#11	5036.6	5048.193	11.59	5331.111	294.51	
#12	5452.51	5459.323	6.81	5330.923	-121.59	
#13	5260	5063.407	-196.59	4773.403	-486.60	
#14	5372.82	5390.081	17.26	5176.495	-196.33	
#15	4597.01	4598.772	1.76	4537.837	-59.17	
#16	4889.86	4890.044	0.18	4984.867	95.01	-232.45
#17	6219.7	6233.208	13.51	6020.806	-198.89	
#18	3199.63	3199.741	0.11	3262.837	63.21	
#19	5950.18	5952.154	1.97	5758.408	-191.77	

6.2.2 **Same Allocation, Optimized Template Location**

If we use the same allocation but with template location optimized, the result is shown in Table. 6-1 and Table. 6-2. The optimized template position makes some wellbores longer, as the blue color indicates in Table. 6-1, but it guarantees the total length of all wellbores connected to the same template to be minimum.

Table. 6-2 Comparison of Template Location

Template	Given Data		Optimized Location	
	North	East	North	East
#1	0	0	277	72
#2	1678	1198	1919	420
#3	4702	2276	4558	2623
#4	4246	17222	4361	17601

6.2.3 **Arbitrary User-defined Costs and Constraints**

Unfortunately, Equinor cannot provide the cost items or functions, therefore we cannot tell if their allocation is the economically global optimum. But we demonstrated the power of handling various user-defined costs and constraints, which is very similar to the Case Study in Section 5.3. Table. 6-3 and Fig. 6.5 show some cases: from case (a) to (b), we can see the effect of cst_{site} on the optimal layout; from case (b) to (c), we can see how the constraint on the number of templates affects the optimal layout; case (d) and (e) show how we can manipulate the user-defined cost or/and constraints to get the same allocation as the given one.

Table. 6-3 Examples of Different User-defined Costs and Constraints

Case	User-defined Costs		User-defined Constraints	Optimal Layout Allocation
	Subsea Facility	Drilling Site		
(a)	$cst_{SF,1} = 20$ $cst_{SF,2} = 70$ $cst_{SF,3} = 70$ $cst_{SF,4} = 70$ $cst_{SF,5} = 70$ $cst_{SF,6} = 70$	$cst_{site} = 500$		[1,2,3] [4,8,9] [10,12,15] [16,18,19]; [6,7] [13,14]; [5] [11] [17]
(b)		$cst_{site} = 1000$		[4,6,8,9] [10,11,12,15]; [1,2,3] [16,18,19]; [5,7] [13,14]; [17]
(c)		$cst_{site} = 1000$	Number of templates ≤ 5	[10,11,12,13,14,15]; [4,6,8,9] [16,17,18,19]; [1,2,3]; [5,7]
(d)		$cst_{site} = 1000$	Number of templates $= 4$	[10,11,12,13,14,15]; [5,6,7,8,9]; [1,2,3,4] [16,17,18,19] (Given Allocation)
(e)		$cst_{site} = 2500$		

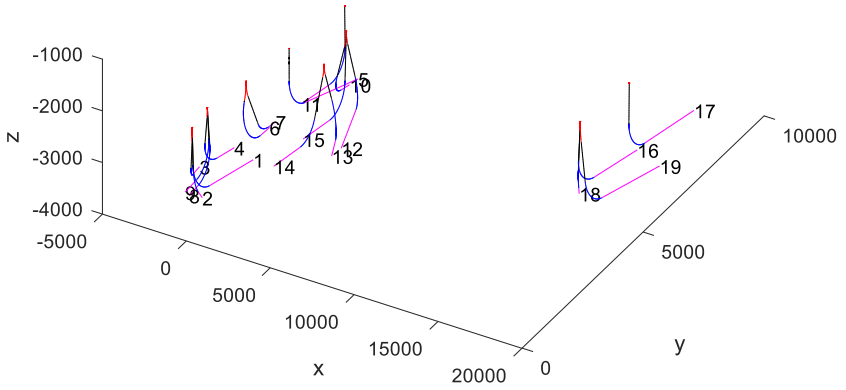
-1000
-2000
-3000
-4000
z
-5000
0
5000
10000
15000
20000
x
0
5000
10000
y
0
1
2
3
4
5
6
7
8
9
10
11
12
13
14
15
16
17
18
19

(a)

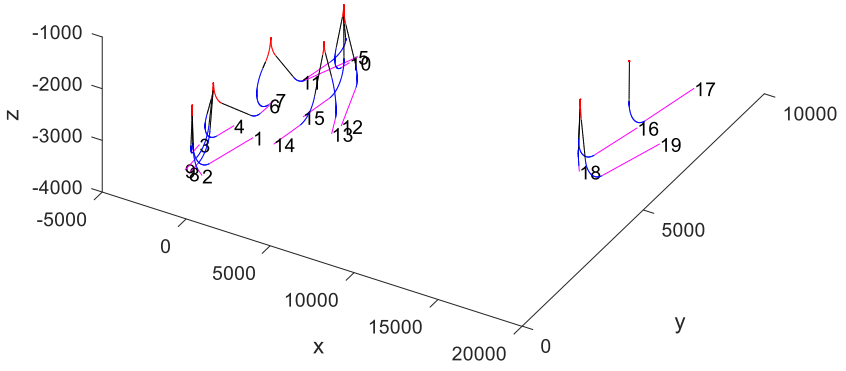
-1000
-2000
-3000
-4000
z
-5000
0
5000
10000
15000
20000
x
0
5000
10000
y
0
1
2
3
4
5
6
7
8
9
10
11
12
13
14
15
16
17
18
19

(b)

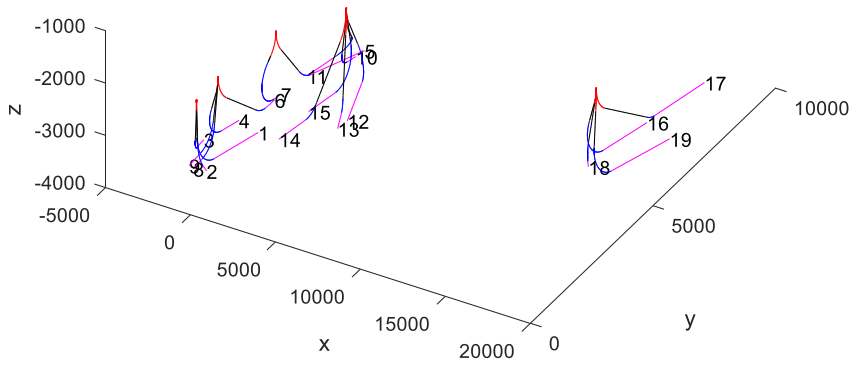

(c)

Fig. 6.5 Optimal Layout of Different User-defined Costs and Constraints

6.3 Summary

This chapter shows the real field data test provided by Equinor. This test is a solid validation of our method. Besides, we accidentally find our method can also mitigate the numerical errors in the trajectory design compared to the current method used by Equinor. Even though limited by the available data, the most lucrative part --- BLP method for optimal allocation --- is yet to be compared, we have demonstrated the flexibility of our method in handling user-defined costs and constraints. The Equinor engineer was very impressed that our method could get the results --- which cost them two weeks --- within just a coffee break!

Chapter 7. Conclusion and Suggestion for Future Work

This study has successfully built an efficient systematic method to optimize the subsea field layout with the aim of minimizing the overall field development cost. The complex optimization problem has been divided into 3 parts and conquered one by one:

Based on the CSC family of 2D Dubins Curve, we have proposed the 3D Dubins Curve for well trajectory design. As for the location-allocation problem, we have proposed a BLP method which is far more efficient than the conventional MINLP method or ILP method to get the global optimum. At last, we have systematically combined these two methods to solve the complex subsea field layout optimization problem.

Abundant case studies and a real field test provided by Equinor have demonstrated the big advantage of our method in both accuracy and efficiency.

As for the future work, we suggest exploring the application of the 3D Dubins Curve method in complex underground formations. The BLP method for the location-allocation problem in continuous space should have a much wider application in more disciplines. Our systematic method for subsea field layout optimization method will be developed into an industrial software to benefit the petroleum industry better. For a better application of our method in the petroleum industry, we will also explore a better way to help users build the user-defined cost functions based on the users' available cost data.

Reference

[1] K. Skaugset, "Subsea Cost Reduction," OG21, April 2015. Available on 2019/2/1. https://www.og21.no/contentassets/f826df43db324d79b148a14cfcf912c4/tta4-subsea-cost-report.pdf

[2] M. Devine and W. Lesso, "Models for the minimum cost development of offshore oil fields," *Management Science,* vol. 18, pp. B-378-B-387, 1972. https://doi.org/10.1287/mnsc.18.8.B378

[3] L. Frair and M. Devine, "Economic Optimization of Offshore Petroleum Development," *Management Science,* vol. 21, pp. 1370-1379, 1975. https://doi.org/10.1287/mnsc.21.12.1370

[4] S. Dogru, "Selection of Optimal Platform Locations," *SPE Drilling Engineering,* vol. 2, pp. 382-386, 1987. https://doi.org/10.2118/10754-PA

[5] P. Hansen, E. de Luna Pedrosa Filho, and C. Carneiro Ribeiro, "Location and sizing of offshore platforms for oil exploration," *European Journal of Operational Research,* vol. 58, pp. 202-214, 1992. https://doi.org/10.1016/0377-2217(92)90207-P

[6] J. C. Garcia-Diaz, R. Startzman, and G. L. Hogg, "A New Methodology for Minimizing Investment in the Development of Offshore Fields," *SPE Production & Facilities,* vol. 11, pp. 22-29, 1996. https://doi.org/10.2118/26018-PA

[7] R. R. Iyer, I. E. Grossmann, S. Vasantharajan, and A. S. Cullick, "Optimal Planning and Scheduling of Offshore Oil Field Infrastructure Investment and Operations," *Industrial & Engineering Chemistry Research,* vol. 37, pp. 1380-1397, 1998. https://doi.org/10.1021/ie970532x

[8] V. Goel and I. E. Grossmann, "A stochastic programming approach to planning of offshore gas field developments under uncertainty in reserves," *Computers & Chemical Engineering,* vol. 28, pp. 1409-1429, 2004. https://doi.org/10.1016/j.compchemeng.2003.10.005

[9] M. S. Tavallali, I. A. Karimi, A. Halim, D. Baxendale, and K. M. Teo, "Well Placement, Infrastructure Design, Facility Allocation, and Production Planning in Multireservoir Oil Fields with Surface Facility Networks," *Industrial & Engineering Chemistry Research,* vol. 53, pp. 11033-11049, 2014. https://doi.org/10.1021/ie403574e

[10] Y. Wang, S. F. Estefen, M. I. Lourenço, and C. Hong, "Optimal design and scheduling for offshore oil-field development," *Computers & Chemical Engineering,* vol. 123, pp. 300-316, 2019. https://doi.org/10.1016/j.compchemeng.2019.01.005

[11] C. Hong, "Optimization of subsea arrangement for production system," PhD Dissertation, Universidade Federal do Rio de Janeiro, 2019. Available on 2019/8/2. https://pantheon.ufrj.br/bitstream/11422/13655/1/ChengHong-min.pdf

[12] M. C. A. Carvalho and J. M. Pinto, "An MILP model and solution technique for the planning of infrastructure in offshore oilfields," *Journal of Petroleum Science and Engineering,* vol. 51, pp. 97-110, 2006. https://doi.org/10.1016/j.petrol.2005.11.012

[13] N. P. Directorate. *Investments and operating costs*. Available on 2021/8/23. https://www.norskpetroleum.no/en/economy/investments-operating-costs/

[14] H. Liu, T. B. Gjersvik, and A. Faanes, "Subsea field layout optimization (Part I) – directional well trajectory planning based on 3D Dubins Curve," *Journal of Petroleum Science and Engineering,* p. 109450, 2021. https://doi.org/10.1016/j.petrol.2021.109450

[15] H. Liu, T. B. Gjersvik, and A. Faanes, "Subsea field layout optimization (part II)– the location-allocation problem of manifolds," *Journal of Petroleum Science and Engineering,* vol. 208, p. 109273, 2022. https://doi.org/10.1016/j.petrol.2021.109273
[16] H. Liu, T. B. Gjersvik, and A. Faanes, "Subsea field layout optimization (part III) -- - the location-allocation problem of drilling sites," *Journal of Petroleum Science and Engineering,* p. 109336, 2021. https://doi.org/10.1016/j.petrol.2021.109336
[17] D. S. Amorim Jr., O. L. A. Santos, and R. C. d. Azevedo, "A statistical solution for cost estimation in oil well drilling," *REM - International Engineering Journal,* vol. 72, pp. 675-683, 2019. https://doi.org/10.1590/0370-44672018720183
[18] H. L. Taylor and M. C. Mason, "A Systematic Approach to Well Surveying Calculations," *Society of Petroleum Engineers Journal,* vol. 12, pp. 474-488, 1972. https://doi.org/10.2118/3362-PA
[19] W. A. Zaremba, "Directional Survey by the Circular Arc Method," *Society of Petroleum Engineers Journal,* vol. 13, pp. 5-11, 1973. https://doi.org/10.2118/3664-PA
[20] J. Shengzong, W. Xilu, C. Limin, and L. Kunfang, "A New Method for Designing 3D Trajectory in Sidetracking Horizontal Wells Under Multi-constraints," presented at the SPE Asia Pacific Improved Oil Recovery Conference, Kuala Lumpur, Malaysia, 1999. https://doi.org/10.2118/57282-MS
[21] S. J. Sawaryn and J. L. Thorogood, "A Compendium of Directional Calculations Based on the Minimum Curvature Method," *SPE Drilling & Completion,* vol. 20, pp. 24-36, 2005. https://doi.org/10.2118/84246-PA
[22] R. Samuel, "A New Well-Path Design Using Clothoid Spiral (Curvature Bridging) for Ultra-Extended-Reach Drilling," *SPE Drilling & Completion,* vol. 25, pp. 363-371, 2010. https://doi.org/10.2118/119459-PA
[23] R. R. Ilyasov, L. A. Svechnikov, M. R. Karimov, M. Z. Kravets, A. N. Solodov, and I. O. Porolo, "Automation of Optimal Well Trajectory Calculations," presented at the SPE Russian Oil and Gas Exploration & Production Technical Conference and Exhibition, Moscow, Russia, 2014. https://doi.org/10.2118/171326-MS
[24] Z. Liu and R. Samuel, "Wellbore Trajectory Control using Minimum Well Profile Energy Criterion for Drilling Automation," presented at the SPE Annual Technical Conference and Exhibition, Amsterdam, The Netherlands, 2014. https://doi.org/10.2118/170861-MS
[25] P. Yi and R. Samuel, "Downhole Automation Using Spline, Catenary, and Clothoid Curves Based On Minimum Wellpath Energy," presented at the SPE/IADC Drilling Conference and Exhibition, London, England, UK, 2015. https://doi.org/10.2118/173096-MS
[26] M. Mittal and R. Samuel, "3D Downhole Drilling Automation Based on Minimum Well Profile Energy," presented at the SPE Annual Technical Conference and Exhibition, Dubai, UAE, 2016. https://doi.org/10.2118/181381-MS
[27] Z. Wang, D. Gao, and J. Yang, "Design and Calculation of Complex Directional-Well Trajectories on the Basis of the Minimum-Curvature Method," *SPE Drilling & Completion,* vol. 34, pp. 173-188, 2019. https://doi.org/10.2118/194511-PA
[28] L. E. Dubins, "On curves of minimal length with a constraint on average curvature, and with prescribed initial and terminal positions and tangents," *American Journal of mathematics,* vol. 79, pp. 497-516, 1957. https://doi.org/10.2307/2372560

[29] H. H. Johnson, "An application of the maximum principle to the geometry of plane curves," in *Proceedings of the American Mathematical Society,* vol. 44, pp. 432-435, 1974. https://doi.org/10.2307/2040451
[30] H. J. Sussmann, "Shortest 3-dimensional paths with a prescribed curvature bound," *Proceedings of 1995 34th IEEE Conference on Decision and Control*, vol.4, pp. 3306-3312, 1995. https://doi.org/10.1109/CDC.1995.478997
[31] V. S. Patsko and V. L. Turova, "From Dubins' car to Reeds and Shepp's mobile robot," *Computing and Visualization in Science,* vol. 12, pp. 345-364, 2009. https://doi.org/10.1007/S00791-008-0109-X
[32] H. Chitsaz and S. M. Lavalle, "Time-optimal paths for a Dubins airplane," in *2007 46th IEEE Conference on Decision and Control*, 2008. https://doi.org/10.1109/CDC.2007.4434966
[33] S. Hota and D. Ghose, "Optimal geometrical path in 3D with curvature constraint," in *2010 IEEE/RSJ International Conference on Intelligent Robots and Systems*, 2010. https://doi.org/10.1109/IROS.2010.5653663
[34] M. Owen, R. W. Beard, and T. W. McLain, "Implementing Dubins Airplane Paths on Fixed-Wing UAVs*," in: Valavanis K., Vachtsevanos G. (eds) Handbook of Unmanned Aerial Vehicles. Springer, Dordrecht. pp. 1677-1701, 2015. https://doi.org/10.1007/978-90-481-9707-1_120
[35] P. Pharpatara, B. Hérissé, and Y. Bestaoui, "3D-shortest paths for a hypersonic glider in a heterogeneous environment," *IFAC-PapersOnLine,* vol. 48, pp. 186-191, 2015. https://doi.org/10.1016/j.ifacol.2015.08.081
[36] Y. H. Wang, "3D Dubins Curves for multi-vehicle path planning," MSc Thesis, Electrical and Computer Engineering, Missouri University of Science and Technology, 2018. Available on 2019/8/20. https://scholarsmine.mst.edu/masters_theses/7839/
[37] Y. Y. Wang, M. L. Duan, M. H. Xu, D. G. Wang, and W. Feng, "A mathematical model for subsea wells partition in the layout of cluster manifolds," *Applied Ocean Research,* vol. 36, pp. 26-35, 2012. https://doi.org/10.1016/j.apor.2012.02.002
[38] H. Zhang, Y. Liang, M. Wu, C. Qian, K. Li, and Y. Yan, "Study on the Optimal Topological Structure of the Producing Pipeline Network System of CBM Fields," presented at the International Petroleum Technology Conference, Doha, Qatar, 2015. https://doi.org/10.2523/IPTC-18466-MS
[39] C. Hong, S. F. Estefen, Y. X. Wang, and M. I. Lourenco, "An integrated optimization model for the layout design of a subsea production system," *Applied Ocean Research,* vol. 77, pp. 1-13, 2018. https://doi.org/10.1016/j.apor.2018.05.009
[40] Z. Duan, Q. Liao, M. Wu, H. Zhang, and Y. Liang, "Optimization of Pipeline Network Structure of CBM Fields Considering Three-Dimensional Geographical Factors." *Proceedings of the 2016 11th International Pipeline Conference*, vol. 2, 2016. V002T02A002. ASME. https://doi.org/10.1115/IPC2016-64020
[41] R. Wang, Y. Wu, Y. Wang, and X. Feng, "An industrial area layout design methodology considering piping and safety using genetic algorithm," *Journal of Cleaner Production,* vol. 167, pp. 23-31, 2017. https://doi.org/10.1016/j.jclepro.2017.08.147
[42] H. Zhang, Y. Liang, J. Ma, C. Qian, and X. Yan, "An MILP method for optimal offshore oilfield gathering system," *Ocean Engineering,* vol. 141, pp. 25-34, 2017. https://doi.org/10.1016/j.oceaneng.2017.06.011

[43] V. Ramos Rosa, E. Camponogara, and V. J. Martins Ferreira Filho, "Design optimization of oilfield subsea infrastructures with manifold placement and pipeline layout," *Computers & Chemical Engineering,* vol. 108, pp. 163-178, 2018. https://doi.org/10.1016/j.compchemeng.2017.08.009
[44] O. Huisman, "Location allocation problem using genetic algorithm and simulated annealing : a case study based on school in Enschede," MSc Thesis, Geo-information Science and Earth Observation, University of Twente, 2011. Available on 2019/2/20. http://essay.utwente.nl/84903/1/arifin.pdf
[45] J. B. Kruskal, "On the shortest spanning subtree of a graph and the traveling salesman problem," *Proceedings of the American Mathematical society,* vol. 7, pp. 48-50, 1956. https://doi.org/10.2307/2033241
[46] R. C. Prim, "Shortest connection networks and some generalizations," *The Bell System Technical Journal,* vol. 36, pp. 1389-1401, 1957. https://doi.org/10.1002/j.1538-7305.1957.tb01515.x
[47] F. Chin and D. Houck, "Algorithms for updating minimal spanning trees," *Journal of Computer and System Sciences,* vol. 16, pp. 333-344, 1978. https://doi.org/10.1016/0022-0000(78)90022-3
[48] S. Lloyd, "Least squares quantization in PCM," *IEEE transactions on information theory,* vol. 28, pp. 129-137, 1982. https://doi.org/10.1109/TIT.1982.1056489
[49] D. Arthur and S. Vassilvitskii, "k-means++: The advantages of careful seeding," in *Proceedings of the eighteenth annual ACM-SIAM symposium on Discrete algorithms*, 2007, pp. 1027-1035. https://dl.acm.org/doi/10.5555/1283383.1283494
[50] J. Lin, "Exact algorithms for size constrained clustering," PhD Thesis, Department of Mathematics, University of Milan, 2012. Available on 2019/3/11. https://air.unimi.it/retrieve/handle/2434/172513/173785/phd_unimi_R07628.pdf
[51] A. Bertoni, M. Goldwurm, and J. Lin, "Exact algorithms for 2-clustering with size constraints in the Euclidean plane," in *International Conference on Current Trends in Theory and Practice of Informatics*, 2015, pp. 128-139. https://doi.org/10.1007/978-3-662-46078-8_11
[52] S. Zhu, D. Wang, and T. J. K.-B. S. Li, "Data clustering with size constraints," *Knowledge-Based Systems*, vol. 23, pp. 883-889, 2010. https://doi.org/10.1016/j.knosys.2010.06.003
[53] C. L. Lawson, "Transforming triangulations," *Discrete Mathematics,* vol. 3, pp. 365-372, 1972. https://doi.org/10.1016/0012-365X(72)90093-3
[54] A. Bowyer, "Computing Dirichlet tessellations," *The Computer Journal,* vol. 24, pp. 162-166, 1981. https://doi.org/10.1093/comjnl/24.2.162
[55] D. F. Watson, "Computing the n-dimensional Delaunay tessellation with application to Voronoi polytopes," *The Computer Journal,* vol. 24, pp. 167-172, 1981. https://doi.org/10.1093/comjnl/24.2.167
[56] G. Leach, "Improving worst-case optimal Delaunay Triangulation algorithms," in *4th Canadian Conference on Computational Geometry*, 1992, p. 15. http://citeseerx.ist.psu.edu/viewdoc/summary?doi=10.1.1.56.2323
[57] *CPU Performance*. Available on 2021/07/02. https://asteroidsathome.net/boinc/cpu_list.php.
[58] E. Lillevik and I. E. Standal, "The Traveling Circus - Automated generation of parametric wellbore trajectories minimizing wellbore lengths for different subsea field layouts," Master, Department of Geoscience and Petroleum, Norwegian University of Science and Technology, 2018. Available on 2019/1/13 http://hdl.handle.net/11250/2505067

Appendix I. List of Symbols

Chapter 3

k : number of completion intervals;

$P_{1,i}$: kickoff point for the i-th well, 3D coordination is $(Px_1, Py_1, Pz_{1,i})$

$V_{1,i}$: drilling direction vector of the i-th well, in this study all $V_{1,i}$ is $(0, 0, -1)$

$P_{2,i}$: start point of the i-th well completion interval, 3D coordination is $\left(Px_{2,i}, Py_{2,i}, Pz_{2,i}\right)$

$V_{2,i}$: drilling direction vector of the i-th well completion interval, 3D coordination is $\left(Vx_{2,i}, Vy_{2,i}, Vz_{2,i}\right)$

Z_i : highest kickoff point for i-th well

κ : max allowed turning rate/dogleg severity, $^\circ/100\text{m}$

$r_{\min}$: minimum allowed turning radius, m

D : optimal drilling site, 3D coordination is $(Px_1, Py_1, 0)$

Lc : length of the non-straight/circular section

Ls : length of the straight section

θ : deviation angle of the straight section

$cstC\left(Lc\right)$: cost function of the non-straight section

$cstS\left(Ls, \theta\right)$: cost function of the straight section

$COST\left(P_1, V_1, P_2, V_2, r\right)_i$: cost function of the i-th well

T : straight section vector in the Dubins Curve

Note:

1. For the subscription i denoting the parameters of the i-th well, it may be omitted such as $(Px_1, Py_1, Pz_{1,i})$ when all wells share the same value or when we are just focusing on one specific well such as Equation (3-1). The subscription i may also be merged outside the parenthesis such as Equation (3-4).

2. The other symbols related with Dubins Curve are not listed here as they do not show up other than Section 3.3.2.

Chapter 4

k : number of manifolds

m : cluster size, i.e., number of wells connected to the manifold

n : number of all wells

h : number of remaining wells that cannot be clustered into the size of m

i, j, ii, jj : index for computation

N : number of all possible clusters or useful clusters

N_m : number of all useful clusters of size m

N_h : number of all useful clusters of size h

$\mathbf{p}_i$: i -th well position, $(x_i,\ \mathrm{y}_i)$

$\boldsymbol{\delta}$: MINLP integer/binary variable matrix

$\mathbf{C}$: MINLP continuous variable matrix

$\boldsymbol{\gamma}$: BLP binary variable vector

$\mathbf{A}$: BLP coefficient matrix

Chapter 5

$P_{0,j}$: $\left(Px_{0,j}, Py_{0,j}, 0\right)$, drilling site position for j-th cluster, vertically above the corresponding kickoff point(s)

$P_{1,i}$: $(Px_{1,i}, Py_{1,i}, Pz_{1,i})$, highest allowed kickoff point for i-th well

$V_{1,i}$: $(0,0,-1)$, the drilling direction at $P_{1,i}$,

$P_{2,i}$: $\left(Px_{2,i}, Py_{2,i}, Pz_{2,i}\right)$, start point of the i-th completion interval

$P_{3,i}$: $\left(Px_{3,i}, Py_{3,i}, Pz_{3,i}\right)$, end point of the first segment of i-th completion interval

$V_{2,i}$: $\left(Vx_{2,i}, Vy_{2,i}, Vz_{2,i}\right)$, drilling direction at $P_{2,i}$

κ : maximum turning rate/dogleg severity, °/30m

$r_{\min}$: minimum turning rate radius, m

cst_{site} : preparation cost for one drilling site

$cst_{SF,m}$: cost of the subsea facility for a m-slot template; particularly, when m=1, it means satellite well

n : number of all wells

n_{site} : number of drilling site

$n_{SF,m}$: number of m-slot subsea facilities

$cst_{Traj,i}$: wellbore cost of i-th well

$cstT_j$: total cost of j-th cluster

N_m : number of clusters of size m

$\boldsymbol{\gamma}$: BLP binary variable vector

Lc : length of the non-straight/circular section

Ls : length of the straight section

θ : inclination angle of the straight section

$cstC(Lc)$: cost function of the non-straight section

$cstS(Ls,\theta)$: cost function of the straight section

Appendix II. 100 Random Points (Chapter 4)

Index	X	Y	Index	X	Y	Index	X	Y
1	53.71210	15.30460	38	9.55590	11.42190	75	23.98760	9.40300
2	56.54320	21.41880	39	35.66190	9.93330	76	30.33130	6.93480
3	20.10500	15.45620	40	19.86600	15.12240	77	10.15840	12.48190
4	26.24180	18.17600	41	39.51680	16.93710	78	31.48470	8.96400
5	28.26940	29.00110	42	51.81810	23.01590	79	38.47220	20.17310
6	8.95860	24.66350	43	34.05740	23.39600	80	0.97180	28.14770
7	8.15190	9.53250	44	58.82890	14.52290	81	50.21110	10.29440
8	31.94990	17.63090	45	47.50990	24.06640	82	48.20770	16.88890
9	43.54740	3.90610	46	9.15560	14.13040	83	41.86710	3.56670
10	23.92220	7.63060	47	49.98160	6.08280	84	27.71330	5.07060
11	21.50510	24.09090	48	11.51180	17.38840	85	4.95680	8.36690
12	17.11680	20.03540	49	38.33920	19.99500	86	49.24300	16.70440
13	52.11810	0.40880	50	40.14000	20.30300	87	11.58120	14.56770
14	37.58480	16.84740	51	46.32530	28.27530	88	26.72130	28.56670
15	14.47030	13.63680	52	22.78910	23.10450	89	0.77750	6.95760
16	58.68490	27.14850	53	26.49510	22.12210	90	18.52450	14.35980
17	38.43000	8.46480	54	28.98360	25.98790	91	52.52110	15.79570
18	13.79090	1.95100	55	36.48630	29.72840	92	50.11560	23.78160
19	40.88010	14.29780	56	10.55970	15.11780	93	19.98570	5.79020
20	39.94940	29.51140	57	0.12150	18.87260	94	52.84230	27.28800
21	8.08310	27.67050	58	47.41340	23.77830	95	28.78120	27.66590
22	1.34960	16.83590	59	30.81650	13.45950	96	33.64900	0.39800
23	15.73200	19.56970	60	12.79380	15.73070	97	36.95450	23.02650
24	6.99090	23.18040	61	6.20700	5.14420	98	39.71390	28.42030
25	4.15910	3.18530	62	9.44020	3.92000	99	36.99800	24.39920
26	51.17580	0.03220	63	24.45090	6.56340	100	41.10840	27.71490
27	10.81980	16.25290	64	24.46540	3.16440			
28	1.94510	0.20570	65	3.16160	4.24280			
29	44.03560	13.54010	66	56.50890	13.70900			
30	32.19100	5.86990	67	8.99830	23.64400			
31	16.56180	23.61430	68	23.06240	8.43190			
32	22.10750	18.55690	69	18.66350	6.74360			
33	0.77320	0.46560	70	10.11210	27.26620			
34	53.35240	26.72560	71	53.79890	0.21990			
35	51.96120	22.85110	72	19.36350	17.66220			
36	15.25480	27.21110	73	44.03980	16.26350			
37	34.16880	22.75710	74	24.65430	19.60570			

Appendix III. Algorithm of Finding Useful Clusters (Chapter 4)

```
function AllCluster=enumPivot(AdjMatrix,LVL,N)
AM=AdjMatrix;
AllCluster=[]; % Initialize
for pivot=1:N-LVL+1    % LVL: cluster size; N: number of points
    pivotComb=pivot;
    lvl=1;
    while lvl<LVL
        comblvl=[];
        for i=1:size(pivotComb,1)
            AM_temp=AM;
            AM_temp(:,pivotComb(i,:)-(pivot-1))=0; % avoid neighbors from itself
            connection=find( any(AM_temp(pivotComb(i,:)-(pivot-1),:), 1) )+pivot-1;
            %get all the connected points(neighbors) to the pivotComb
            connection=connection(:); % Make sure it's a Column Vector
            pivotComb_New=[repmat(pivotComb(i,:), length(connection),1), connection];
            comblvl=[comblvl; pivotComb_New];
        end
        comblvl=sort(comblvl,2); % sort each cluster by point index
        comblvl=sortrows(comblvl); % sort clusters by its first point index
        comblvl=unique(comblvl,'rows'); % eliminate the repeated
        %-----Prepare for next lvl-----
        lvl=lvl+1;
        pivotComb=comblvl;
    end

    AllCluster=[AllCluster; comblvl];
    %--Delete pivot information for simplification of next pivot--
    AM(1,:)=[];
    AM(:,1)=[];
    %---------------------------------------------------------------
end
end
```

Appendix IV. Distance Matrix, Adjacent Matrix, Modified Adjacent Matrix of the Undirected Graph in Fig. 4.4 (Chapter 4)

IV.1. Distance Matrix

Ind	1	2	3	4	5	6	7	8	9	10	11	12	13	14	15	16	17	18	19	20
1	0	1	2	3	3	4	5	4	4	4	3	3	2	1	2	2	2	3	3	3
2	1	0	1	2	2	3	4	3	4	4	3	3	2	1	2	2	2	3	3	3
3	2	1	0	1	1	2	3	2	3	4	3	2	1	1	2	2	2	3	3	3
4	3	2	1	0	1	2	2	1	2	3	2	1	1	2	2	3	3	4	3	3
5	3	2	1	1	0	1	2	1	2	3	3	2	2	2	3	3	3	4	4	4
6	4	3	2	2	1	0	1	1	2	3	3	2	3	3	3	4	4	5	4	4
7	5	4	3	2	2	1	0	1	1	2	2	2	3	4	3	4	4	4	3	3
8	4	3	2	1	1	1	1	0	1	2	2	1	2	3	2	3	3	4	3	3
9	4	4	3	2	2	2	1	1	0	1	1	1	2	3	2	3	3	3	2	2
10	4	4	4	3	3	3	2	2	1	0	1	2	3	3	2	3	2	2	1	1
11	3	3	3	2	3	3	2	2	1	1	0	1	2	2	1	2	2	3	2	1
12	3	3	2	1	2	2	2	1	1	2	1	0	1	2	1	2	2	3	2	2
13	2	2	1	1	2	3	3	2	2	3	2	1	0	1	1	2	2	3	2	2
14	1	1	1	2	2	3	4	3	3	3	2	2	1	0	1	1	1	2	2	2
15	2	2	2	2	3	3	3	2	2	2	1	1	1	1	0	1	1	2	1	1
16	2	2	2	3	3	4	4	3	3	3	2	2	2	1	1	0	1	2	2	2
17	2	2	2	3	3	4	4	3	3	2	2	2	2	1	1	1	0	1	1	2
18	3	3	3	4	4	5	4	4	3	2	3	3	3	2	2	2	1	0	1	2
19	3	3	3	3	4	4	3	3	2	1	2	2	2	2	1	2	1	1	0	1
20	3	3	3	3	4	4	3	3	2	1	1	2	2	2	1	2	2	2	1	0

IV.2. **Adjacent-1 matrix (distance≤1, conventional adjacency matrix)**

Ind	1	2	3	4	5	6	7	8	9	10	11	12	13	14	15	16	17	18	19	20
1	1	1	0	0	0	0	0	0	0	0	0	0	0	1	0	0	0	0	0	0
2	1	1	1	0	0	0	0	0	0	0	0	0	0	1	0	0	0	0	0	0
3	0	1	1	1	1	0	0	0	0	0	0	0	1	1	0	0	0	0	0	0
4	0	0	1	1	1	0	0	1	0	0	0	1	1	0	0	0	0	0	0	0
5	0	0	1	1	1	1	0	1	0	0	0	0	0	0	0	0	0	0	0	0
6	0	0	0	0	1	1	1	1	0	0	0	0	0	0	0	0	0	0	0	0
7	0	0	0	0	0	1	1	1	1	0	0	0	0	0	0	0	0	0	0	0
8	0	0	0	1	1	1	1	1	1	0	0	1	0	0	0	0	0	0	0	0
9	0	0	0	0	0	0	1	1	1	1	1	1	0	0	0	0	0	0	0	0
10	0	0	0	0	0	0	0	0	1	1	1	0	0	0	0	0	0	0	1	1
11	0	0	0	0	0	0	0	0	1	1	1	1	0	0	1	0	0	0	0	1
12	0	0	0	1	0	0	0	1	1	0	1	1	1	0	1	0	0	0	0	0
13	0	0	1	1	0	0	0	0	0	0	0	1	1	1	1	0	0	0	0	0
14	1	1	1	0	0	0	0	0	0	0	0	0	1	1	1	1	1	0	0	0
15	0	0	0	0	0	0	0	0	0	0	1	1	1	1	1	1	1	0	1	1
16	0	0	0	0	0	0	0	0	0	0	0	0	0	1	1	1	1	0	0	0
17	0	0	0	0	0	0	0	0	0	0	0	0	0	1	1	1	1	1	1	0
18	0	0	0	0	0	0	0	0	0	0	0	0	0	0	0	0	1	1	1	0
19	0	0	0	0	0	0	0	0	0	1	0	0	0	0	1	0	1	1	1	1
20	0	0	0	0	0	0	0	0	0	1	1	0	0	0	1	0	0	0	1	1

IV.3. **Adjacent-2 matrix (distance≤2)**

Ind	1	2	3	4	5	6	7	8	9	10	11	12	13	14	15	16	17	18	19	20
1	1	1	1	0	0	0	0	0	0	0	0	0	1	1	1	1	1	0	0	0
2	1	1	1	1	1	0	0	0	0	0	0	0	1	1	1	1	1	0	0	0
3	1	1	1	1	1	1	0	1	0	0	0	1	1	1	1	1	1	0	0	0
4	0	1	1	1	1	1	1	1	1	0	1	1	1	1	1	0	0	0	0	0
5	0	1	1	1	1	1	1	1	1	0	0	1	1	1	0	0	0	0	0	0
6	0	0	1	1	1	1	1	1	1	0	0	1	0	0	0	0	0	0	0	0
7	0	0	0	1	1	1	1	1	1	1	1	1	0	0	0	0	0	0	0	0
8	0	0	1	1	1	1	1	1	1	1	1	1	1	0	1	0	0	0	0	0
9	0	0	0	1	1	1	1	1	1	1	1	1	1	0	1	0	0	0	1	1
10	0	0	0	0	0	0	1	1	1	1	1	1	0	0	1	0	1	1	1	1
11	0	0	0	1	0	0	1	1	1	1	1	1	1	1	1	1	1	0	1	1
12	0	0	1	1	1	1	1	1	1	1	1	1	1	1	1	1	1	0	1	1
13	1	1	1	1	1	0	0	1	1	0	1	1	1	1	1	1	1	0	1	1
14	1	1	1	1	1	0	0	0	0	0	1	1	1	1	1	1	1	1	1	1
15	1	1	1	1	0	0	0	1	1	1	1	1	1	1	1	1	1	1	1	1
16	1	1	1	0	0	0	0	0	0	0	1	1	1	1	1	1	1	1	1	1
17	1	1	1	0	0	0	0	0	0	1	1	1	1	1	1	1	1	1	1	1
18	0	0	0	0	0	0	0	0	0	1	0	0	0	1	1	1	1	1	1	1
19	0	0	0	0	0	0	0	0	1	1	1	1	1	1	1	1	1	1	1	1
20	0	0	0	0	0	0	0	0	1	1	1	1	1	1	1	1	1	1	1	1

Appendix V. Dataset of Well Completion Intervals (Chapter 5)

V.1. Dataset 1

Well Index	Start Point			End Point		
	x	y	z	x	y	z
1	286	786	2500	71	1500	2500
2	2714	2786	2500	1786	2143	2500
3	2571	2714	2500	1571	3143	2500
4	1786	4143	2500	500	4714	2500
5	2000	4214	2500	2857	4000	2500
6	2786	4429	2500	3786	4500	2500
7	3000	5071	2500	3714	4714	2500
8	3357	5429	2500	3786	5214	2500
9	3714	3357	2500	4500	3429	2500
10	6786	3571	2500	6571	2857	2500
11	7143	4071	2500	6786	3786	2500
12	7500	4500	2500	6786	5286	2500
13	7500	4071	2500	8714	3929	2500
14	9429	6571	2500	8857	5929	2500
15	9571	4429	2500	10000	4286	2500
16	11357	4500	2500	11929	4143	2500
17	10214	5214	2500	10714	5643	2500
18	7857	6286	2500	8857	5821	2500
19	8429	4500	2500	7714	5357	2500
20	9643	3571	2500	9071	2857	2500
21	7714	3786	2500	7857	2857	2500
22	7571	893	2500	7143	571	2500
23	5357	3143	2500	4714	1929	2500
24	4500	4500	2500	5000	5143	2500
25	3357	1143	2500	3000	571	2500
26	1071	1714	2500	1500	2714	2500
27	786	786	2500	500	1571	2500
28	2643	5929	2500	1643	5429	2500
29	5929	2286	2500	6214	1071	2500
30	10571	3429	2500	11571	2571	2500

V.2. **Dataset 2**

Well Index	Start Point			End Point		
	x	y	z	x	y	z
1	5565	5364	3850	5614	5335	4852
2	7578	6922	4368	8166	7252	4451
3	6939	5918	4179	6997	5920	4801
4	6630	5944	2066	6869	6075	2235
5	7188	5004	4311	6978	4553	4567
6	10500	6606	4284	10939	6969	4352
7	9586	5938	4143	10034	5781	4438
8	8661	5646	4117	8550	5311	4536
9	3595	3324	4409	3434	2902	4698
10	3918	4803	4219	3921	4524	4870
11	6960	7764	4361	6976	7785	4962
12	5957	7304	4234	5993	7303	4965
13	14262	8338	3992	14268	8316	4512
14	13577	8829	3527	13614	8788	4614
15	14984	9513	4086	15315	9737	4640
16	11993	6938	4114	11769	6560	4434
17	11972	8424	4009	12029	8426	4667
18	13520	6981	3800	13554	6945	4422
19	10463	7570	3939	10484	7545	4737
20	13283	7731	4355	13757	7882	4434
21	8287	9189	4858	7848	8910	4949
22	9330	8699	4299	9357	8534	4848
23	11658	9918	4265	11700	9881	4855
24	10356	9062	4278	10400	8892	4825
25	14367	10650	3584	14434	10507	4795
26	12852	11499	4474	12480	11367	4967
27	14568	10649	1901	14632	10176	2195
28	13977	15499	4540	13963	15852	5030
29	14467	12996	4712	14803	12691	5011
30	12748	11346	4424	12541	10953	4929
31	14652	14836	4163	14696	14954	5054

Appendix VI. Drilling Site Positions (Grid Value) for Case Study (Chapter 5)

VI.1. Case 1

Well Index	Drilling Site Position		Difference
	Grid Value	Accurate Value	
1	[5550;5350;-500]	[5564;5364;-500]	[14;14;0]
2	[7150;6700;-500]	[7139;6676;-500]	[-11;-24;0]
3	[6950;5900;-500]	[6937;5918;-500]	[-13;18;0]
4	[6400;5800;-500]	[6392;5814;-500]	[-8;14;0]
5	[7300;5300;-500]	[7319;5286;-500]	[19;-14;0]
6	[10100;6300;-500]	[10111;6284;-500]	[11;-16;0]
7	[9350;6050;-500]	[9331;6028;-500]	[-19;-22;0]
8	[8700;5750;-500]	[8703;5774;-500]	[3;24;0]
9	[3700;3550;-500]	[3689;3571;-500]	[-11;21;0]
10	[3900;4850;-500]	[3917;4849;-500]	[17;-1;0]
11	[6950;7750;-500]	[6960;7764;-500]	[10;14;0]
12	[5950;7300;-500]	[5956;7304;-500]	[6;4;0]
13	[14250;8350;-500]	[14262;8339;-500]	[12;-11;0]
14	[13600;8850;-500]	[13576;8830;-500]	[-24;-20;0]
15	[14900;9450;-500]	[14894;9452;-500]	[-6;2;0]
16	[12100;7150;-500]	[12113;7141;-500]	[13;-9;0]
17	[11950;8400;-500]	[11968;8422;-500]	[18;22;0]
18	[13500;7000;-500]	[13519;6982;-500]	[19;-18;0]
19	[10450;7550;-500]	[10463;7570;-500]	[13;20;0]
20	[12800;7600;-500]	[12823;7584;-500]	[23;-16;0]
21	[8700;9450;-500]	[8687;9443;-500]	[-13;-7;0]
22	[9350;8700;-500]	[9326;8724;-500]	[-24;24;0]
23	[11650;9900;-500]	[11656;9920;-500]	[6;20;0]
24	[10350;9100;-500]	[10349;9089;-500]	[-1;-11;0]
25	[14350;10650;-500]	[14365;10654;-500]	[15;4;0]
26	[12950;11550;-500]	[12970;11541;-500]	[20;-9;0]
27	[14550;10900;-500]	[14531;10919;-500]	[-19;19;0]
28	[14000;15400;-500]	[13981;15391;-500]	[-19;-9;0]
29	[14300;13150;-500]	[14276;13169;-500]	[-24;19;0]
30	[12800;11450;-500]	[12814;11472;-500]	[14;22;0]
31	[14650;14850;-500]	[14650;14831;-500]	[0;-19;0]

VI.2. **Case 2.1**

Well Index	Drilling Site Position
1	[6200;5700;-500]
2	[7050;7200;-500]
3	[7100;5600;-500]
4	[6200;5700;-500]
5	[7100;5600;-500]
6	[10250;6950;-500]
7	[9050;5900;-500]
8	[9050;5900;-500]
9	[3800;4200;-500]
10	[3800;4200;-500]
11	[7050;7200;-500]
12	[5950;7300;-500]
13	[13900;8600;-500]
14	[13900;8600;-500]
15	[14900;9450;-500]
16	[12050;7750;-500]
17	[12050;7750;-500]
18	[13200;7250;-500]
19	[10250;6950;-500]
20	[13200;7250;-500]
21	[9050;9050;-500]
22	[9050;9050;-500]
23	[11000;9500;-500]
24	[11000;9500;-500]
25	[14500;10850;-500]
26	[12900;11500;-500]
27	[14500;10850;-500]
28	[14350;15100;-500]
29	[14300;13150;-500]
30	[12900;11500;-500]
31	[14350;15100;-500]

VI.3. **Case 2.2**

Well Index	Drilling Site Position
1	[6200;5700;-500]
2	[7050;7200;-500]
3	[7100;5600;-500]
4	[6200;5700;-500]
5	[7100;5600;-500]
6	[10100;6300;-500]
7	[9050;5900;-500]
8	[9050;5900;-500]
9	[3700;3550;-500]
10	[3900;4850;-500]
11	[7050;7200;-500]
12	[5950;7300;-500]
13	[13900;8600;-500]
14	[13900;8600;-500]
15	[14900;9450;-500]
16	[12450;7350;-500]
17	[11950;8400;-500]
18	[13500;7000;-500]
19	[10450;7550;-500]
20	[12450;7350;-500]
21	[9050;9050;-500]
22	[9050;9050;-500]
23	[11650;9900;-500]
24	[10350;9100;-500]
25	[14500;10850;-500]
26	[12900;11500;-500]
27	[14500;10850;-500]
28	[14350;15100;-500]
29	[14300;13150;-500]
30	[12900;11500;-500]
31	[14350;15100;-500]

VI.4. **Case 3.1**

Well Index	Drilling Site Position
1	[6450;5900;-500]
2	[6450;5900;-500]
3	[6450;5900;-500]
4	[6450;5900;-500]
5	[8900;5800;-500]
6	[8900;5800;-500]
7	[8900;5800;-500]
8	[8900;5800;-500]
9	[3700;3550;-500]
10	[3900;4850;-500]
11	[6950;7750;-500]
12	[5950;7300;-500]
13	[14250;8350;-500]
14	[13600;8850;-500]
15	[14900;9450;-500]
16	[12600;7500;-500]
17	[12600;7500;-500]
18	[12600;7500;-500]
19	[9750;8650;-500]
20	[12600;7500;-500]
21	[9750;8650;-500]
22	[9750;8650;-500]
23	[11650;9900;-500]
24	[9750;8650;-500]
25	[14000;11050;-500]
26	[14000;11050;-500]
27	[14000;11050;-500]
28	[14000;15400;-500]
29	[14300;13150;-500]
30	[14000;11050;-500]
31	[14650;14850;-500]

VI.5. **Case 3.2**

Well Index	Drilling Site Position
1	[5550;5350;-500]
2	[6750;5850;-500]
3	[6750;5850;-500]
4	[6750;5850;-500]
5	[6750;5850;-500]
6	[10250;6950;-500]
7	[9050;5900;-500]
8	[9050;5900;-500]
9	[3800;4200;-500]
10	[3800;4200;-500]
11	[6450;7550;-500]
12	[6450;7550;-500]
13	[13900;8600;-500]
14	[13900;8600;-500]
15	[14900;9450;-500]
16	[12600;7500;-500]
17	[12600;7500;-500]
18	[12600;7500;-500]
19	[10250;6950;-500]
20	[12600;7500;-500]
21	[9050;9050;-500]
22	[9050;9050;-500]
23	[11000;9500;-500]
24	[11000;9500;-500]
25	[14500;10850;-500]
26	[12900;11500;-500]
27	[14500;10850;-500]
28	[14350;15100;-500]
29	[14300;13150;-500]
30	[12900;11500;-500]
31	[14350;15100;-500]

VI.6. **Case 3.3**

Well Index	Drilling Site Position		Difference
	Grid Value	Accurate Value	
1	[6200;5700;-500]	[6183;5702;-500]	[-17;2;0]
2	[7050;7200;-500]	[7037;7211;-500]	[-13;11;0]
3	[7100;5600;-500]	[7122;5594;-500]	[22;-6;0]
4	[6200;5700;-500]	[6183;5702;-500]	[-17;2;0]
5	[7100;5600;-500]	[7122;5594;-500]	[22;-6;0]
6	[10100;6300;-500]	[10111;6284;-500]	[11;-16;0]
7	[9050;5900;-500]	[9025;5890;-500]	[-25;-10;0]
8	[9050;5900;-500]	[9025;5890;-500]	[-25;-10;0]
9	[3700;3550;-500]	[3689;3571;-500]	[-11;21;0]
10	[3900;4850;-500]	[3917;4849;-500]	[17;-1;0]
11	[7050;7200;-500]	[7037;7211;-500]	[-13;11;0]
12	[5950;7300;-500]	[5956;7304;-500]	[6;4;0]
13	[13900;8600;-500]	[13892;8604;-500]	[-8;4;0]
14	[13900;8600;-500]	[13892;8604;-500]	[-8;4;0]
15	[14900;9450;-500]	[14894;9452;-500]	[-6;2;0]
16	[12450;7350;-500]	[12470;7347;-500]	[20;-3;0]
17	[11950;8400;-500]	[11968;8422;-500]	[18;22;0]
18	[13500;7000;-500]	[13519;6982;-500]	[19;-18;0]
19	[10450;7550;-500]	[10463;7570;-500]	[13;20;0]
20	[12450;7350;-500]	[12470;7347;-500]	[20;-3;0]
21	[9050;9050;-500]	[9025;9052;-500]	[-25;2;0]
22	[9050;9050;-500]	[9025;9052;-500]	[-25;2;0]
23	[11650;9900;-500]	[11656;9920;-500]	[6;20;0]
24	[10350;9100;-500]	[10349;9089;-500]	[-1;-11;0]
25	[14500;10850;-500]	[14482;10858;-500]	[-18;8;0]
26	[12900;11500;-500]	[12893;11505;-500]	[-7;5;0]
27	[14500;10850;-500]	[14482;10858;-500]	[-18;8;0]
28	[14350;15100;-500]	[14329;15104;-500]	[-21;4;0]
29	[14300;13150;-500]	[14276;13169;-500]	[-24;19;0]
30	[12900;11500;-500]	[12893;11505;-500]	[-7;5;0]
31	[14350;15100;-500]	[14329;15104;-500]	[-21;4;0]

VI.7. **Case 4**

Well Index	Drilling Site Position
1	[6500;5650;-500]
2	[6700;7250;-500]
3	[6500;5650;-500]
4	[6500;5650;-500]
5	[6500;5650;-500]
6	[10250;6950;-500]
7	[9050;5900;-500]
8	[9050;5900;-500]
9	[3800;4200;-500]
10	[3800;4200;-500]
11	[6700;7250;-500]
12	[6700;7250;-500]
13	[14200;8900;-500]
14	[14200;8900;-500]
15	[14200;8900;-500]
16	[12850;7200;-500]
17	[11800;9150;-500]
18	[12850;7200;-500]
19	[10250;6950;-500]
20	[12850;7200;-500]
21	[9500;9050;-500]
22	[9500;9050;-500]
23	[11800;9150;-500]
24	[9500;9050;-500]
25	[14500;10850;-500]
26	[12900;11500;-500]
27	[14500;10850;-500]
28	[14350;15100;-500]
29	[14300;13150;-500]
30	[12900;11500;-500]
31	[14350;15100;-500]

Appendix VII. Real Field Data from SUBPRO Industrial Partner (Chapter 6)

VII.1. Trajectory of Well #1a (#1)

Depth (m)	Inclination (°)	Azimuth (°)	TVD (m)	North (m)	East (m)	VS (m)	DLS $(°/30m)$
1170	0	0	1170	0	0	0	0
1800	0	0	1800	0	0	0	0
1830	3	71.975	1829.99	0.24	0.75	0.65	3
1860	6	71.975	1859.89	0.97	2.98	2.59	3
1890	9	71.975	1889.63	2.18	6.71	5.82	3
1920	12	71.975	1919.12	3.87	11.91	10.33	3
1950	15	71.975	1948.29	6.04	18.56	16.11	3
1980	18	71.975	1977.05	8.68	26.67	23.14	3
2006.31	20.631	71.975	2001.88	11.37	34.94	30.32	3
2010	20.631	71.975	2005.33	11.77	36.18	31.4	0
2040	20.631	71.975	2033.41	15.04	46.23	40.12	0
2070	20.631	71.975	2061.49	18.31	56.28	48.84	0
2100	20.631	71.975	2089.56	21.58	66.33	57.57	0
2130	20.631	71.975	2117.64	24.86	76.38	66.29	0
2160	20.631	71.975	2145.71	28.13	86.44	75.01	0
2190	20.631	71.975	2173.79	31.4	96.49	83.74	0
2220	20.631	71.975	2201.87	34.67	106.54	92.46	0
2250	20.631	71.975	2229.94	37.94	116.59	101.18	0
2280	20.631	71.975	2258.02	41.21	126.64	109.91	0
2310	20.631	71.975	2286.09	44.48	136.7	118.63	0
2340	20.631	71.975	2314.17	47.75	146.75	127.36	0
2370	20.631	71.975	2342.25	51.02	156.8	136.08	0
2400	20.631	71.975	2370.32	54.29	166.85	144.8	0
2430	20.631	71.975	2398.4	57.56	176.9	153.53	0
2460	20.631	71.975	2426.47	60.83	186.95	162.25	0
2490	20.631	71.975	2454.55	64.11	197.01	170.97	0
2520	20.631	71.975	2482.63	67.38	207.06	179.7	0
2550	20.631	71.975	2510.7	70.65	217.11	188.42	0
2580	20.631	71.975	2538.78	73.92	227.16	197.14	0
2610	20.631	71.975	2566.85	77.19	237.21	205.87	0
2640	20.631	71.975	2594.93	80.46	247.27	214.59	0
2670	20.631	71.975	2623.01	83.73	257.32	223.31	0
2700	20.631	71.975	2651.08	87	267.37	232.04	0
2730	20.631	71.975	2679.16	90.27	277.42	240.76	0
2736.67	20.631	71.975	2685.4	91	279.66	242.7	0
2760	22.369	67.723	2707.11	93.96	287.67	249.93	3
2790	24.74	63.119	2734.61	98.96	298.56	260.54	3

2820	27.229	59.291	2761.58	105.3	310.06	272.58	3
2850	29.806	56.069	2787.93	112.97	322.15	286.03	3
2880	32.449	53.322	2813.61	121.94	334.79	300.85	3
2910	35.144	50.95	2838.54	132.19	347.96	317.01	3
2940	37.879	48.877	2862.65	143.69	361.6	334.44	3
2970	40.646	47.045	2885.88	156.41	375.7	353.12	3
3000	43.439	45.41	2908.16	170.31	390.2	372.98	3
3030	46.253	43.935	2929.43	185.36	405.06	393.97	3
3060	49.085	42.593	2949.63	201.51	420.26	416.04	3
3090	51.93	41.362	2968.71	218.72	435.73	439.12	3
3120	54.788	40.223	2986.61	236.95	451.46	463.15	3
3150	57.655	39.162	3003.29	256.14	467.38	488.06	3
3180	60.531	38.166	3018.69	276.23	483.45	513.8	3
3210	63.414	37.225	3032.79	297.19	499.64	540.28	3
3240	66.303	36.331	3045.53	318.94	515.9	567.43	3
3270	69.196	35.475	3056.89	341.43	532.18	595.18	3
3300	72.094	34.652	3066.83	364.59	548.43	623.45	3
3330	74.995	33.855	3075.33	388.37	564.62	652.17	3
3360	77.899	33.079	3082.36	412.7	580.7	681.26	3
3390	80.805	32.32	3087.9	437.51	596.63	710.63	3
3420	83.712	31.574	3091.94	462.73	612.36	740.21	3
3450	86.621	30.836	3094.47	488.3	627.84	769.91	3
3480	89.53	30.102	3095.48	514.14	643.04	799.66	3
3485.08	90.022	29.978	3095.5	518.53	645.59	804.7	3
3510	90.022	29.978	3095.49	540.12	658.04	829.4	0
3540	90.022	29.978	3095.48	566.11	673.03	859.13	0
3570	90.022	29.978	3095.47	592.09	688.02	888.87	0
3600	90.022	29.978	3095.46	618.08	703.01	918.6	0
3630	90.022	29.978	3095.44	644.07	718	948.34	0
3660	90.022	29.978	3095.43	670.05	732.99	978.07	0
3690	90.022	29.978	3095.42	696.04	747.98	1007.81	0
3720	90.022	29.978	3095.41	722.03	762.97	1037.55	0
3750	90.022	29.978	3095.4	748.01	777.96	1067.28	0
3780	90.022	29.978	3095.39	774	792.95	1097.02	0
3810	90.022	29.978	3095.37	799.99	807.94	1126.75	0
3840	90.022	29.978	3095.36	825.97	822.93	1156.49	0
3870	90.022	29.978	3095.35	851.96	837.92	1186.22	0
3900	90.022	29.978	3095.34	877.95	852.91	1215.96	0
3930	90.022	29.978	3095.33	903.93	867.9	1245.7	0
3960	90.022	29.978	3095.32	929.92	882.89	1275.43	0
3990	90.022	29.978	3095.3	955.9	897.88	1305.17	0
4020	90.022	29.978	3095.29	981.89	912.87	1334.9	0
4050	90.022	29.978	3095.28	1007.88	927.86	1364.64	0
4080	90.022	29.978	3095.27	1033.86	942.85	1394.37	0
4110	90.022	29.978	3095.26	1059.85	957.84	1424.11	0
4140	90.022	29.978	3095.25	1085.84	972.83	1453.84	0

4170	90.022	29.978	3095.24	1111.82	987.82	1483.58	0
4200	90.022	29.978	3095.22	1137.81	1002.81	1513.32	0
4230	90.022	29.978	3095.21	1163.8	1017.8	1543.05	0
4260	90.022	29.978	3095.2	1189.78	1032.79	1572.79	0
4290	90.022	29.978	3095.19	1215.77	1047.78	1602.52	0
4320	90.022	29.978	3095.18	1241.76	1062.77	1632.26	0
4350	90.022	29.978	3095.17	1267.74	1077.76	1661.99	0
4380	90.022	29.978	3095.15	1293.73	1092.75	1691.73	0
4410	90.022	29.978	3095.14	1319.72	1107.74	1721.46	0
4440	90.022	29.978	3095.13	1345.7	1122.73	1751.2	0
4470	90.022	29.978	3095.12	1371.69	1137.72	1780.94	0
4500	90.022	29.978	3095.11	1397.68	1152.7	1810.67	0
4530	90.022	29.978	3095.1	1423.66	1167.69	1840.41	0
4560	90.022	29.978	3095.08	1449.65	1182.68	1870.14	0
4590	90.022	29.978	3095.07	1475.64	1197.67	1899.88	0
4620	90.022	29.978	3095.06	1501.62	1212.66	1929.61	0
4650	90.022	29.978	3095.05	1527.61	1227.65	1959.35	0
4680	90.022	29.978	3095.04	1553.6	1242.64	1989.09	0
4710	90.022	29.978	3095.03	1579.58	1257.63	2018.82	0
4740	90.022	29.978	3095.01	1605.57	1272.62	2048.56	0
4770	90.022	29.978	3095	1631.56	1287.61	2078.29	0
4800	90.022	29.978	3094.99	1657.54	1302.6	2108.03	0
4830	90.022	29.978	3094.98	1683.53	1317.59	2137.76	0
4860	90.022	29.978	3094.97	1709.52	1332.58	2167.5	0
4890	90.022	29.978	3094.96	1735.5	1347.57	2197.23	0
4920	90.022	29.978	3094.95	1761.49	1362.56	2226.97	0
4950	90.022	29.978	3094.93	1787.48	1377.55	2256.71	0
4958.99	90.022	29.978	3094.93	1795.26	1382.04	2265.61	0

VII.2. **Trajectory of Well #1b (#2)**

Depth (m)	Inclination $(°)$	Azimuth $(°)$	TVD (m)	North (m)	East (m)	VS (m)	DLS $(°/30m)$
1170	0	0	1170	0	0	0	0
1800	0	0	1800	0	0	0	0
1830	3	94.204	1829.99	-0.06	0.78	0.63	3
1860	6	94.204	1859.89	-0.23	3.13	2.52	3
1890	9	94.204	1889.63	-0.52	7.04	5.67	3
1920	12	94.204	1919.12	-0.92	12.49	10.06	3
1950	15	94.204	1948.29	-1.43	19.47	15.69	3
1980	18	94.204	1977.05	-2.06	27.97	22.53	3
2010	21	94.204	2005.33	-2.79	37.95	30.57	3
2040	24	94.204	2033.04	-3.63	49.4	39.8	3
2070	27	94.204	2060.12	-4.58	62.28	50.17	3
2087.18	28.718	94.204	2075.3	-5.17	70.28	56.62	3
2100	28.718	94.204	2086.55	-5.62	76.43	61.57	0
2130	28.718	94.204	2112.86	-6.68	90.81	73.15	0
2160	28.718	94.204	2139.17	-7.73	105.18	84.73	0
2190	28.718	94.204	2165.48	-8.79	119.56	96.31	0
2220	28.718	94.204	2191.79	-9.85	133.93	107.9	0
2250	28.718	94.204	2218.1	-10.9	148.31	119.48	0
2280	28.718	94.204	2244.41	-11.96	162.69	131.06	0
2310	28.718	94.204	2270.72	-13.02	177.06	142.64	0
2340	28.718	94.204	2297.03	-14.07	191.44	154.22	0
2370	28.718	94.204	2323.34	-15.13	205.81	165.8	0
2400	28.718	94.204	2349.65	-16.19	220.19	177.38	0
2430	28.718	94.204	2375.96	-17.24	234.57	188.96	0
2460	28.718	94.204	2402.27	-18.3	248.94	200.54	0
2490	28.718	94.204	2428.58	-19.36	263.32	212.12	0
2520	28.718	94.204	2454.89	-20.41	277.69	223.71	0
2550	28.718	94.204	2481.2	-21.47	292.07	235.29	0
2580	28.718	94.204	2507.51	-22.53	306.45	246.87	0
2610	28.718	94.204	2533.82	-23.58	320.82	258.45	0
2640	28.718	94.204	2560.13	-24.64	335.2	270.03	0
2670	28.718	94.204	2586.44	-25.7	349.57	281.61	0
2700	28.718	94.204	2612.75	-26.75	363.95	293.19	0
2710.49	28.718	94.204	2621.94	-27.12	368.97	297.24	0
2730	27.718	90.659	2639.14	-27.52	378.19	304.81	3
2760	26.373	84.757	2665.86	-26.99	391.8	316.6	3
2790	25.292	78.331	2692.87	-25.08	404.72	328.53	3
2820	24.511	71.448	2720.09	-21.81	416.9	340.57	3
2850	24.059	64.232	2747.44	-17.17	428.31	352.69	3
2880	23.954	56.859	2774.85	-11.18	438.91	364.86	3
2910	24.201	49.526	2802.25	-3.86	448.69	377.04	3
2940	24.79	42.427	2829.55	4.78	457.62	389.2	3

2970	25.697	35.717	2856.69	14.7	465.66	401.3	3
3000	26.89	29.499	2883.59	25.89	472.8	413.32	3
3030	28.332	23.819	2910.18	38.31	479.02	425.22	3
3060	29.987	18.681	2936.38	51.93	484.29	436.96	3
3090	31.822	14.058	2962.13	66.71	488.62	448.52	3
3120	33.808	9.905	2987.34	82.61	491.97	459.86	3
3150	35.918	6.174	3011.96	99.58	494.36	470.95	3
3180	38.133	2.812	3035.91	117.58	495.76	481.76	3
3210	40.435	359.772	3059.13	136.57	496.17	492.27	3
3227.16	41.785	358.16	3072.06	147.85	495.97	498.13	3
3240	41.785	358.16	3081.63	156.4	495.69	502.47	0
3270	41.785	358.16	3104	176.38	495.05	512.62	0
3300	41.785	358.16	3126.37	196.36	494.41	522.76	0
3330	41.785	358.16	3148.74	216.34	493.77	532.91	0
3360	41.785	358.16	3171.11	236.32	493.13	543.05	0
3390	41.785	358.16	3193.48	256.3	492.48	553.2	0
3420	41.785	358.16	3215.85	276.28	491.84	563.34	0
3450	41.785	358.16	3238.22	296.26	491.2	573.49	0
3471.67	41.785	358.16	3254.38	310.69	490.74	580.82	0

VII.3. **Trajectory of Well #1c (#3)**

Depth (m)	Inclination (°)	Azimuth (°)	TVD (m)	North (m)	East (m)	VS (m)	DLS $(°/30m)$
1170	0	0	1170	0	0	0	0
1800	0	0	1800	0	0	0	0
1830	3	319.358	1829.99	0.6	-0.51	0.78	3
1860	6	319.358	1859.89	2.38	-2.04	3.14	3
1890	9	319.358	1889.63	5.35	-4.59	7.05	3
1920	12	319.358	1919.12	9.5	-8.15	12.52	3
1950	15	319.358	1948.29	14.81	-12.72	19.52	3
1980	18	319.358	1977.05	21.28	-18.26	28.03	3
2010	21	319.358	2005.33	28.88	-24.79	38.04	3
2040	24	319.358	2033.04	37.59	-32.26	49.51	3
2070	27	319.358	2060.12	47.39	-40.67	62.42	3
2075.81	27.581	319.358	2065.28	49.41	-42.41	65.09	3
2100	27.581	319.358	2086.72	57.91	-49.7	76.28	0
2130	27.581	319.358	2113.31	68.45	-58.75	90.17	0
2160	27.581	319.358	2139.9	78.98	-67.8	104.05	0
2190	27.581	319.358	2166.49	89.52	-76.85	117.94	0
2220	27.581	319.358	2193.08	100.06	-85.89	131.82	0
2250	27.581	319.358	2219.68	110.6	-94.94	145.7	0
2280	27.581	319.358	2246.27	121.14	-103.99	159.59	0
2310	27.581	319.358	2272.86	131.68	-113.03	173.47	0
2340	27.581	319.358	2299.45	142.22	-122.08	187.36	0
2370	27.581	319.358	2326.04	152.76	-131.13	201.24	0
2400	27.581	319.358	2352.63	163.3	-140.17	215.13	0
2430	27.581	319.358	2379.22	173.84	-149.22	229.01	0
2460	27.581	319.358	2405.81	184.38	-158.27	242.9	0
2490	27.581	319.358	2432.4	194.92	-167.32	256.78	0
2520	27.581	319.358	2458.99	205.46	-176.36	270.66	0
2550	27.581	319.358	2485.58	216	-185.41	284.55	0
2580	27.581	319.358	2512.17	226.54	-194.46	298.43	0
2610	27.581	319.358	2538.76	237.08	-203.5	312.32	0
2640	27.581	319.358	2565.36	247.62	-212.55	326.2	0
2670	27.581	319.358	2591.95	258.16	-221.6	340.09	0
2700	27.581	319.358	2618.54	268.7	-230.64	353.97	0
2730	27.581	319.358	2645.13	279.24	-239.69	367.86	0
2760	27.581	319.358	2671.72	289.78	-248.74	381.74	0
2790	27.581	319.358	2698.31	300.32	-257.79	395.62	0
2820	27.581	319.358	2724.9	310.86	-266.83	409.51	0
2848.88	27.581	319.358	2750.5	321	-275.54	422.87	0
2850	27.693	319.371	2751.49	321.4	-275.88	423.39	3
2880	30.689	319.694	2777.68	332.53	-285.37	438.02	3
2910	33.685	319.965	2803.06	344.74	-295.68	453.99	3
2940	36.682	320.197	2827.58	358	-306.77	471.28	3

2970	39.68	320.398	2851.16	372.26	-318.61	489.82	3
3000	42.677	320.575	2873.74	387.5	-331.18	509.57	3
3030	45.675	320.733	2895.25	403.67	-344.43	530.47	3
3060	48.674	320.875	2915.64	420.72	-358.34	552.47	3
3090	51.672	321.005	2934.85	438.6	-372.85	575.51	3
3120	54.67	321.125	2952.83	457.28	-387.94	599.52	3
3150	57.669	321.236	2969.53	476.7	-403.56	624.44	3
3180	60.668	321.341	2984.91	496.79	-419.67	650.19	3
3210	63.666	321.439	2998.91	517.52	-436.22	676.72	3
3240	66.665	321.532	3011.51	538.82	-453.17	703.94	3
3270	69.664	321.621	3022.67	560.64	-470.48	731.78	3
3300	72.663	321.706	3032.35	582.91	-488.09	760.17	3
3330	75.662	321.789	3040.54	605.57	-505.95	789.03	3
3344.18	77.079	321.828	3043.88	616.4	-514.47	802.8	3
3360	77.079	321.828	3047.42	628.52	-524	818.22	0
3390	77.079	321.828	3054.13	651.51	-542.07	847.46	0
3420	77.079	321.828	3060.83	674.5	-560.15	876.7	0
3450	77.079	321.828	3067.54	697.48	-578.22	905.93	0
3480	77.079	321.828	3074.25	720.47	-596.29	935.17	0
3510	77.079	321.828	3080.96	743.46	-614.36	964.41	0
3540	77.079	321.828	3087.67	766.45	-632.43	993.65	0
3570	77.079	321.828	3094.37	789.43	-650.5	1022.88	0
3600	77.079	321.828	3101.08	812.42	-668.57	1052.12	0
3630	77.079	321.828	3107.79	835.41	-686.65	1081.36	0
3660	77.079	321.828	3114.5	858.4	-704.72	1110.59	0
3690	77.079	321.828	3121.21	881.38	-722.79	1139.83	0
3720	77.079	321.828	3127.91	904.37	-740.86	1169.07	0
3750	77.079	321.828	3134.62	927.36	-758.93	1198.31	0
3780	77.079	321.828	3141.33	950.35	-777	1227.54	0
3810	77.079	321.828	3148.04	973.33	-795.07	1256.78	0
3840	77.079	321.828	3154.75	996.32	-813.15	1286.02	0
3870	77.079	321.828	3161.45	1019.31	-831.22	1315.26	0
3900	77.079	321.828	3168.16	1042.3	-849.29	1344.49	0
3930	77.079	321.828	3174.87	1065.28	-867.36	1373.73	0
3960	77.079	321.828	3181.58	1088.27	-885.43	1402.97	0
3990	77.079	321.828	3188.29	1111.26	-903.5	1432.2	0
4020	77.079	321.828	3194.99	1134.25	-921.57	1461.44	0
4050	77.079	321.828	3201.7	1157.23	-939.65	1490.68	0
4080	77.079	321.828	3208.41	1180.22	-957.72	1519.92	0
4110	77.079	321.828	3215.12	1203.21	-975.79	1549.15	0
4140	77.079	321.828	3221.83	1226.2	-993.86	1578.39	0
4147.22	77.079	321.828	3223.44	1231.73	-998.21	1585.42	0

VII.4. **Trajectory of Well #1d (#4)**

Depth (m)	Inclination (°)	Azimuth (°)	TVD (m)	North (m)	East (m)	VS (m)	DLS $(°/30m)$
1170	0	0	1170	0	0	0	0
1800	0	0	1800	0	0	0	0
1830	3	342.967	1829.99	0.75	-0.23	0.77	3
1860	6	342.967	1859.89	3	-0.92	3.07	3
1890	9	342.967	1889.63	6.74	-2.07	6.91	3
1920	12	342.967	1919.12	11.97	-3.67	12.26	3
1950	15	342.967	1948.29	18.67	-5.72	19.11	3
1980	18	342.967	1977.05	26.81	-8.21	27.45	3
2010	21	342.967	2005.33	36.39	-11.15	37.26	3
2040	24	342.967	2033.04	47.36	-14.51	48.5	3
2070	27	342.967	2060.12	59.71	-18.29	61.14	3
2100	30	342.967	2086.48	73.39	-22.49	75.15	3
2130	33	342.967	2112.06	88.38	-27.08	90.5	3
2160	36	342.967	2136.78	104.63	-32.05	107.13	3
2190	39	342.967	2160.57	122.09	-37.4	125.01	3
2220	42	342.967	2183.38	140.71	-43.11	144.08	3
2250	45	342.967	2205.14	160.45	-49.16	164.3	3
2280	48	342.967	2225.79	181.26	-55.53	185.6	3
2310	51	342.967	2245.27	203.07	-62.21	207.93	3
2337.36	53.736	342.967	2261.97	223.78	-68.56	229.14	3
2340	53.736	342.967	2263.54	225.82	-69.18	231.23	0
2370	53.736	342.967	2281.28	248.95	-76.27	254.91	0
2400	53.736	342.967	2299.03	272.07	-83.35	278.59	0
2430	53.736	342.967	2316.77	295.2	-90.44	302.27	0
2460	53.736	342.967	2334.52	318.33	-97.52	325.96	0
2490	53.736	342.967	2352.26	341.46	-104.61	349.64	0
2520	53.736	342.967	2370.01	364.59	-111.7	373.32	0
2550	53.736	342.967	2387.75	387.71	-118.78	397	0
2580	53.736	342.967	2405.5	410.84	-125.87	420.68	0
2610	53.736	342.967	2423.24	433.97	-132.95	444.37	0
2640	53.736	342.967	2440.99	457.1	-140.04	468.05	0
2670	53.736	342.967	2458.74	480.23	-147.12	491.73	0
2700	53.736	342.967	2476.48	503.35	-154.21	515.41	0
2730	53.736	342.967	2494.23	526.48	-161.29	539.09	0
2760	53.736	342.967	2511.97	549.61	-168.38	562.78	0
2790	53.736	342.967	2529.72	572.74	-175.47	586.46	0
2820	53.736	342.967	2547.46	595.86	-182.55	610.14	0
2850	53.736	342.967	2565.21	618.99	-189.64	633.82	0
2880	53.736	342.967	2582.95	642.12	-196.72	657.5	0
2910	53.736	342.967	2600.7	665.25	-203.81	681.19	0
2940	53.736	342.967	2618.44	688.38	-210.89	704.87	0
2970	53.736	342.967	2636.19	711.5	-217.98	728.55	0

3000	53.736	342.967	2653.93	734.63	-225.06	752.23	0
3030	53.736	342.967	2671.68	757.76	-232.15	775.91	0
3060	53.736	342.967	2689.42	780.89	-239.23	799.6	0
3090	53.736	342.967	2707.17	804.02	-246.32	823.28	0
3120	53.736	342.967	2724.91	827.14	-253.41	846.96	0
3150	53.736	342.967	2742.66	850.27	-260.49	870.64	0
3180	53.736	342.967	2760.41	873.4	-267.58	894.32	0
3210	53.736	342.967	2778.15	896.53	-274.66	918.01	0
3240	53.736	342.967	2795.9	919.66	-281.75	941.69	0
3270	53.736	342.967	2813.64	942.78	-288.83	965.37	0
3300	53.736	342.967	2831.39	965.91	-295.92	989.05	0
3330	53.736	342.967	2849.13	989.04	-303	1012.73	0
3360	53.736	342.967	2866.88	1012.17	-310.09	1036.42	0
3390	53.736	342.967	2884.62	1035.3	-317.18	1060.1	0
3420	53.736	342.967	2902.37	1058.42	-324.26	1083.78	0
3450	53.736	342.967	2920.11	1081.55	-331.35	1107.46	0
3480	53.736	342.967	2937.86	1104.68	-338.43	1131.14	0
3510	53.736	342.967	2955.6	1127.81	-345.52	1154.83	0
3518.99	53.736	342.967	2960.92	1134.74	-347.64	1161.93	0
3540	55.096	344.936	2973.15	1151.16	-352.36	1178.71	3
3570	57.09	347.636	2989.88	1175.34	-358.26	1203.33	3
3600	59.14	350.216	3005.73	1200.34	-363.14	1228.67	3
3630	61.239	352.686	3020.65	1226.08	-367.01	1254.65	3
3660	63.382	355.059	3034.59	1252.48	-369.84	1281.21	3
3690	65.562	357.343	3047.52	1279.49	-371.62	1308.27	3
3720	67.775	359.548	3059.4	1307.03	-372.37	1335.75	3
3750	70.017	1.685	3070.2	1335.01	-372.06	1363.59	3
3780	72.284	3.762	3079.89	1363.36	-370.71	1391.7	3
3810	74.572	5.786	3088.45	1392.01	-368.31	1420.01	3
3840	76.878	7.766	3095.85	1420.88	-364.88	1448.44	3
3870	79.199	9.71	3102.07	1449.88	-360.42	1476.91	3
3900	81.532	11.623	3107.09	1478.95	-354.95	1505.34	3
3930	83.874	13.513	3110.9	1507.99	-348.47	1533.66	3
3942.66	84.865	14.306	3112.14	1520.22	-345.44	1545.56	3
3960	84.865	14.306	3113.69	1536.95	-341.17	1561.83	0
3990	84.865	14.306	3116.38	1565.9	-333.79	1589.98	0
4020	84.865	14.306	3119.06	1594.86	-326.41	1618.13	0
4050	84.865	14.306	3121.75	1623.81	-319.02	1646.28	0
4080	84.865	14.306	3124.43	1652.76	-311.64	1674.43	0
4110	84.865	14.306	3127.12	1681.72	-304.26	1702.58	0
4140	84.865	14.306	3129.8	1710.67	-296.88	1730.73	0
4170	84.865	14.306	3132.49	1739.62	-289.49	1758.88	0
4200	84.865	14.306	3135.17	1768.58	-282.11	1787.04	0
4230	84.865	14.306	3137.86	1797.53	-274.73	1815.19	0
4260	84.865	14.306	3140.54	1826.48	-267.34	1843.34	0
4290	84.865	14.306	3143.23	1855.43	-259.96	1871.49	0

4320	84.865	14.306	3145.91	1884.39	-252.58	1899.64	0
4350	84.865	14.306	3148.6	1913.34	-245.19	1927.79	0
4380	84.865	14.306	3151.28	1942.29	-237.81	1955.94	0
4410	84.865	14.306	3153.97	1971.25	-230.43	1984.09	0
4440	84.865	14.306	3156.65	2000.2	-223.04	2012.24	0
4470	84.865	14.306	3159.34	2029.15	-215.66	2040.39	0
4500	84.865	14.306	3162.02	2058.11	-208.28	2068.54	0
4530	84.865	14.306	3164.71	2087.06	-200.9	2096.69	0
4553.71	84.865	14.306	3166.83	2109.94	-195.06	2118.94	0

VII.5. **Trajectory of Well #2a (#5)**

Depth (m)	Inclination $(°)$	Azimuth $(°)$	TVD (m)	North (m)	East (m)	VS (m)	DLS $(°/30m)$
1170	0	0	1170	0	0	0	0
1800	0	0	1800	0	0	0	0
1830	3	356.123	1829.99	0.78	-0.05	0.74	3
1860	6	356.123	1859.89	3.13	-0.21	2.97	3
1890	9	356.123	1889.63	7.04	-0.48	6.67	3
1920	12	356.123	1919.12	12.49	-0.85	11.84	3
1950	15	356.123	1948.29	19.48	-1.32	18.46	3
1980	18	356.123	1977.05	27.98	-1.9	26.52	3
2010	21	356.123	2005.33	37.97	-2.57	35.99	3
2040	24	356.123	2033.04	49.42	-3.35	46.84	3
2070	27	356.123	2060.12	62.31	-4.22	59.06	3
2100	30	356.123	2086.48	76.59	-5.19	72.59	3
2130	33	356.123	2112.06	92.22	-6.25	87.41	3
2160	36	356.123	2136.78	109.17	-7.4	103.48	3
2190	39	356.123	2160.57	127.39	-8.63	120.75	3
2220	42	356.123	2183.38	146.83	-9.95	139.17	3
2250	45	356.123	2205.14	167.43	-11.35	158.7	3
2280	48	356.123	2225.79	189.14	-12.82	179.28	3
2310	51	356.123	2245.27	211.9	-14.36	200.85	3
2340	54	356.123	2263.53	235.64	-15.97	223.35	3
2370	57	356.123	2280.52	260.31	-17.64	246.73	3
2400	60	356.123	2296.2	285.82	-19.37	270.92	3
2430	63	356.123	2310.51	312.12	-21.15	295.85	3
2460	66	356.123	2323.42	339.14	-22.98	321.45	3
2490	69	356.123	2334.9	366.79	-24.85	347.66	3
2497.07	69.707	356.123	2337.4	373.39	-25.3	353.92	3
2520	69.707	356.123	2345.35	394.85	-26.76	374.25	0
2550	69.707	356.123	2355.75	422.92	-28.66	400.86	0
2580	69.707	356.123	2366.16	450.99	-30.56	427.47	0
2610	69.707	356.123	2376.56	479.07	-32.46	454.08	0
2640	69.707	356.123	2386.96	507.14	-34.37	480.69	0
2670	69.707	356.123	2397.37	535.21	-36.27	507.3	0
2700	69.707	356.123	2407.77	563.29	-38.17	533.91	0
2730	69.707	356.123	2418.18	591.36	-40.07	560.52	0
2760	69.707	356.123	2428.58	619.43	-41.97	587.13	0
2790	69.707	356.123	2438.99	647.51	-43.88	613.74	0
2820	69.707	356.123	2449.39	675.58	-45.78	640.35	0
2850	69.707	356.123	2459.8	703.66	-47.68	666.96	0
2880	69.707	356.123	2470.2	731.73	-49.58	693.57	0
2910	69.707	356.123	2480.6	759.8	-51.49	720.18	0
2940	69.707	356.123	2491.01	787.88	-53.39	746.79	0
2970	69.707	356.123	2501.41	815.95	-55.29	773.4	0

3000	69.707	356.123	2511.82	844.02	-57.19	800.01	0
3030	69.707	356.123	2522.22	872.1	-59.1	826.62	0
3060	69.707	356.123	2532.63	900.17	-61	853.23	0
3090	69.707	356.123	2543.03	928.24	-62.9	879.84	0
3120	69.707	356.123	2553.44	956.32	-64.8	906.45	0
3150	69.707	356.123	2563.84	984.39	-66.7	933.06	0
3180	69.707	356.123	2574.24	1012.47	-68.61	959.66	0
3210	69.707	356.123	2584.65	1040.54	-70.51	986.27	0
3240	69.707	356.123	2595.05	1068.61	-72.41	1012.88	0
3270	69.707	356.123	2605.46	1096.69	-74.31	1039.49	0
3300	69.707	356.123	2615.86	1124.76	-76.22	1066.1	0
3330	69.707	356.123	2626.27	1152.83	-78.12	1092.71	0
3360	69.707	356.123	2636.67	1180.91	-80.02	1119.32	0
3390	69.707	356.123	2647.08	1208.98	-81.92	1145.93	0
3420	69.707	356.123	2657.48	1237.05	-83.83	1172.54	0
3450	69.707	356.123	2667.88	1265.13	-85.73	1199.15	0
3480	69.707	356.123	2678.29	1293.2	-87.63	1225.76	0
3510	69.707	356.123	2688.69	1321.28	-89.53	1252.37	0
3540	69.707	356.123	2699.1	1349.35	-91.44	1278.98	0
3570	69.707	356.123	2709.5	1377.42	-93.34	1305.59	0
3600	69.707	356.123	2719.91	1405.5	-95.24	1332.2	0
3630	69.707	356.123	2730.31	1433.57	-97.14	1358.81	0
3660	69.707	356.123	2740.72	1461.64	-99.04	1385.42	0
3690	69.707	356.123	2751.12	1489.72	-100.95	1412.03	0
3720	69.707	356.123	2761.52	1517.79	-102.85	1438.64	0
3750	69.707	356.123	2771.93	1545.86	-104.75	1465.25	0
3780	69.707	356.123	2782.33	1573.94	-106.65	1491.86	0
3810	69.707	356.123	2792.74	1602.01	-108.56	1518.47	0
3840	69.707	356.123	2803.14	1630.09	-110.46	1545.08	0
3870	69.707	356.123	2813.55	1658.16	-112.36	1571.69	0
3900	69.707	356.123	2823.95	1686.23	-114.26	1598.3	0
3930	69.707	356.123	2834.35	1714.31	-116.17	1624.9	0
3960	69.707	356.123	2844.76	1742.38	-118.07	1651.51	0
3990	69.707	356.123	2855.16	1770.45	-119.97	1678.12	0
4020	69.707	356.123	2865.57	1798.53	-121.87	1704.73	0
4050	69.707	356.123	2875.97	1826.6	-123.78	1731.34	0
4080	69.707	356.123	2886.38	1854.67	-125.68	1757.95	0
4110	69.707	356.123	2896.78	1882.75	-127.58	1784.56	0
4140	69.707	356.123	2907.19	1910.82	-129.48	1811.17	0
4170	69.707	356.123	2917.59	1938.9	-131.38	1837.78	0
4200	69.707	356.123	2927.99	1966.97	-133.29	1864.39	0
4230	69.707	356.123	2938.4	1995.04	-135.19	1891	0
4255.3	69.707	356.123	2947.17	2018.72	-136.79	1913.44	0
4260	69.86	356.597	2948.8	2023.12	-137.07	1917.62	3
4290	70.865	359.599	2958.88	2051.36	-138.01	1944.64	3
4320	71.917	2.563	2968.46	2079.78	-137.47	1972.22	3

4350	73.014	5.492	2977.5	2108.31	-135.46	2000.29	3
4380	74.152	8.385	2985.98	2136.87	-131.98	2028.77	3
4410	75.329	11.246	2993.87	2165.38	-127.05	2057.59	3
4440	76.54	14.076	3001.17	2193.77	-120.67	2086.66	3
4470	77.782	16.877	3007.83	2221.96	-112.86	2115.9	3
4500	79.052	19.651	3013.86	2249.86	-103.65	2145.24	3
4530	80.347	22.401	3019.22	2277.41	-93.06	2174.6	3
4560	81.664	25.13	3023.91	2304.53	-81.12	2203.89	3
4590	83	27.841	3027.92	2331.13	-67.86	2233.03	3
4620	84.35	30.536	3031.22	2357.16	-53.32	2261.94	3
4650	85.713	33.219	3033.82	2382.54	-37.54	2290.55	3
4680	87.086	35.892	3035.71	2407.19	-20.56	2318.78	3
4682.69	87.209	36.131	3035.84	2409.37	-18.97	2321.29	3
4710	87.209	36.131	3037.17	2431.4	-2.89	2346.75	0
4740	87.209	36.131	3038.63	2455.6	14.78	2374.72	0
4770	87.209	36.131	3040.09	2479.8	32.44	2402.69	0
4800	87.209	36.131	3041.55	2504	50.11	2430.65	0
4830	87.209	36.131	3043.01	2528.2	67.78	2458.62	0
4860	87.209	36.131	3044.47	2552.4	85.45	2486.59	0
4890	87.209	36.131	3045.93	2576.6	103.12	2514.56	0
4920	87.209	36.131	3047.39	2600.81	120.79	2542.52	0
4950	87.209	36.131	3048.85	2625.01	138.45	2570.49	0
4980	87.209	36.131	3050.32	2649.21	156.12	2598.46	0
5010	87.209	36.131	3051.78	2673.41	173.79	2626.42	0
5040	87.209	36.131	3053.24	2697.61	191.46	2654.39	0
5070	87.209	36.131	3054.7	2721.81	209.13	2682.36	0
5100	87.209	36.131	3056.16	2746.01	226.8	2710.33	0
5130	87.209	36.131	3057.62	2770.21	244.46	2738.29	0
5160	87.209	36.131	3059.08	2794.42	262.13	2766.26	0
5190	87.209	36.131	3060.54	2818.62	279.8	2794.23	0
5220	87.209	36.131	3062	2842.82	297.47	2822.2	0
5250	87.209	36.131	3063.46	2867.02	315.14	2850.16	0
5280	87.209	36.131	3064.92	2891.22	332.8	2878.13	0
5310	87.209	36.131	3066.38	2915.42	350.47	2906.1	0
5340	87.209	36.131	3067.84	2939.62	368.14	2934.07	0
5370	87.209	36.131	3069.3	2963.82	385.81	2962.03	0
5400	87.209	36.131	3070.76	2988.03	403.48	2990	0
5430	87.209	36.131	3072.22	3012.23	421.15	3017.97	0
5460	87.209	36.131	3073.68	3036.43	438.81	3045.93	0
5490	87.209	36.131	3075.15	3060.63	456.48	3073.9	0
5520	87.209	36.131	3076.61	3084.83	474.15	3101.87	0
5550	87.209	36.131	3078.07	3109.03	491.82	3129.84	0
5580	87.209	36.131	3079.53	3133.23	509.49	3157.8	0
5610	87.209	36.131	3080.99	3157.43	527.15	3185.77	0
5640	87.209	36.131	3082.45	3181.64	544.82	3213.74	0
5670	87.209	36.131	3083.91	3205.84	562.49	3241.71	0

5700	87.209	36.131	3085.37	3230.04	580.16	3269.67	0
5730	87.209	36.131	3086.83	3254.24	597.83	3297.64	0
5760	87.209	36.131	3088.29	3278.44	615.5	3325.61	0
5790	87.209	36.131	3089.75	3302.64	633.16	3353.58	0
5820	87.209	36.131	3091.21	3326.84	650.83	3381.54	0
5850	87.209	36.131	3092.67	3351.04	668.5	3409.51	0
5880	87.209	36.131	3094.13	3375.25	686.17	3437.48	0
5910	87.209	36.131	3095.59	3399.45	703.84	3465.44	0
5940	87.209	36.131	3097.05	3423.65	721.5	3493.41	0
5970	87.209	36.131	3098.52	3447.85	739.17	3521.38	0
6000	87.209	36.131	3099.98	3472.05	756.84	3549.35	0
6030	87.209	36.131	3101.44	3496.25	774.51	3577.31	0
6060	87.209	36.131	3102.9	3520.45	792.18	3605.28	0
6090	87.209	36.131	3104.36	3544.65	809.85	3633.25	0
6120	87.209	36.131	3105.82	3568.86	827.51	3661.22	0
6150	87.209	36.131	3107.28	3593.06	845.18	3689.18	0
6180	87.209	36.131	3108.74	3617.26	862.85	3717.15	0
6210	87.209	36.131	3110.2	3641.46	880.52	3745.12	0
6240	87.209	36.131	3111.66	3665.66	898.19	3773.09	0
6270	87.209	36.131	3113.12	3689.86	915.85	3801.05	0
6300	87.209	36.131	3114.58	3714.06	933.52	3829.02	0
6330	87.209	36.131	3116.04	3738.26	951.19	3856.99	0
6360	87.209	36.131	3117.5	3762.47	968.86	3884.95	0
6390	87.209	36.131	3118.96	3786.67	986.53	3912.92	0
6420	87.209	36.131	3120.42	3810.87	1004.2	3940.89	0
6450	87.209	36.131	3121.89	3835.07	1021.86	3968.86	0
6480	87.209	36.131	3123.35	3859.27	1039.53	3996.82	0
6483.78	87.209	36.131	3123.53	3862.32	1041.76	4000.35	0

VII.6. **Trajectory of Well #2b (#6)**

Depth (m)	Inclination (°)	Azimuth (°)	TVD (m)	North (m)	East (m)	VS (m)	DLS $(°/30m)$
1170	0	0	1170	0	0	0	0
1800	0	0	1800	0	0	0	0
1830	3	315.615	1829.99	0.56	-0.55	0.7	3
1860	6	315.615	1859.89	2.24	-2.2	2.79	3
1890	9	315.615	1889.63	5.04	-4.93	6.27	3
1920	12	315.615	1919.12	8.95	-8.76	11.12	3
1950	15	315.615	1948.29	13.95	-13.66	17.34	3
1980	18	315.615	1977.05	20.04	-19.62	24.91	3
2010	21	315.615	2005.33	27.2	-26.62	33.8	3
2040	24	315.615	2033.04	35.4	-34.65	44	3
2070	27	315.615	2060.12	44.63	-43.68	55.47	3
2097.13	29.713	315.615	2083.99	53.84	-52.69	66.92	3
2100	29.713	315.615	2086.48	54.85	-53.69	68.18	0
2130	29.713	315.615	2112.54	65.48	-64.09	81.39	0
2160	29.713	315.615	2138.59	76.11	-74.49	94.6	0
2190	29.713	315.615	2164.65	86.73	-84.89	107.81	0
2220	29.713	315.615	2190.7	97.36	-95.29	121.02	0
2250	29.713	315.615	2216.76	107.99	-105.69	134.23	0
2280	29.713	315.615	2242.82	118.61	-116.1	147.43	0
2310	29.713	315.615	2268.87	129.24	-126.5	160.64	0
2340	29.713	315.615	2294.93	139.87	-136.9	173.85	0
2370	29.713	315.615	2320.98	150.49	-147.3	187.06	0
2400	29.713	315.615	2347.04	161.12	-157.7	200.27	0
2430	29.713	315.615	2373.09	171.75	-168.1	213.48	0
2460	29.713	315.615	2399.15	182.38	-178.5	226.69	0
2490	29.713	315.615	2425.2	193	-188.9	239.9	0
2520	29.713	315.615	2451.26	203.63	-199.3	253.11	0
2550	29.713	315.615	2477.31	214.26	-209.71	266.31	0
2580	29.713	315.615	2503.37	224.88	-220.11	279.52	0
2610	29.713	315.615	2529.43	235.51	-230.51	292.73	0
2640	29.713	315.615	2555.48	246.14	-240.91	305.94	0
2670	29.713	315.615	2581.54	256.76	-251.31	319.15	0
2700	29.713	315.615	2607.59	267.39	-261.71	332.36	0
2730	29.713	315.615	2633.65	278.02	-272.11	345.57	0
2741.39	29.713	315.615	2643.54	282.05	-276.06	350.58	0
2760	30.868	318.509	2659.61	288.92	-282.45	359.03	3
2790	32.854	322.771	2685.09	301.17	-292.47	373.67	3
2820	34.969	326.587	2709.99	314.83	-302.13	389.56	3
2850	37.192	330.01	2734.24	329.86	-311.4	406.65	3
2880	39.503	333.095	2757.77	346.23	-320.25	424.89	3
2910	41.888	335.887	2780.51	363.88	-328.67	444.24	3
2940	44.334	338.428	2802.41	382.78	-336.61	464.63	3

2970	46.833	340.755	2823.41	402.86	-344.08	486.02	3
3000	49.374	342.896	2843.44	424.07	-351.03	508.34	3
3030	51.952	344.88	2862.46	446.36	-357.46	531.54	3
3060	54.562	346.728	2880.4	469.67	-363.35	555.54	3
3090	57.197	348.459	2897.23	493.92	-368.68	580.29	3
3120	59.855	350.09	2912.89	519.06	-373.44	605.72	3
3150	62.533	351.636	2927.35	545.01	-377.6	631.75	3
3180	65.226	353.107	2940.56	571.7	-381.18	658.32	3
3210	67.933	354.516	2952.48	599.07	-384.14	685.35	3
3240	70.652	355.872	2963.09	627.03	-386.49	712.77	3
3270	73.381	357.183	2972.35	655.51	-388.21	740.51	3
3300	76.117	358.457	2980.24	684.43	-389.31	768.48	3
3330	78.86	359.702	2986.74	713.71	-389.78	796.61	3
3360	81.608	0.923	2991.83	743.27	-389.62	824.83	3
3390	84.36	2.128	2995.49	773.03	-388.82	853.05	3
3420	87.114	3.32	2997.72	802.91	-387.4	881.2	3
3447.75	89.663	4.419	2998.5	830.59	-385.53	907.11	3
3450	89.663	4.419	2998.51	832.83	-385.36	909.2	0
3480	89.663	4.419	2998.69	862.74	-383.05	937.12	0
3510	89.663	4.419	2998.87	892.65	-380.73	965.04	0
3540	89.663	4.419	2999.04	922.56	-378.42	992.96	0
3570	89.663	4.419	2999.22	952.47	-376.11	1020.88	0
3600	89.663	4.419	2999.39	982.38	-373.8	1048.8	0
3630	89.663	4.419	2999.57	1012.29	-371.49	1076.71	0
3660	89.663	4.419	2999.75	1042.2	-369.18	1104.63	0
3690	89.663	4.419	2999.92	1072.11	-366.87	1132.55	0
3720	89.663	4.419	3000.1	1102.02	-364.56	1160.47	0
3750	89.663	4.419	3000.28	1131.93	-362.24	1188.39	0
3780	89.663	4.419	3000.45	1161.84	-359.93	1216.31	0
3789.73	89.663	4.419	3000.51	1171.54	-359.18	1225.37	0

VII.7. **Trajectory of Well #2c (#7)**

Depth (m)	Inclination (°)	Azimuth (°)	TVD (m)	North (m)	East (m)	VS (m)	DLS $(°/30m)$
1170	0	0	1170	0	0	0	0
1800	0	0	1800	0	0	0	0
1830	3	321.307	1829.99	0.61	-0.49	0.77	3
1860	6	321.307	1859.89	2.45	-1.96	3.08	3
1890	9	321.307	1889.63	5.51	-4.41	6.93	3
1920	12	321.307	1919.12	9.77	-7.83	12.3	3
1950	15	321.307	1948.29	15.24	-12.2	19.18	3
1980	18	321.307	1977.05	21.89	-17.53	27.55	3
2010	21	321.307	2005.33	29.7	-23.79	37.39	3
2040	24	321.307	2033.04	38.66	-30.97	48.67	3
2070	27	321.307	2060.12	48.74	-39.04	61.35	3
2100	30	321.307	2086.48	59.91	-47.99	75.41	3
2130	33	321.307	2112.06	72.15	-57.79	90.81	3
2160	36	321.307	2136.78	85.41	-68.41	107.5	3
2190	39	321.307	2160.57	99.66	-79.82	125.45	3
2220	42	321.307	2183.38	114.86	-92	144.58	3
2250	45	321.307	2205.14	130.98	-104.91	164.87	3
2280	48	321.307	2225.79	147.96	-118.51	186.25	3
2310	51	321.307	2245.27	165.77	-132.77	208.66	3
2340	54	321.307	2263.53	184.34	-147.65	232.04	3
2365.12	56.512	321.307	2277.85	200.45	-160.55	252.31	3
2370	56.512	321.307	2280.54	203.63	-163.1	256.31	0
2400	56.512	321.307	2297.09	223.16	-178.74	280.89	0
2430	56.512	321.307	2313.65	242.68	-194.38	305.47	0
2460	56.512	321.307	2330.2	262.21	-210.02	330.06	0
2490	56.512	321.307	2346.75	281.74	-225.66	354.64	0
2520	56.512	321.307	2363.3	301.27	-241.3	379.22	0
2550	56.512	321.307	2379.86	320.8	-256.94	403.8	0
2580	56.512	321.307	2396.41	340.33	-272.58	428.38	0
2610	56.512	321.307	2412.96	359.85	-288.23	452.96	0
2640	56.512	321.307	2429.52	379.38	-303.87	477.54	0
2670	56.512	321.307	2446.07	398.91	-319.51	502.12	0
2700	56.512	321.307	2462.62	418.44	-335.15	526.7	0
2730	56.512	321.307	2479.18	437.97	-350.79	551.28	0
2760	56.512	321.307	2495.73	457.49	-366.43	575.86	0
2790	56.512	321.307	2512.28	477.02	-382.07	600.45	0
2820	56.512	321.307	2528.83	496.55	-397.71	625.03	0
2850	56.512	321.307	2545.39	516.08	-413.35	649.61	0
2880	56.512	321.307	2561.94	535.61	-429	674.19	0
2910	56.512	321.307	2578.49	555.14	-444.64	698.77	0
2940	56.512	321.307	2595.05	574.66	-460.28	723.35	0
2970	56.512	321.307	2611.6	594.19	-475.92	747.93	0

3000	56.512	321.307	2628.15	613.72	-491.56	772.51	0
3030	56.512	321.307	2644.7	633.25	-507.2	797.09	0
3060	56.512	321.307	2661.26	652.78	-522.84	821.67	0
3090	56.512	321.307	2677.81	672.31	-538.48	846.25	0
3120	56.512	321.307	2694.36	691.83	-554.13	870.84	0
3150	56.512	321.307	2710.92	711.36	-569.77	895.42	0
3180	56.512	321.307	2727.47	730.89	-585.41	920	0
3210	56.512	321.307	2744.02	750.42	-601.05	944.58	0
3240	56.512	321.307	2760.58	769.95	-616.69	969.16	0
3270	56.512	321.307	2777.13	789.48	-632.33	993.74	0
3300	56.512	321.307	2793.68	809	-647.97	1018.32	0
3330	56.512	321.307	2810.23	828.53	-663.61	1042.9	0
3360	56.512	321.307	2826.79	848.06	-679.25	1067.48	0
3390	56.512	321.307	2843.34	867.59	-694.9	1092.06	0
3420	56.512	321.307	2859.89	887.12	-710.54	1116.64	0
3450	56.512	321.307	2876.45	906.65	-726.18	1141.23	0
3480	56.512	321.307	2893	926.17	-741.82	1165.81	0
3510	56.512	321.307	2909.55	945.7	-757.46	1190.39	0
3540	56.512	321.307	2926.1	965.23	-773.1	1214.97	0
3570	56.512	321.307	2942.66	984.76	-788.74	1239.55	0
3600	56.512	321.307	2959.21	1004.29	-804.38	1264.13	0
3630	56.512	321.307	2975.76	1023.81	-820.03	1288.71	0
3660	56.512	321.307	2992.32	1043.34	-835.67	1313.29	0
3690	56.512	321.307	3008.87	1062.87	-851.31	1337.87	0
3720	56.512	321.307	3025.42	1082.4	-866.95	1362.45	0
3750	56.512	321.307	3041.98	1101.93	-882.59	1387.03	0
3780	56.512	321.307	3058.53	1121.46	-898.23	1411.62	0
3809.13	56.512	321.307	3074.6	1140.42	-913.42	1435.48	0
3810	56.547	321.402	3075.08	1140.98	-913.87	1436.2	3
3840	57.813	324.639	3091.34	1161.12	-929.03	1461.09	3
3870	59.159	327.785	3107.03	1182.38	-943.25	1486.53	3
3900	60.578	330.841	3122.09	1204.69	-956.48	1512.44	3
3930	62.066	333.811	3136.49	1227.99	-968.7	1538.75	3
3960	63.615	336.698	3150.18	1252.23	-979.86	1565.4	3
3990	65.22	339.508	3163.14	1277.34	-989.95	1592.3	3
4020	66.877	342.245	3175.32	1303.24	-998.93	1619.39	3
4050	68.58	344.914	3186.69	1329.87	-1006.77	1646.59	3
4080	70.324	347.521	3197.22	1357.14	-1013.46	1673.82	3
4110	72.105	350.071	3206.88	1385	-1018.97	1701.01	3
4140	73.918	352.57	3215.65	1413.36	-1023.3	1728.09	3
4170	75.76	355.024	3223.5	1442.14	-1026.42	1754.99	3
4200	77.627	357.437	3230.4	1471.27	-1028.34	1781.62	3
4230	79.514	359.817	3236.35	1500.67	-1029.04	1807.91	3
4260	81.419	2.167	3241.32	1530.24	-1028.53	1833.8	3
4290	83.338	4.493	3245.3	1559.92	-1026.8	1859.21	3
4320	85.268	6.802	3248.27	1589.63	-1023.86	1884.07	3

4345.26	86.899	8.736	3250	1614.6	-1020.46	1904.54	3
4350	86.899	8.736	3250.26	1619.27	-1019.74	1908.33	0
4380	86.899	8.736	3251.88	1648.88	-1015.19	1932.36	0
4410	86.899	8.736	3253.5	1678.49	-1010.64	1956.38	0
4440	86.899	8.736	3255.12	1708.1	-1006.09	1980.4	0
4470	86.899	8.736	3256.75	1737.71	-1001.54	2004.43	0
4500	86.899	8.736	3258.37	1767.32	-996.99	2028.45	0
4530	86.899	8.736	3259.99	1796.92	-992.44	2052.48	0
4560	86.899	8.736	3261.62	1826.53	-987.89	2076.5	0
4588.19	86.899	8.736	3263.14	1854.35	-983.62	2099.08	0

VII.8. **Trajectory of Well #2d (#8)**

Depth (m)	Inclination (°)	Azimuth (°)	TVD (m)	North (m)	East (m)	VS (m)	DLS $(°/30m)$
1170	0	0	1170	0	0	0	0
1800	0	0	1800	0	0	0	0
1830	3	337.186	1829.99	0.72	-0.3	-0.39	3
1860	6	337.186	1859.89	2.89	-1.22	-1.55	3
1890	9	337.186	1889.63	6.5	-2.74	-3.48	3
1920	12	337.186	1919.12	11.54	-4.85	-6.17	3
1950	15	337.186	1948.29	18	-7.57	-9.63	3
1980	18	337.186	1977.05	25.85	-10.87	-13.83	3
2010	21	337.186	2005.33	35.08	-14.76	-18.77	3
2040	24	337.186	2033.04	45.66	-19.21	-24.43	3
2070	27	337.186	2060.12	57.56	-24.21	-30.8	3
2100	30	337.186	2086.48	70.76	-29.76	-37.85	3
2130	33	337.186	2112.06	85.2	-35.84	-45.58	3
2160	36	337.186	2136.78	100.86	-42.43	-53.96	3
2161.19	36.119	337.186	2137.74	101.51	-42.7	-54.31	3
2190	36.119	337.186	2161.01	117.16	-49.29	-62.68	0
2220	36.119	337.186	2185.24	133.46	-56.14	-71.4	0
2250	36.119	337.186	2209.48	149.77	-63	-80.12	0
2280	36.119	337.186	2233.71	166.07	-69.86	-88.85	0
2310	36.119	337.186	2257.95	182.37	-76.71	-97.57	0
2340	36.119	337.186	2282.18	198.67	-83.57	-106.29	0
2370	36.119	337.186	2306.41	214.97	-90.43	-115.01	0
2400	36.119	337.186	2330.65	231.27	-97.28	-123.73	0
2419.93	36.119	337.186	2346.74	242.09	-101.84	-129.52	0
2430	35.485	335.848	2354.91	247.5	-104.18	-132.37	3
2460	33.689	331.612	2379.61	262.77	-111.7	-139.87	3
2490	32.052	326.978	2404.81	276.77	-120	-145.88	3
2520	30.6	321.927	2430.45	289.45	-129.05	-150.41	3
2550	29.359	316.458	2456.44	300.8	-138.83	-153.42	3
2580	28.357	310.596	2482.72	310.77	-149.3	-154.91	3
2610	27.622	304.396	2509.21	319.33	-160.46	-154.89	3
2640	27.175	297.946	2535.85	326.47	-172.25	-153.34	3
2670	27.029	291.366	2562.56	332.17	-184.65	-150.28	3
2700	27.191	284.79	2589.27	336.4	-197.63	-145.7	3
2730	27.654	278.351	2615.91	339.17	-211.15	-139.64	3
2760	28.405	272.167	2642.4	340.45	-225.17	-132.09	3
2790	29.419	266.325	2668.66	340.24	-239.66	-123.08	3
2820	30.672	260.878	2694.64	338.56	-254.57	-112.64	3
2850	32.136	255.85	2720.24	335.39	-269.86	-100.79	3
2880	33.782	251.238	2745.42	330.76	-285.5	-87.57	3
2910	35.585	247.022	2770.09	324.67	-301.44	-73.02	3
2940	37.522	243.174	2794.19	317.14	-317.63	-57.16	3

2970	39.574	239.66	2817.66	308.18	-334.03	-40.06	3
3000	41.722	236.444	2840.42	297.84	-350.61	-21.75	3
3030	43.952	233.493	2862.42	286.12	-367.3	-2.28	3
3060	46.253	230.774	2883.59	273.07	-384.06	18.3	3
3090	48.613	228.259	2903.89	258.73	-400.86	39.91	3
3120	51.024	225.922	2923.24	243.12	-417.64	62.52	3
3150	53.479	223.74	2941.61	226.29	-434.35	86.05	3
3180	55.971	221.694	2958.94	208.3	-450.96	110.44	3
3210	58.495	219.765	2975.17	189.18	-467.41	135.63	3
3240	61.046	217.938	2990.28	168.99	-483.66	161.54	3
3270	63.621	216.199	3004.2	147.79	-499.67	188.11	3
3300	66.216	214.537	3016.92	125.63	-515.4	215.25	3
3330	68.828	212.939	3028.39	102.58	-530.79	242.9	3
3360	71.455	211.398	3038.58	78.7	-545.81	270.99	3
3390	74.093	209.903	3047.47	54.05	-560.41	299.43	3
3420	76.742	208.447	3055.02	28.7	-574.56	328.14	3
3450	79.398	207.023	3061.22	2.73	-588.22	357.05	3
3480	82.061	205.623	3066.05	-23.81	-601.34	386.08	3
3510	84.729	204.241	3069.5	-50.83	-613.9	415.15	3
3540	87.4	202.871	3071.56	-78.26	-625.86	444.17	3
3547.84	88.098	202.514	3071.87	-85.49	-628.88	451.74	3
3553.1	88.541	202.798	3072.02	-90.34	-630.91	456.82	3
3570	88.541	202.798	3072.45	-105.92	-637.45	473.15	0
3600	88.541	202.798	3073.22	-133.57	-649.08	502.14	0
3630	88.541	202.798	3073.98	-161.21	-660.7	531.13	0
3660	88.541	202.798	3074.75	-188.86	-672.32	560.12	0
3690	88.541	202.798	3075.51	-216.51	-683.94	589.11	0
3720	88.541	202.798	3076.28	-244.15	-695.56	618.1	0
3750	88.541	202.798	3077.04	-271.8	-707.18	647.09	0
3780	88.541	202.798	3077.8	-299.45	-718.8	676.08	0
3810	88.541	202.798	3078.57	-327.1	-730.42	705.07	0
3840	88.541	202.798	3079.33	-354.74	-742.04	734.06	0
3870	88.541	202.798	3080.1	-382.39	-753.66	763.05	0
3900	88.541	202.798	3080.86	-410.04	-765.28	792.04	0
3930	88.541	202.798	3081.62	-437.69	-776.9	821.03	0
3960	88.541	202.798	3082.39	-465.33	-788.52	850.02	0
3990	88.541	202.798	3083.15	-492.98	-800.14	879.01	0
4020	88.541	202.798	3083.92	-520.63	-811.76	908	0
4050	88.541	202.798	3084.68	-548.28	-823.38	936.99	0
4080	88.541	202.798	3085.44	-575.92	-835	965.98	0
4110	88.541	202.798	3086.21	-603.57	-846.62	994.97	0
4140	88.541	202.798	3086.97	-631.22	-858.24	1023.96	0
4170	88.541	202.798	3087.74	-658.87	-869.87	1052.95	0
4200	88.541	202.798	3088.5	-686.51	-881.49	1081.94	0
4230	88.541	202.798	3089.26	-714.16	-893.11	1110.93	0
4260	88.541	202.798	3090.03	-741.81	-904.73	1139.92	0

4290	88.541	202.798	3090.79	-769.46	-916.35	1168.91	0
4320	88.541	202.798	3091.56	-797.1	-927.97	1197.9	0
4350	88.541	202.798	3092.32	-824.75	-939.59	1226.89	0
4380	88.541	202.798	3093.08	-852.4	-951.21	1255.88	0
4410	88.541	202.798	3093.85	-880.05	-962.83	1284.87	0
4440	88.541	202.798	3094.61	-907.69	-974.45	1313.86	0
4470	88.541	202.798	3095.38	-935.34	-986.07	1342.85	0
4500	88.541	202.798	3096.14	-962.99	-997.69	1371.84	0
4530	88.541	202.798	3096.9	-990.64	-1009.31	1400.83	0
4560	88.541	202.798	3097.67	-1018.28	-1020.93	1429.82	0
4590	88.541	202.798	3098.43	-1045.93	-1032.55	1458.81	0
4620	88.541	202.798	3099.2	-1073.58	-1044.17	1487.8	0
4650	88.541	202.798	3099.96	-1101.22	-1055.79	1516.79	0
4680	88.541	202.798	3100.73	-1128.87	-1067.41	1545.78	0
4708.28	88.541	202.798	3101.45	-1154.94	-1078.37	1573.11	0
4710	88.396	202.705	3101.49	-1156.52	-1079.03	1574.77	3
4740	85.871	201.084	3102.99	-1184.32	-1090.21	1603.6	3
4770	83.348	199.452	3105.81	-1212.33	-1100.55	1632.1	3
4800	80.832	197.803	3109.94	-1240.49	-1110.04	1660.19	3
4824.17	78.809	196.458	3114.21	-1263.22	-1117.05	1682.47	3
4830	78.809	196.458	3115.34	-1268.7	-1118.67	1687.81	0
4860	78.809	196.458	3121.16	-1296.93	-1127.01	1715.25	0
4890	78.809	196.458	3126.99	-1325.15	-1135.35	1742.69	0
4920	78.809	196.458	3132.81	-1353.38	-1143.68	1770.13	0
4950	78.809	196.458	3138.63	-1381.6	-1152.02	1797.57	0
4980	78.809	196.458	3144.45	-1409.82	-1160.36	1825.02	0
5010	78.809	196.458	3150.27	-1438.05	-1168.7	1852.46	0
5040	78.809	196.458	3156.1	-1466.27	-1177.04	1879.9	0
5070	78.809	196.458	3161.92	-1494.49	-1185.37	1907.34	0
5100	78.809	196.458	3167.74	-1522.72	-1193.71	1934.78	0
5130	78.809	196.458	3173.56	-1550.94	-1202.05	1962.22	0
5143.43	78.809	196.458	3176.17	-1563.58	-1205.78	1974.51	0

VII.9. **Trajectory of Well #2e (#9)**

Depth (m)	Inclination (°)	Azimuth (°)	TVD (m)	North (m)	East (m)	VS (m)	DLS $(°/30m)$
1170	0	0	1170	0	0	0	0
1800	0	0	1800	0	0	0	0
1830	3	244.197	1829.99	-0.34	-0.71	0.71	3
1860	6	244.197	1859.89	-1.37	-2.83	2.83	3
1890	9	244.197	1889.63	-3.07	-6.35	6.37	3
1920	12	244.197	1919.12	-5.45	-11.27	11.3	3
1950	15	244.197	1948.29	-8.5	-17.58	17.62	3
1980	18	244.197	1977.05	-12.21	-25.25	25.31	3
2010	21	244.197	2005.33	-16.56	-34.26	34.34	3
2040	24	244.197	2033.04	-21.56	-44.6	44.7	3
2070	27	244.197	2060.12	-27.18	-56.22	56.35	3
2100	30	244.197	2086.48	-33.41	-69.11	69.27	3
2130	33	244.197	2112.06	-40.23	-83.22	83.41	3
2160	36	244.197	2136.78	-47.63	-98.52	98.75	3
2190	39	244.197	2160.57	-55.58	-114.96	115.22	3
2220	42	244.197	2183.38	-64.06	-132.49	132.8	3
2250	45	244.197	2205.14	-73.05	-151.08	151.44	3
2280	48	244.197	2225.79	-82.52	-170.67	171.07	3
2310	51	244.197	2245.27	-92.44	-191.21	191.66	3
2332.14	53.214	244.197	2258.87	-100.05	-206.94	207.42	3
2340	53.214	244.197	2263.58	-102.79	-212.61	213.1	0
2370	53.214	244.197	2281.54	-113.25	-234.24	234.78	0
2400	53.214	244.197	2299.51	-123.71	-255.87	256.47	0
2430	53.214	244.197	2317.47	-134.16	-277.5	278.15	0
2460	53.214	244.197	2335.43	-144.62	-299.13	299.83	0
2490	53.214	244.197	2353.4	-155.08	-320.76	321.51	0
2520	53.214	244.197	2371.36	-165.54	-342.39	343.19	0
2550	53.214	244.197	2389.33	-176	-364.02	364.87	0
2580	53.214	244.197	2407.29	-186.45	-385.65	386.56	0
2610	53.214	244.197	2425.26	-196.91	-407.28	408.24	0
2640	53.214	244.197	2443.22	-207.37	-428.91	429.92	0
2670	53.214	244.197	2461.19	-217.83	-450.55	451.6	0
2700	53.214	244.197	2479.15	-228.29	-472.18	473.28	0
2730	53.214	244.197	2497.12	-238.74	-493.81	494.96	0
2760	53.214	244.197	2515.08	-249.2	-515.44	516.65	0
2790	53.214	244.197	2533.05	-259.66	-537.07	538.33	0
2820	53.214	244.197	2551.01	-270.12	-558.7	560.01	0
2850	53.214	244.197	2568.98	-280.58	-580.33	581.69	0
2880	53.214	244.197	2586.94	-291.03	-601.96	603.37	0
2910	53.214	244.197	2604.91	-301.49	-623.59	625.05	0
2940	53.214	244.197	2622.87	-311.95	-645.22	646.74	0
2970	53.214	244.197	2640.84	-322.41	-666.86	668.42	0

3000	53.214	244.197	2658.8	-332.87	-688.49	690.1	0
3030	53.214	244.197	2676.77	-343.32	-710.12	711.78	0
3060	53.214	244.197	2694.73	-353.78	-731.75	733.46	0
3090	53.214	244.197	2712.69	-364.24	-753.38	755.14	0
3120	53.214	244.197	2730.66	-374.7	-775.01	776.83	0
3150	53.214	244.197	2748.62	-385.16	-796.64	798.51	0
3180	53.214	244.197	2766.59	-395.61	-818.27	820.19	0
3210	53.214	244.197	2784.55	-406.07	-839.9	841.87	0
3222.73	53.214	244.197	2792.18	-410.51	-849.08	851.07	0
3240	53.89	242.222	2802.44	-416.77	-861.48	863.71	3
3270	55.139	238.872	2819.86	-428.78	-882.74	886.37	3
3300	56.477	235.625	2836.72	-442.21	-903.6	909.89	3
3330	57.897	232.481	2852.98	-457.01	-924.01	934.2	3
3360	59.392	229.435	2868.59	-473.15	-943.9	959.23	3
3390	60.956	226.484	2883.51	-490.58	-963.22	984.91	3
3420	62.583	223.622	2897.7	-509.25	-981.92	1011.17	3
3450	64.266	220.846	2911.13	-529.12	-999.95	1037.94	3
3480	66.001	218.147	2923.74	-550.12	-1017.25	1065.16	3
3510	67.781	215.522	2935.52	-572.2	-1033.79	1092.73	3
3540	69.603	212.963	2946.42	-595.31	-1049.51	1120.59	3
3570	71.461	210.465	2956.42	-619.37	-1064.38	1148.66	3
3600	73.351	208.02	2965.49	-644.32	-1078.34	1176.87	3
3630	75.269	205.624	2973.6	-670.09	-1091.37	1205.13	3
3660	77.211	203.27	2980.74	-696.61	-1103.42	1233.37	3
3690	79.174	200.952	2986.88	-723.82	-1114.47	1261.52	3
3720	81.154	198.665	2992.01	-751.62	-1124.49	1289.48	3
3750	83.147	196.402	2996.1	-779.96	-1133.44	1317.2	3
3780	85.152	194.158	2999.16	-808.75	-1141.3	1344.58	3
3805.01	86.828	192.297	3000.91	-833.03	-1147.01	1367.11	3
3810	87.077	192.319	3001.18	-837.9	-1148.07	1371.58	1.5
3822.55	87.702	192.374	3001.75	-850.15	-1150.75	1382.81	1.5
3840	87.702	192.374	3002.45	-867.18	-1154.49	1398.44	0
3870	87.702	192.374	3003.65	-896.46	-1160.91	1425.32	0
3900	87.702	192.374	3004.85	-925.74	-1167.34	1452.19	0
3930	87.702	192.374	3006.06	-955.02	-1173.76	1479.06	0
3960	87.702	192.374	3007.26	-984.3	-1180.18	1505.93	0
3990	87.702	192.374	3008.46	-1013.57	-1186.61	1532.81	0
4020	87.702	192.374	3009.67	-1042.85	-1193.03	1559.68	0
4050	87.702	192.374	3010.87	-1072.13	-1199.45	1586.55	0
4080	87.702	192.374	3012.07	-1101.41	-1205.88	1613.43	0
4110	87.702	192.374	3013.27	-1130.69	-1212.3	1640.3	0
4114.56	87.702	192.374	3013.46	-1135.15	-1213.28	1644.39	0
4140	86.435	192.263	3014.76	-1159.96	-1218.7	1667.15	1.5
4170	84.94	192.132	3017.01	-1189.2	-1225.02	1693.93	1.5
4200	83.446	192	3020.05	-1218.39	-1231.26	1720.61	1.5
4230	81.952	191.868	3023.86	-1247.5	-1237.41	1747.18	1.5

4236.36	81.635	191.839	3024.77	-1253.67	-1238.7	1752.8	1.5
4260	81.635	191.839	3028.21	-1276.55	-1243.5	1773.67	0
4290	81.635	191.839	3032.57	-1305.6	-1249.59	1800.16	0
4320	81.635	191.839	3036.94	-1334.65	-1255.68	1826.64	0
4350	81.635	191.839	3041.3	-1363.7	-1261.77	1853.13	0
4380	81.635	191.839	3045.67	-1392.75	-1267.86	1879.61	0
4410	81.635	191.839	3050.03	-1421.8	-1273.95	1906.1	0
4440	81.635	191.839	3054.39	-1450.85	-1280.04	1932.58	0
4470	81.635	191.839	3058.76	-1479.9	-1286.13	1959.06	0
4500	81.635	191.839	3063.12	-1508.95	-1292.22	1985.55	0
4530	81.635	191.839	3067.49	-1538	-1298.31	2012.03	0
4560	81.635	191.839	3071.85	-1567.05	-1304.4	2038.52	0
4590	81.635	191.839	3076.22	-1596.1	-1310.49	2065	0
4620	81.635	191.839	3080.58	-1625.15	-1316.58	2091.49	0
4647.63	81.635	191.839	3084.6	-1651.9	-1322.18	2115.88	0

VII.10. **Trajectory of Well #3a (#10)**

Depth (m)	Inclination (°)	Azimuth (°)	TVD (m)	North (m)	East (m)	VS (m)	DLS $(°/30m)$
1170	0	0	1170	0	0	0	0
1800	0	0	1800	0	0	0	0
1830	3	278.931	1829.99	0.12	-0.78	0.54	3
1860	6	278.931	1859.89	0.49	-3.1	2.15	3
1890	9	278.931	1889.63	1.1	-6.97	4.82	3
1920	12	278.931	1919.12	1.94	-12.37	8.56	3
1950	15	278.931	1948.29	3.03	-19.29	13.35	3
1980	18	278.931	1977.05	4.35	-27.7	19.18	3
1987.49	18.749	278.931	1984.17	4.72	-30.04	20.79	3
2010	18.749	278.931	2005.48	5.84	-37.18	25.74	0
2040	18.749	278.931	2033.89	7.34	-46.71	32.34	0
2070	18.749	278.931	2062.29	8.84	-56.23	38.93	0
2100	18.749	278.931	2090.7	10.33	-65.76	45.53	0
2130	18.749	278.931	2119.11	11.83	-75.29	52.12	0
2160	18.749	278.931	2147.52	13.33	-84.81	58.72	0
2190	18.749	278.931	2175.93	14.83	-94.34	65.31	0
2220	18.749	278.931	2204.33	16.32	-103.86	71.9	0
2250	18.749	278.931	2232.74	17.82	-113.39	78.5	0
2280	18.749	278.931	2261.15	19.32	-122.92	85.09	0
2310	18.749	278.931	2289.56	20.81	-132.44	91.69	0
2340	18.749	278.931	2317.97	22.31	-141.97	98.28	0
2370	18.749	278.931	2346.37	23.81	-151.49	104.88	0
2400	18.749	278.931	2374.78	25.31	-161.02	111.47	0
2430	18.749	278.931	2403.19	26.8	-170.55	118.07	0
2460	18.749	278.931	2431.6	28.3	-180.07	124.66	0
2490	18.749	278.931	2460.01	29.8	-189.6	131.26	0
2520	18.749	278.931	2488.41	31.29	-199.12	137.85	0
2550	18.749	278.931	2516.82	32.79	-208.65	144.45	0
2580	18.749	278.931	2545.23	34.29	-218.18	151.04	0
2610	18.749	278.931	2573.64	35.79	-227.7	157.64	0
2640	18.749	278.931	2602.05	37.28	-237.23	164.23	0
2670	18.749	278.931	2630.45	38.78	-246.75	170.83	0
2700	18.749	278.931	2658.86	40.28	-256.28	177.42	0
2730	18.749	278.931	2687.27	41.77	-265.81	184.02	0
2760	18.749	278.931	2715.68	43.27	-275.33	190.61	0
2781.73	18.749	278.931	2736.25	44.35	-282.23	195.39	0
2790	18.998	281.371	2744.08	44.83	-284.87	197.26	3
2820	20.15	289.649	2772.35	47.53	-294.52	204.92	3
2850	21.645	296.949	2800.38	51.77	-304.32	213.94	3
2880	23.418	303.272	2828.09	57.55	-314.24	224.3	3
2910	25.41	308.705	2855.41	64.85	-324.25	235.96	3
2940	27.574	313.367	2882.27	73.64	-334.32	248.9	3

2970	29.873	317.382	2908.57	83.91	-344.43	263.07	3
3000	32.276	320.863	2934.27	95.63	-354.55	278.45	3
3030	34.764	323.902	2959.28	108.75	-364.64	294.98	3
3060	37.318	326.579	2983.54	123.26	-374.69	312.63	3
3090	39.925	328.958	3006.98	139.1	-384.67	331.34	3
3120	42.576	331.088	3029.53	156.23	-394.54	351.06	3
3150	45.263	333.014	3051.14	174.62	-404.29	371.74	3
3180	47.979	334.767	3071.74	194.2	-413.87	393.32	3
3210	50.719	336.376	3091.28	214.92	-423.28	415.74	3
3240	53.48	337.863	3109.71	236.73	-432.48	438.95	3
3270	56.259	339.247	3126.97	259.56	-441.44	462.87	3
3300	59.052	340.545	3143.02	283.36	-450.15	487.45	3
3330	61.856	341.768	3157.82	308.06	-458.57	512.61	3
3360	64.672	342.929	3171.31	333.59	-466.69	538.29	3
3390	67.496	344.036	3183.47	359.88	-474.49	564.41	3
3420	70.327	345.1	3194.27	386.86	-481.93	590.9	3
3450	73.164	346.126	3203.66	414.45	-489.01	617.7	3
3480	76.006	347.122	3211.64	442.59	-495.69	644.73	3
3497.08	77.626	347.678	3215.53	458.81	-499.32	660.18	3
3510	77.626	347.678	3218.3	471.14	-502.02	671.89	0
3540	77.626	347.678	3224.73	499.77	-508.27	699.08	0
3570	77.626	347.678	3231.16	528.4	-514.52	726.27	0
3600	77.626	347.678	3237.59	557.03	-520.78	753.46	0
3630	77.626	347.678	3244.01	585.66	-527.03	780.65	0
3660	77.626	347.678	3250.44	614.28	-533.28	807.84	0
3690	77.626	347.678	3256.87	642.91	-539.54	835.03	0
3720	77.626	347.678	3263.3	671.54	-545.79	862.22	0
3750	77.626	347.678	3269.73	700.17	-552.04	889.41	0
3780	77.626	347.678	3276.16	728.8	-558.3	916.6	0
3810	77.626	347.678	3282.59	757.42	-564.55	943.79	0
3840	77.626	347.678	3289.02	786.05	-570.8	970.98	0
3870	77.626	347.678	3295.45	814.68	-577.06	998.17	0
3900	77.626	347.678	3301.87	843.31	-583.31	1025.36	0
3922.29	77.626	347.678	3306.65	864.58	-587.95	1045.55	0

VII.11. **Trajectory of Well #3b (#11)**

Depth (m)	Inclination (°)	Azimuth (°)	TVD (m)	North (m)	East (m)	VS (m)	DLS $(°/30m)$
1170	0	0	1170	0	0	0	0
1800	0	0	1800	0	0	0	0
1830	3	321.691	1829.99	0.62	-0.49	0.37	3
1860	6	321.691	1859.89	2.46	-1.95	1.46	3
1890	9	321.691	1889.63	5.54	-4.37	3.28	3
1920	12	321.691	1919.12	9.82	-7.76	5.83	3
1950	15	321.691	1948.29	15.32	-12.1	9.09	3
1980	18	321.691	1977.05	22	-17.38	13.05	3
2010	21	321.691	2005.33	29.86	-23.59	17.71	3
2040	24	321.691	2033.04	38.87	-30.71	23.06	3
2070	27	321.691	2060.12	49	-38.71	29.07	3
2100	30	321.691	2086.48	60.23	-47.58	35.73	3
2130	33	321.691	2112.06	72.53	-57.3	43.02	3
2160	36	321.691	2136.78	85.86	-67.83	50.93	3
2190	39	321.691	2160.57	100.19	-79.15	59.43	3
2220	42	321.691	2183.38	115.48	-91.23	68.5	3
2250	45	321.691	2205.14	131.68	-104.03	78.11	3
2280	48	321.691	2225.79	148.75	-117.52	88.24	3
2310	51	321.691	2245.27	166.65	-131.66	98.85	3
2316.69	51.669	321.691	2249.45	170.75	-134.89	101.28	3
2340	51.669	321.691	2263.91	185.1	-146.23	109.79	0
2370	51.669	321.691	2282.51	203.57	-160.82	120.75	0
2400	51.669	321.691	2301.12	222.03	-175.41	131.7	0
2430	51.669	321.691	2319.73	240.5	-190	142.65	0
2460	51.669	321.691	2338.33	258.96	-204.58	153.61	0
2490	51.669	321.691	2356.94	277.43	-219.17	164.56	0
2520	51.669	321.691	2375.55	295.9	-233.76	175.51	0
2550	51.669	321.691	2394.15	314.36	-248.35	186.47	0
2580	51.669	321.691	2412.76	332.83	-262.94	197.42	0
2610	51.669	321.691	2431.36	351.29	-277.53	208.37	0
2640	51.669	321.691	2449.97	369.76	-292.11	219.33	0
2670	51.669	321.691	2468.58	388.23	-306.7	230.28	0
2700	51.669	321.691	2487.18	406.69	-321.29	241.23	0
2730	51.669	321.691	2505.79	425.16	-335.88	252.19	0
2760	51.669	321.691	2524.4	443.62	-350.47	263.14	0
2790	51.669	321.691	2543	462.09	-365.05	274.09	0
2820	51.669	321.691	2561.61	480.56	-379.64	285.05	0
2850	51.669	321.691	2580.21	499.02	-394.23	296	0
2880	51.669	321.691	2598.82	517.49	-408.82	306.96	0
2910	51.669	321.691	2617.43	535.95	-423.41	317.91	0
2940	51.669	321.691	2636.03	554.42	-438	328.86	0
2970	51.669	321.691	2654.64	572.89	-452.58	339.82	0

3000	51.669	321.691	2673.24	591.35	-467.17	350.77	0
3030	51.669	321.691	2691.85	609.82	-481.76	361.72	0
3060	51.669	321.691	2710.46	628.28	-496.35	372.68	0
3060.82	51.669	321.691	2710.97	628.79	-496.75	372.98	0
3090	50.977	318.06	2729.2	646.2	-511.42	384.2	3
3120	50.385	314.258	2748.22	662.94	-527.49	396.93	3
3150	49.919	310.398	2767.44	678.45	-544.51	410.82	3
3180	49.583	306.492	2786.83	692.68	-562.44	425.83	3
3210	49.379	302.554	2806.33	705.6	-581.22	441.92	3
3240	49.31	298.6	2825.88	717.17	-600.8	459.05	3
3270	49.375	294.646	2845.43	727.37	-621.14	477.17	3
3300	49.575	290.708	2864.93	736.16	-642.18	496.24	3
3330	49.908	286.801	2884.32	743.51	-663.85	516.19	3
3360	50.37	282.939	2903.55	749.42	-686.1	536.98	3
3390	50.959	279.135	2922.57	753.85	-708.86	558.55	3
3420	51.669	275.401	2941.33	756.81	-732.09	580.84	3
3450	52.494	271.744	2959.77	758.28	-755.7	603.78	3
3480	53.43	268.173	2977.84	758.26	-779.64	627.32	3
3510	54.47	264.693	2995.5	756.75	-803.84	651.38	3
3540	55.607	261.305	3012.69	753.75	-828.24	675.92	3
3570	56.835	258.011	3029.37	749.27	-852.76	700.85	3
3600	58.147	254.812	3045.5	743.32	-877.35	726.11	3
3630	59.537	251.705	3061.02	735.92	-901.92	751.62	3
3660	60.999	248.688	3075.9	727.09	-926.43	777.33	3
3690	62.526	245.756	3090.1	716.86	-950.79	803.16	3
3720	64.112	242.907	3103.57	705.24	-974.94	829.03	3
3750	65.753	240.134	3116.28	692.28	-998.82	854.88	3
3780	67.443	237.432	3128.2	678.01	-1022.36	880.64	3
3810	69.177	234.797	3139.29	662.47	-1045.5	906.24	3
3840	70.95	232.223	3149.52	645.7	-1068.17	931.6	3
3870	72.758	229.704	3158.86	627.74	-1090.31	956.65	3
3900	74.596	227.233	3167.3	608.65	-1111.85	981.34	3
3930	76.462	224.807	3174.79	588.48	-1132.75	1005.58	3
3960	78.351	222.418	3181.34	567.29	-1152.94	1029.32	3
3990	80.259	220.062	3186.9	545.12	-1172.37	1052.48	3
4020	82.183	217.733	3191.48	522.05	-1190.99	1075.01	3
4050	84.119	215.425	3195.06	498.13	-1208.73	1096.85	3
4080	86.065	213.133	3197.63	473.44	-1225.57	1117.92	3
4080.32	86.086	213.109	3197.65	473.16	-1225.74	1118.15	3
4110	86.086	213.109	3199.68	448.37	-1241.91	1138.59	0
4140	86.086	213.109	3201.72	423.29	-1258.26	1159.26	0
4170	86.086	213.109	3203.77	398.22	-1274.61	1179.93	0
4200	86.086	213.109	3205.82	373.15	-1290.96	1200.6	0
4230	86.086	213.109	3207.87	348.08	-1307.31	1221.27	0
4260	86.086	213.109	3209.91	323.01	-1323.66	1241.94	0
4290	86.086	213.109	3211.96	297.94	-1340.01	1262.61	0

4320	86.086	213.109	3214.01	272.87	-1356.35	1283.28	0
4350	86.086	213.109	3216.06	247.8	-1372.7	1303.95	0
4380	86.086	213.109	3218.1	222.73	-1389.05	1324.62	0
4410	86.086	213.109	3220.15	197.66	-1405.4	1345.29	0
4440	86.086	213.109	3222.2	172.59	-1421.75	1365.96	0
4470	86.086	213.109	3224.25	147.52	-1438.1	1386.63	0
4500	86.086	213.109	3226.29	122.45	-1454.45	1407.3	0
4530	86.086	213.109	3228.34	97.38	-1470.8	1427.97	0
4560	86.086	213.109	3230.39	72.31	-1487.14	1448.64	0
4590	86.086	213.109	3232.44	47.24	-1503.49	1469.31	0
4620	86.086	213.109	3234.49	22.17	-1519.84	1489.98	0
4650	86.086	213.109	3236.53	-2.9	-1536.19	1510.66	0
4680	86.086	213.109	3238.58	-27.97	-1552.54	1531.33	0
4710	86.086	213.109	3240.63	-53.04	-1568.89	1552	0
4740	86.086	213.109	3242.68	-78.11	-1585.24	1572.67	0
4770	86.086	213.109	3244.72	-103.18	-1601.58	1593.34	0
4800	86.086	213.109	3246.77	-128.26	-1617.93	1614.01	0
4830	86.086	213.109	3248.82	-153.33	-1634.28	1634.68	0
4860	86.086	213.109	3250.87	-178.4	-1650.63	1655.35	0
4890	86.086	213.109	3252.91	-203.47	-1666.98	1676.02	0
4920	86.086	213.109	3254.96	-228.54	-1683.33	1696.69	0
4950	86.086	213.109	3257.01	-253.61	-1699.68	1717.36	0
4980	86.086	213.109	3259.06	-278.68	-1716.03	1738.03	0
5010	86.086	213.109	3261.1	-303.75	-1732.37	1758.7	0
5036.6	86.086	213.109	3262.92	-325.98	-1746.87	1777.02	0

VII.12. **Trajectory of Well #3c (#12)**

Depth (m)	Inclination (°)	Azimuth (°)	TVD (m)	North (m)	East (m)	VS (m)	DLS $(°/30m)$
1170	0	0	1170	0	0	0	0
1800	0	0	1800	0	0	0	0
1830	3	74.581	1829.99	0.21	0.76	0.52	3
1860	6	74.581	1859.89	0.83	3.03	2.1	3
1890	9	74.581	1889.63	1.88	6.8	4.71	3
1920	12	74.581	1919.12	3.33	12.07	8.36	3
1950	15	74.581	1948.29	5.19	18.82	13.04	3
1980	18	74.581	1977.05	7.46	27.03	18.73	3
2010	21	74.581	2005.33	10.12	36.69	25.42	3
2040	24	74.581	2033.04	13.17	47.75	33.08	3
2070	27	74.581	2060.12	16.6	60.2	41.71	3
2100	30	74.581	2086.48	20.41	74	51.27	3
2130	33	74.581	2112.06	24.58	89.11	61.73	3
2160	36	74.581	2136.78	29.09	105.49	73.08	3
2189.41	38.941	74.581	2160.11	33.85	122.73	85.03	3
2190	38.941	74.581	2160.57	33.95	123.09	85.27	0
2220	38.941	74.581	2183.91	38.96	141.27	97.87	0
2250	38.941	74.581	2207.24	43.98	159.44	110.46	0
2280	38.941	74.581	2230.58	48.99	177.62	123.05	0
2310	38.941	74.581	2253.91	54	195.8	135.64	0
2340	38.941	74.581	2277.24	59.02	213.97	148.24	0
2370	38.941	74.581	2300.58	64.03	232.15	160.83	0
2400	38.941	74.581	2323.91	69.04	250.33	173.42	0
2430	38.941	74.581	2347.25	74.06	268.5	186.02	0
2460	38.941	74.581	2370.58	79.07	286.68	198.61	0
2490	38.941	74.581	2393.91	84.08	304.86	211.2	0
2520	38.941	74.581	2417.25	89.1	323.03	223.79	0
2550	38.941	74.581	2440.58	94.11	341.21	236.39	0
2580	38.941	74.581	2463.91	99.12	359.39	248.98	0
2610	38.941	74.581	2487.25	104.14	377.56	261.57	0
2640	38.941	74.581	2510.58	109.15	395.74	274.16	0
2670	38.941	74.581	2533.92	114.16	413.92	286.76	0
2700	38.941	74.581	2557.25	119.18	432.1	299.35	0
2730	38.941	74.581	2580.58	124.19	450.27	311.94	0
2760	38.941	74.581	2603.92	129.2	468.45	324.53	0
2790	38.941	74.581	2627.25	134.22	486.63	337.13	0
2820	38.941	74.581	2650.59	139.23	504.8	349.72	0
2850	38.941	74.581	2673.92	144.24	522.98	362.31	0
2880	38.941	74.581	2697.25	149.26	541.16	374.9	0
2910	38.941	74.581	2720.59	154.27	559.33	387.5	0
2940	38.941	74.581	2743.92	159.28	577.51	400.09	0
2970	38.941	74.581	2767.26	164.3	595.69	412.68	0

3000	38.941	74.581	2790.59	169.31	613.86	425.27	0
3030	38.941	74.581	2813.92	174.32	632.04	437.87	0
3046.56	38.941	74.581	2826.8	177.09	642.07	444.82	0
3060	39.346	76.612	2837.23	179.2	650.29	450.6	3
3090	40.374	81.01	2860.26	182.92	669.14	464.45	3
3120	41.561	85.213	2882.92	185.27	688.66	479.61	3
3150	42.894	89.213	2905.14	186.24	708.79	496.03	3
3180	44.359	93.008	2926.85	185.83	729.48	513.67	3
3210	45.943	96.603	2948.01	184.04	750.66	532.47	3
3240	47.634	100.003	2968.56	180.87	772.29	552.38	3
3270	49.42	103.221	2988.43	176.34	794.3	573.35	3
3300	51.29	106.268	3007.57	170.46	816.63	595.33	3
3330	53.236	109.156	3025.93	163.23	839.23	618.24	3
3360	55.248	111.899	3043.47	154.69	862.02	642.04	3
3390	57.318	114.509	3060.12	144.85	884.94	666.65	3
3420	59.44	117	3075.85	133.75	907.95	692	3
3450	61.607	119.383	3090.61	121.41	930.96	718.04	3
3480	63.814	121.67	3104.37	107.87	953.92	744.67	3
3510	66.056	123.871	3117.08	93.15	976.76	771.85	3
3540	68.328	125.996	3128.71	77.32	999.43	799.47	3
3570	70.627	128.055	3139.22	60.4	1021.85	827.49	3
3600	72.948	130.056	3148.6	42.44	1043.98	855.8	3
3630	75.288	132.008	3156.81	23.5	1065.74	884.35	3
3660	77.644	133.919	3163.83	3.62	1087.08	913.04	3
3690	80.013	135.795	3169.64	-17.14	1107.94	941.81	3
3720	82.392	137.644	3174.23	-38.72	1128.26	970.56	3
3750	84.779	139.473	3177.58	-61.06	1147.99	999.24	3
3780	87.172	141.287	3179.69	-84.11	1167.07	1027.74	3
3795.64	88.42	142.23	3180.29	-96.39	1176.74	1042.51	3
3810	88.42	142.23	3180.69	-107.73	1185.53	1056.04	0
3840	88.42	142.23	3181.51	-131.44	1203.9	1084.3	0
3870	88.42	142.23	3182.34	-155.15	1222.27	1112.56	0
3900	88.42	142.23	3183.17	-178.85	1240.64	1140.82	0
3930	88.42	142.23	3183.99	-202.56	1259	1169.08	0
3960	88.42	142.23	3184.82	-226.26	1277.37	1197.34	0
3990	88.42	142.23	3185.65	-249.97	1295.74	1225.6	0
4020	88.42	142.23	3186.48	-273.67	1314.11	1253.86	0
4050	88.42	142.23	3187.3	-297.38	1332.48	1282.12	0
4080	88.42	142.23	3188.13	-321.08	1350.84	1310.37	0
4110	88.42	142.23	3188.96	-344.79	1369.21	1338.63	0
4140	88.42	142.23	3189.79	-368.49	1387.58	1366.89	0
4170	88.42	142.23	3190.61	-392.2	1405.95	1395.15	0
4200	88.42	142.23	3191.44	-415.9	1424.31	1423.41	0
4230	88.42	142.23	3192.27	-439.61	1442.68	1451.67	0
4260	88.42	142.23	3193.09	-463.31	1461.05	1479.93	0
4290	88.42	142.23	3193.92	-487.02	1479.42	1508.19	0

4320	88.42	142.23	3194.75	-510.72	1497.79	1536.45	0
4350	88.42	142.23	3195.58	-534.43	1516.15	1564.71	0
4380	88.42	142.23	3196.4	-558.13	1534.52	1592.97	0
4410	88.42	142.23	3197.23	-581.84	1552.89	1621.23	0
4440	88.42	142.23	3198.06	-605.55	1571.26	1649.49	0
4470	88.42	142.23	3198.88	-629.25	1589.62	1677.75	0
4500	88.42	142.23	3199.71	-652.96	1607.99	1706.01	0
4530	88.42	142.23	3200.54	-676.66	1626.36	1734.27	0
4560	88.42	142.23	3201.37	-700.37	1644.73	1762.53	0
4590	88.42	142.23	3202.19	-724.07	1663.1	1790.79	0
4620	88.42	142.23	3203.02	-747.78	1681.46	1819.05	0
4650	88.42	142.23	3203.85	-771.48	1699.83	1847.31	0
4680	88.42	142.23	3204.67	-795.19	1718.2	1875.57	0
4710	88.42	142.23	3205.5	-818.89	1736.57	1903.83	0
4740	88.42	142.23	3206.33	-842.6	1754.94	1932.09	0
4770	88.42	142.23	3207.16	-866.3	1773.3	1960.35	0
4800	88.42	142.23	3207.98	-890.01	1791.67	1988.61	0
4830	88.42	142.23	3208.81	-913.71	1810.04	2016.87	0
4860	88.42	142.23	3209.64	-937.42	1828.41	2045.13	0
4890	88.42	142.23	3210.46	-961.12	1846.77	2073.39	0
4920	88.42	142.23	3211.29	-984.83	1865.14	2101.65	0
4950	88.42	142.23	3212.12	-1008.53	1883.51	2129.91	0
4980	88.42	142.23	3212.95	-1032.24	1901.88	2158.16	0
5010	88.42	142.23	3213.77	-1055.95	1920.25	2186.42	0
5040	88.42	142.23	3214.6	-1079.65	1938.61	2214.68	0
5070	88.42	142.23	3215.43	-1103.36	1956.98	2242.94	0
5100	88.42	142.23	3216.25	-1127.06	1975.35	2271.2	0
5130	88.42	142.23	3217.08	-1150.77	1993.72	2299.46	0
5160	88.42	142.23	3217.91	-1174.47	2012.08	2327.72	0
5190	88.42	142.23	3218.74	-1198.18	2030.45	2355.98	0
5220	88.42	142.23	3219.56	-1221.88	2048.82	2384.24	0
5250	88.42	142.23	3220.39	-1245.59	2067.19	2412.5	0
5280	88.42	142.23	3221.22	-1269.29	2085.56	2440.76	0
5310	88.42	142.23	3222.05	-1293	2103.92	2469.02	0
5340	88.42	142.23	3222.87	-1316.7	2122.29	2497.28	0
5370	88.42	142.23	3223.7	-1340.41	2140.66	2525.54	0
5400	88.42	142.23	3224.53	-1364.11	2159.03	2553.8	0
5430	88.42	142.23	3225.35	-1387.82	2177.39	2582.06	0
5452.51	88.42	142.23	3225.97	-1405.61	2191.18	2603.27	0

VII.13. **Trajectory of Well #3d (#13)**

Depth (m)	Inclination (°)	Azimuth (°)	TVD (m)	North (m)	East (m)	VS (m)	DLS $(°/30m)$
1170	0	0	1170	0	0	0	0
1800	0	0	1800	0	0	0	0
1830	3	139.805	1829.99	-0.6	0.51	0.77	3
1860	6	139.805	1859.89	-2.4	2.03	3.09	3
1890	9	139.805	1889.63	-5.39	4.55	6.95	3
1920	12	139.805	1919.12	-9.56	8.08	12.33	3
1950	15	139.805	1948.29	-14.91	12.6	19.22	3
1980	18	139.805	1977.05	-21.42	18.1	27.61	3
2010	21	139.805	2005.33	-29.07	24.56	37.47	3
2040	24	139.805	2033.04	-37.84	31.97	48.78	3
2070	27	139.805	2060.12	-47.7	40.3	61.49	3
2100	30	139.805	2086.48	-58.63	49.54	75.59	3
2130	33	139.805	2112.06	-70.61	59.66	91.02	3
2160	36	139.805	2136.78	-83.58	70.62	107.75	3
2173.48	37.348	139.805	2147.59	-89.74	75.82	115.68	3
2190	37.348	139.805	2160.72	-97.39	82.29	125.55	0
2220	37.348	139.805	2184.57	-111.29	94.03	143.47	0
2250	37.348	139.805	2208.42	-125.19	105.78	161.39	0
2280	37.348	139.805	2232.27	-139.1	117.52	179.31	0
2310	37.348	139.805	2256.12	-153	129.27	197.23	0
2340	37.348	139.805	2279.96	-166.9	141.02	215.15	0
2370	37.348	139.805	2303.81	-180.8	152.76	233.07	0
2400	37.348	139.805	2327.66	-194.7	164.51	251	0
2430	37.348	139.805	2351.51	-208.61	176.25	268.92	0
2460	37.348	139.805	2375.36	-222.51	188	286.84	0
2490	37.348	139.805	2399.21	-236.41	199.75	304.76	0
2520	37.348	139.805	2423.06	-250.31	211.49	322.68	0
2550	37.348	139.805	2446.91	-264.21	223.24	340.6	0
2580	37.348	139.805	2470.76	-278.12	234.98	358.52	0
2610	37.348	139.805	2494.6	-292.02	246.73	376.45	0
2640	37.348	139.805	2518.45	-305.92	258.48	394.37	0
2670	37.348	139.805	2542.3	-319.82	270.22	412.29	0
2700	37.348	139.805	2566.15	-333.72	281.97	430.21	0
2730	37.348	139.805	2590	-347.62	293.71	448.13	0
2760	37.348	139.805	2613.85	-361.53	305.46	466.05	0
2790	37.348	139.805	2637.7	-375.43	317.21	483.97	0
2820	37.348	139.805	2661.55	-389.33	328.95	501.89	0
2850	37.348	139.805	2685.39	-403.23	340.7	519.82	0
2880	37.348	139.805	2709.24	-417.13	352.44	537.74	0
2910	37.348	139.805	2733.09	-431.04	364.19	555.66	0
2940	37.348	139.805	2756.94	-444.94	375.94	573.58	0
2970	37.348	139.805	2780.79	-458.84	387.68	591.5	0

3000	37.348	139.805	2804.64	-472.74	399.43	609.42	0
3030	37.348	139.805	2828.49	-486.64	411.17	627.34	0
3060	37.348	139.805	2852.34	-500.55	422.92	645.26	0
3090	37.348	139.805	2876.19	-514.45	434.67	663.19	0
3120	37.348	139.805	2900.03	-528.35	446.41	681.11	0
3150	37.348	139.805	2923.88	-542.25	458.16	699.03	0
3180	37.348	139.805	2947.73	-556.15	469.9	716.95	0
3210	37.348	139.805	2971.58	-570.06	481.65	734.87	0
3240	37.348	139.805	2995.43	-583.96	493.4	752.79	0
3259.24	37.348	139.805	3010.73	-592.88	500.93	764.29	0
3270	38.295	138.97	3019.22	-597.88	505.22	770.79	3
3300	40.962	136.816	3042.33	-612.07	518.06	789.73	3
3330	43.665	134.883	3064.51	-626.55	532.13	809.81	3
3360	46.398	133.133	3085.71	-641.29	547.4	830.97	3
3390	49.155	131.536	3105.87	-656.24	563.82	853.16	3
3420	51.932	130.066	3124.94	-671.37	581.36	876.32	3
3450	54.727	128.705	3142.85	-686.63	599.96	900.38	3
3480	57.535	127.435	3159.57	-701.99	619.57	925.27	3
3510	60.356	126.242	3175.04	-717.39	640.14	950.94	3
3540	63.187	125.114	3189.23	-732.8	661.61	977.3	3
3570	66.026	124.041	3202.1	-748.18	683.92	1004.29	3
3600	68.872	123.014	3213.6	-763.48	707.01	1031.82	3
3630	71.724	122.027	3223.71	-778.66	730.83	1059.84	3
3660	74.582	121.071	3232.41	-793.68	755.29	1088.25	3
3690	77.443	120.141	3239.66	-808.5	780.35	1116.99	3
3720	80.307	119.232	3245.45	-823.07	805.92	1145.97	3
3750	83.174	118.338	3249.75	-837.36	831.94	1175.11	3
3780	86.042	117.454	3252.57	-851.34	858.33	1204.33	3
3810	88.911	116.577	3253.89	-864.95	885.03	1233.56	3
3819.61	89.831	116.297	3254	-869.23	893.63	1242.91	3
3840	89.848	114.938	3254.06	-878.04	912.02	1262.68	2
3870	89.874	112.938	3254.13	-890.21	939.43	1291.54	2
3900	89.9	110.938	3254.19	-901.42	967.26	1320.1	2
3930	89.926	108.938	3254.23	-911.65	995.46	1348.32	2
3950.92	89.945	107.544	3254.26	-918.2	1015.33	1367.78	2
3960	89.945	107.544	3254.27	-920.94	1023.99	1376.18	0
3990	89.945	107.544	3254.3	-929.98	1052.59	1403.95	0
4020	89.945	107.544	3254.32	-939.02	1081.2	1431.73	0
4050	89.945	107.544	3254.35	-948.07	1109.8	1459.5	0
4080	89.945	107.544	3254.38	-957.11	1138.4	1487.27	0
4109.69	89.945	107.544	3254.41	-966.06	1166.72	1514.76	0
4110	89.945	107.564	3254.41	-966.15	1167.01	1515.04	2
4140	89.918	109.564	3254.45	-975.7	1195.45	1543.01	2
4170	89.892	111.564	3254.5	-986.24	1223.53	1571.34	2
4200	89.866	113.564	3254.56	-997.75	1251.24	1599.99	2
4230	89.84	115.563	3254.64	-1010.22	1278.52	1628.94	2

4260	89.814	117.563	3254.73	-1023.63	1305.35	1658.14	2
4290	89.789	119.563	3254.83	-1037.98	1331.7	1687.57	2
4320	89.764	121.563	3254.95	-1053.23	1357.53	1717.18	2
4350	89.739	123.563	3255.08	-1069.38	1382.81	1746.94	2
4380	89.714	125.563	3255.22	-1086.4	1407.52	1776.82	2
4410	89.69	127.563	3255.38	-1104.27	1431.61	1806.77	2
4440	89.666	129.563	3255.55	-1122.97	1455.07	1836.76	2
4470	89.643	131.562	3255.73	-1142.47	1477.86	1866.76	2
4500	89.62	133.562	3255.92	-1162.76	1499.95	1896.72	2
4517.78	89.606	134.748	3256.04	-1175.15	1512.71	1914.45	2
4530	89.606	134.748	3256.12	-1183.75	1521.38	1926.62	0
4560	89.606	134.748	3256.33	-1204.87	1542.69	1956.51	0
4590	89.606	134.748	3256.54	-1225.99	1564	1986.39	0
4620	89.606	134.748	3256.74	-1247.11	1585.3	2016.28	0
4650	89.606	134.748	3256.95	-1268.23	1606.61	2046.16	0
4680	89.606	134.748	3257.15	-1289.35	1627.91	2076.05	0
4710	89.606	134.748	3257.36	-1310.46	1649.22	2105.94	0
4740	89.606	134.748	3257.57	-1331.58	1670.53	2135.82	0
4770	89.606	134.748	3257.77	-1352.7	1691.83	2165.71	0
4800	89.606	134.748	3257.98	-1373.82	1713.14	2195.59	0
4830	89.606	134.748	3258.19	-1394.94	1734.44	2225.48	0
4860	89.606	134.748	3258.39	-1416.06	1755.75	2255.37	0
4890	89.606	134.748	3258.6	-1437.18	1777.06	2285.25	0
4920	89.606	134.748	3258.8	-1458.3	1798.36	2315.14	0
4950	89.606	134.748	3259.01	-1479.42	1819.67	2345.02	0
4980	89.606	134.748	3259.22	-1500.54	1840.97	2374.91	0
5010	89.606	134.748	3259.42	-1521.66	1862.28	2404.8	0
5040	89.606	134.748	3259.63	-1542.77	1883.58	2434.68	0
5070	89.606	134.748	3259.83	-1563.89	1904.89	2464.57	0
5100	89.606	134.748	3260.04	-1585.01	1926.2	2494.46	0
5130	89.606	134.748	3260.25	-1606.13	1947.5	2524.34	0
5160	89.606	134.748	3260.45	-1627.25	1968.81	2554.23	0
5190	89.606	134.748	3260.66	-1648.37	1990.11	2584.11	0
5220	89.606	134.748	3260.87	-1669.49	2011.42	2614	0
5250	89.606	134.748	3261.07	-1690.61	2032.73	2643.89	0
5260	89.606	134.748	3261.14	-1697.65	2039.83	2653.84	0

VII.14. **Trajectory of Well #3e (#14)**

Depth (m)	Inclination (°)	Azimuth (°)	TVD (m)	North (m)	East (m)	VS (m)	DLS $(°/30m)$
1170	0	0	1170	0	0	0	0
1800	0	0	1800	0	0	0	0
1830	3	158.444	1829.99	-0.73	0.29	0.76	3
1860	6	158.444	1859.89	-2.92	1.15	3.03	3
1890	9	158.444	1889.63	-6.56	2.59	6.81	3
1920	12	158.444	1919.12	-11.64	4.6	12.09	3
1950	15	158.444	1948.29	-18.16	7.17	18.85	3
1980	18	158.444	1977.05	-26.08	10.3	27.08	3
2010	21	158.444	2005.33	-35.39	13.98	36.75	3
2040	24	158.444	2033.04	-46.07	18.2	47.83	3
2070	27	158.444	2060.12	-58.08	22.94	60.3	3
2100	30	158.444	2086.48	-71.39	28.2	74.13	3
2130	33	158.444	2112.06	-85.97	33.96	89.26	3
2160	36	158.444	2136.78	-101.77	40.2	105.67	3
2190	39	158.444	2160.57	-118.76	46.91	123.3	3
2220	42	158.444	2183.38	-136.87	54.07	142.12	3
2250	45	158.444	2205.14	-156.08	61.66	162.05	3
2280	48	158.444	2225.79	-176.31	69.65	183.07	3
2310	51	158.444	2245.27	-197.53	78.03	205.09	3
2340	54	158.444	2263.53	-219.66	86.78	228.07	3
2370	57	158.444	2280.52	-242.65	95.86	251.95	3
2400	60	158.444	2296.2	-266.44	105.26	276.64	3
2430	63	158.444	2310.51	-290.96	114.94	302.1	3
2444.18	64.418	158.444	2316.79	-302.78	119.61	314.38	3
2460	64.418	158.444	2323.62	-316.05	124.86	328.16	0
2490	64.418	158.444	2336.58	-341.22	134.8	354.29	0
2520	64.418	158.444	2349.53	-366.39	144.74	380.42	0
2550	64.418	158.444	2362.48	-391.55	154.68	406.55	0
2580	64.418	158.444	2375.44	-416.72	164.62	432.68	0
2610	64.418	158.444	2388.39	-441.89	174.57	458.81	0
2640	64.418	158.444	2401.35	-467.05	184.51	484.94	0
2670	64.418	158.444	2414.3	-492.22	194.45	511.07	0
2700	64.418	158.444	2427.25	-517.39	204.39	537.2	0
2730	64.418	158.444	2440.21	-542.55	214.33	563.33	0
2760	64.418	158.444	2453.16	-567.72	224.28	589.46	0
2790	64.418	158.444	2466.12	-592.88	234.22	615.59	0
2820	64.418	158.444	2479.07	-618.05	244.16	641.72	0
2850	64.418	158.444	2492.03	-643.22	254.1	667.85	0
2880	64.418	158.444	2504.98	-668.38	264.04	693.98	0
2910	64.418	158.444	2517.93	-693.55	273.99	720.11	0
2940	64.418	158.444	2530.89	-718.72	283.93	746.24	0
2970	64.418	158.444	2543.84	-743.88	293.87	772.37	0

3000	64.418	158.444	2556.8	-769.05	303.81	798.5	0
3030	64.418	158.444	2569.75	-794.22	313.75	824.63	0
3060	64.418	158.444	2582.7	-819.38	323.7	850.76	0
3090	64.418	158.444	2595.66	-844.55	333.64	876.89	0
3120	64.418	158.444	2608.61	-869.71	343.58	903.02	0
3150	64.418	158.444	2621.57	-894.88	353.52	929.15	0
3180	64.418	158.444	2634.52	-920.05	363.46	955.28	0
3210	64.418	158.444	2647.48	-945.21	373.4	981.41	0
3240	64.418	158.444	2660.43	-970.38	383.35	1007.54	0
3270	64.418	158.444	2673.38	-995.55	393.29	1033.67	0
3300	64.418	158.444	2686.34	-1020.71	403.23	1059.8	0
3330	64.418	158.444	2699.29	-1045.88	413.17	1085.93	0
3360	64.418	158.444	2712.25	-1071.05	423.11	1112.06	0
3390	64.418	158.444	2725.2	-1096.21	433.06	1138.19	0
3420	64.418	158.444	2738.15	-1121.38	443	1164.32	0
3450	64.418	158.444	2751.11	-1146.54	452.94	1190.45	0
3480	64.418	158.444	2764.06	-1171.71	462.88	1216.58	0
3510	64.418	158.444	2777.02	-1196.88	472.82	1242.71	0
3540	64.418	158.444	2789.97	-1222.04	482.77	1268.84	0
3570	64.418	158.444	2802.93	-1247.21	492.71	1294.97	0
3600	64.418	158.444	2815.88	-1272.38	502.65	1321.1	0
3630	64.418	158.444	2828.83	-1297.54	512.59	1347.23	0
3660	64.418	158.444	2841.79	-1322.71	522.53	1373.36	0
3690	64.418	158.444	2854.74	-1347.88	532.48	1399.49	0
3720	64.418	158.444	2867.7	-1373.04	542.42	1425.62	0
3750	64.418	158.444	2880.65	-1398.21	552.36	1451.75	0
3780	64.418	158.444	2893.6	-1423.38	562.3	1477.88	0
3810	64.418	158.444	2906.56	-1448.54	572.24	1504.01	0
3840	64.418	158.444	2919.51	-1473.71	582.19	1530.14	0
3870	64.418	158.444	2932.47	-1498.87	592.13	1556.27	0
3900	64.418	158.444	2945.42	-1524.04	602.07	1582.4	0
3930	64.418	158.444	2958.38	-1549.21	612.01	1608.53	0
3960	64.418	158.444	2971.33	-1574.37	621.95	1634.66	0
3985.14	64.418	158.444	2982.19	-1595.46	630.28	1656.56	0
3990	64.635	158.925	2984.28	-1599.55	631.88	1660.8	3
4020	66.008	161.861	2996.8	-1625.23	641.02	1687.35	3
4050	67.436	164.733	3008.66	-1651.62	648.94	1714.47	3
4080	68.914	167.546	3019.82	-1678.65	655.6	1742.08	3
4110	70.437	170.302	3030.24	-1706.26	661	1770.12	3
4140	72.002	173.006	3039.9	-1734.36	665.12	1798.51	3
4170	73.603	175.661	3048.77	-1762.87	667.95	1827.16	3
4200	75.237	178.273	3056.83	-1791.73	669.48	1856	3
4230	76.9	180.846	3064.05	-1820.84	669.7	1884.95	3
4260	78.588	183.384	3070.42	-1850.13	668.61	1913.93	3
4290	80.298	185.892	3075.92	-1879.52	666.23	1942.86	3
4320	82.025	188.374	3080.53	-1908.93	662.55	1971.67	3

4350	83.768	190.835	3084.24	-1938.28	657.58	2000.27	3
4380	85.521	193.28	3087.04	-1967.49	651.34	2028.58	3
4410	87.283	195.713	3088.92	-1996.47	643.84	2056.53	3
4440	89.049	198.139	3089.88	-2025.16	635.11	2084.04	3
4450.86	89.689	199.016	3090	-2035.44	631.66	2093.87	3
4470	89.689	199.016	3090.1	-2053.54	625.42	2111.15	0
4500	89.689	199.016	3090.27	-2081.91	615.64	2138.22	0
4530	89.689	199.016	3090.43	-2110.27	605.87	2165.29	0
4560	89.689	199.016	3090.59	-2138.63	596.09	2192.37	0
4590	89.689	199.016	3090.75	-2166.99	586.32	2219.44	0
4620	89.689	199.016	3090.92	-2195.36	576.54	2246.51	0
4650	89.689	199.016	3091.08	-2223.72	566.77	2273.59	0
4680	89.689	199.016	3091.24	-2252.08	556.99	2300.66	0
4710	89.689	199.016	3091.41	-2280.44	547.22	2327.73	0
4740	89.689	199.016	3091.57	-2308.8	537.44	2354.81	0
4770	89.689	199.016	3091.73	-2337.17	527.67	2381.88	0
4800	89.689	199.016	3091.89	-2365.53	517.89	2408.95	0
4830	89.689	199.016	3092.06	-2393.89	508.12	2436.03	0
4860	89.689	199.016	3092.22	-2422.25	498.34	2463.1	0
4890	89.689	199.016	3092.38	-2450.62	488.57	2490.17	0
4920	89.689	199.016	3092.54	-2478.98	478.79	2517.25	0
4950	89.689	199.016	3092.71	-2507.34	469.02	2544.32	0
4980	89.689	199.016	3092.87	-2535.7	459.24	2571.39	0
5010	89.689	199.016	3093.03	-2564.07	449.47	2598.47	0
5040	89.689	199.016	3093.2	-2592.43	439.69	2625.54	0
5070	89.689	199.016	3093.36	-2620.79	429.92	2652.61	0
5100	89.689	199.016	3093.52	-2649.15	420.14	2679.69	0
5130	89.689	199.016	3093.68	-2677.52	410.37	2706.76	0
5160	89.689	199.016	3093.85	-2705.88	400.59	2733.83	0
5190	89.689	199.016	3094.01	-2734.24	390.82	2760.91	0
5220	89.689	199.016	3094.17	-2762.6	381.04	2787.98	0
5250	89.689	199.016	3094.33	-2790.96	371.27	2815.05	0
5280	89.689	199.016	3094.5	-2819.33	361.49	2842.13	0
5310	89.689	199.016	3094.66	-2847.69	351.72	2869.2	0
5340	89.689	199.016	3094.82	-2876.05	341.94	2896.27	0
5370	89.689	199.016	3094.98	-2904.41	332.17	2923.35	0
5372.82	89.689	199.016	3095	-2907.08	331.25	2925.89	0

VII.15. **Trajectory of Well #3f (#15)**

Depth (m)	Inclination (°)	Azimuth (°)	TVD (m)	North (m)	East (m)	VS (m)	DLS $(°/30m)$
1170	0	0	1170	0	0	0	0
1800	0	0	1800	0	0	0	0
1830	3	82.282	1829.99	0.11	0.78	-0.11	3
1860	6	82.282	1859.89	0.42	3.11	-0.46	3
1890	9	82.282	1889.63	0.95	6.99	-1.03	3
1920	12	82.282	1919.12	1.68	12.41	-1.82	3
1950	15	82.282	1948.29	2.62	19.35	-2.84	3
1980	18	82.282	1977.05	3.77	27.79	-4.08	3
1994.98	19.498	82.282	1991.24	4.41	32.56	-4.78	3
2010	19.498	82.282	2005.4	5.09	37.53	-5.51	0
2040	19.498	82.282	2033.68	6.43	47.45	-6.96	0
2070	19.498	82.282	2061.96	7.78	57.37	-8.42	0
2100	19.498	82.282	2090.24	9.12	67.29	-9.87	0
2130	19.498	82.282	2118.52	10.46	77.22	-11.33	0
2160	19.498	82.282	2146.8	11.81	87.14	-12.79	0
2190	19.498	82.282	2175.07	13.15	97.06	-14.24	0
2220	19.498	82.282	2203.35	14.5	106.98	-15.7	0
2250	19.498	82.282	2231.63	15.84	116.91	-17.15	0
2280	19.498	82.282	2259.91	17.19	126.83	-18.61	0
2310	19.498	82.282	2288.19	18.53	136.75	-20.07	0
2340	19.498	82.282	2316.47	19.88	146.67	-21.52	0
2370	19.498	82.282	2344.75	21.22	156.6	-22.98	0
2400	19.498	82.282	2373.03	22.57	166.52	-24.43	0
2430	19.498	82.282	2401.31	23.91	176.44	-25.89	0
2460	19.498	82.282	2429.59	25.26	186.36	-27.34	0
2490	19.498	82.282	2457.87	26.6	196.29	-28.8	0
2520	19.498	82.282	2486.15	27.95	206.21	-30.26	0
2550	19.498	82.282	2514.43	29.29	216.13	-31.71	0
2580	19.498	82.282	2542.71	30.64	226.05	-33.17	0
2610	19.498	82.282	2570.99	31.98	235.98	-34.62	0
2640	19.498	82.282	2599.27	33.32	245.9	-36.08	0
2670	19.498	82.282	2627.55	34.67	255.82	-37.54	0
2681.88	19.498	82.282	2638.75	35.2	259.75	-38.11	0
2700	18.817	87.401	2655.87	35.74	265.67	-38.72	3
2730	18.025	96.568	2684.33	35.43	275.11	-38.51	3
2760	17.695	106.301	2712.89	33.62	284.1	-36.8	3
2790	17.854	116.126	2741.47	30.31	292.61	-33.59	3
2820	18.489	125.538	2769.98	25.52	300.61	-28.89	3
2850	19.554	134.155	2798.35	19.26	308.09	-22.71	3
2880	20.982	141.779	2826.49	11.54	315.01	-15.07	3
2910	22.707	148.385	2854.34	2.39	321.37	-5.99	3
2940	24.664	154.05	2881.82	-8.18	327.15	4.51	3

2970	26.804	158.897	2908.84	-20.12	332.32	16.39	3
3000	29.086	163.057	2935.35	-33.41	336.88	29.63	3
3030	31.479	166.648	2961.25	-48.01	340.82	44.18	3
3060	33.959	169.773	2986.49	-63.88	344.12	60.01	3
3090	36.509	172.516	3011	-80.98	346.77	77.08	3
3120	39.114	174.944	3034.7	-99.25	348.76	95.34	3
3150	41.764	177.113	3057.53	-118.66	350.1	114.73	3
3180	44.451	179.066	3079.43	-139.15	350.78	135.21	3
3210	47.168	180.84	3100.34	-160.66	350.79	156.71	3
3240	49.91	182.465	3120.2	-183.12	350.13	179.19	3
3270	52.673	183.962	3138.96	-206.49	348.81	202.57	3
3300	55.454	185.353	3156.57	-230.7	346.84	226.8	3
3330	58.249	186.654	3172.97	-255.68	344.2	251.8	3
3360	61.057	187.879	3188.12	-281.35	340.93	277.51	3
3390	63.876	189.038	3201.99	-307.66	337.01	303.86	3
3420	66.703	190.143	3214.53	-334.53	332.47	330.78	3
3450	69.537	191.202	3225.71	-361.89	327.31	358.19	3
3480	72.378	192.222	3235.5	-389.65	321.55	386.02	3
3510	75.224	193.211	3243.87	-417.75	315.21	414.19	3
3540	78.074	194.174	3250.79	-446.1	308.3	442.62	3
3570	80.927	195.117	3256.26	-474.64	300.84	471.24	3
3600	83.783	196.045	3260.25	-503.28	292.85	499.96	3
3630	86.64	196.963	3262.76	-531.94	284.36	528.71	3
3660	89.498	197.876	3263.77	-560.54	275.39	557.42	3
3668.59	90.316	198.137	3263.78	-568.71	272.73	565.61	3
3690	90.316	198.137	3263.66	-589.06	266.07	586.04	0
3720	90.316	198.137	3263.5	-617.57	256.73	614.65	0
3750	90.316	198.137	3263.33	-646.07	247.39	643.26	0
3780	90.316	198.137	3263.17	-674.58	238.05	671.87	0
3810	90.316	198.137	3263	-703.09	228.71	700.48	0
3840	90.316	198.137	3262.83	-731.6	219.37	729.1	0
3870	90.316	198.137	3262.67	-760.11	210.04	757.71	0
3900	90.316	198.137	3262.5	-788.62	200.7	786.32	0
3930	90.316	198.137	3262.34	-817.13	191.36	814.93	0
3960	90.316	198.137	3262.17	-845.64	182.02	843.54	0
3990	90.316	198.137	3262.01	-874.15	172.68	872.16	0
4020	90.316	198.137	3261.84	-902.66	163.34	900.77	0
4050	90.316	198.137	3261.68	-931.16	154	929.38	0
4080	90.316	198.137	3261.51	-959.67	144.66	957.99	0
4110	90.316	198.137	3261.35	-988.18	135.33	986.6	0
4140	90.316	198.137	3261.18	-1016.69	125.99	1015.21	0
4170	90.316	198.137	3261.01	-1045.2	116.65	1043.83	0
4200	90.316	198.137	3260.85	-1073.71	107.31	1072.44	0
4230	90.316	198.137	3260.68	-1102.22	97.97	1101.05	0
4260	90.316	198.137	3260.52	-1130.73	88.63	1129.66	0
4290	90.316	198.137	3260.35	-1159.24	79.29	1158.27	0

4320	90.316	198.137	3260.19	-1187.75	69.96	1186.89	0
4350	90.316	198.137	3260.02	-1216.25	60.62	1215.5	0
4380	90.316	198.137	3259.86	-1244.76	51.28	1244.11	0
4410	90.316	198.137	3259.69	-1273.27	41.94	1272.72	0
4440	90.316	198.137	3259.53	-1301.78	32.6	1301.33	0
4470	90.316	198.137	3259.36	-1330.29	23.26	1329.95	0
4500	90.316	198.137	3259.19	-1358.8	13.92	1358.56	0
4530	90.316	198.137	3259.03	-1387.31	4.59	1387.17	0
4560	90.316	198.137	3258.86	-1415.82	-4.75	1415.78	0
4590	90.316	198.137	3258.7	-1444.33	-14.09	1444.39	0
4597.01	90.316	198.137	3258.66	-1450.99	-16.27	1451.08	0

VII.16. **Trajectory of Well #4a (#16)**

Depth (m)	Inclination (°)	Azimuth (°)	TVD (m)	North (m)	East (m)	VS (m)	DLS $(°/30m)$
0	0	0	0	-1	-8.3	0	0
1700	0	360	1700	-1	-8.3	0	0
1709.94	0.994	265.54	1709.94	-1.01	-8.39	-0.04	3
1710	0.994	265.54	1710	-1.01	-8.39	-0.04	0
1740	0.994	265.54	1739.99	-1.05	-8.91	-0.31	0
1770	0.994	265.54	1769.99	-1.09	-9.42	-0.57	0
1800	0.994	265.54	1799.99	-1.13	-9.94	-0.83	0
1830	0.994	265.54	1829.98	-1.17	-10.46	-1.09	0
1860	0.994	265.54	1859.98	-1.21	-10.98	-1.35	0
1890	0.994	265.54	1889.97	-1.25	-11.5	-1.61	0
1920	0.994	265.54	1919.97	-1.29	-12.02	-1.87	0
1950	0.994	265.54	1949.96	-1.33	-12.54	-2.13	0
1980	0.994	265.54	1979.96	-1.37	-13.06	-2.4	0
2010	0.994	265.54	2009.95	-1.41	-13.57	-2.66	0
2040	0.994	265.54	2039.95	-1.45	-14.09	-2.92	0
2070	0.994	265.54	2069.95	-1.49	-14.61	-3.18	0
2100	0.994	265.54	2099.94	-1.53	-15.13	-3.44	0
2130	0.994	265.54	2129.94	-1.57	-15.65	-3.7	0
2160	0.994	265.54	2159.93	-1.61	-16.17	-3.96	0
2190	0.994	265.54	2189.93	-1.65	-16.69	-4.22	0
2220	0.994	265.54	2219.92	-1.69	-17.2	-4.49	0
2250	0.994	265.54	2249.92	-1.73	-17.72	-4.75	0
2280	0.994	265.54	2279.91	-1.78	-18.24	-5.01	0
2310	0.994	265.54	2309.91	-1.82	-18.76	-5.27	0
2340	0.994	265.54	2339.9	-1.86	-19.28	-5.53	0
2370	0.994	265.54	2369.9	-1.9	-19.8	-5.79	0
2400	0.994	265.54	2399.9	-1.94	-20.32	-6.05	0
2430	0.994	265.54	2429.89	-1.98	-20.84	-6.31	0
2460	0.994	265.54	2459.89	-2.02	-21.35	-6.58	0
2490	0.994	265.54	2489.88	-2.06	-21.87	-6.84	0
2516.36	0.994	265.54	2516.24	-2.09	-22.33	-7.07	0
2520	0.866	286.708	2519.88	-2.09	-22.39	-7.09	3
2550	2.981	9.631	2549.86	-1.25	-22.47	-6.37	3
2580	5.918	17.998	2579.77	0.99	-21.86	-4.09	3
2610	8.897	20.803	2609.52	4.63	-20.56	-0.24	3
2640	11.886	22.206	2639.02	9.66	-18.57	5.15	3
2670	14.88	23.052	2668.2	16.06	-15.89	12.09	3
2700	17.876	23.619	2696.98	23.83	-12.54	20.54	3
2730	20.873	24.028	2725.28	32.93	-8.52	30.48	3
2760	23.871	24.338	2753.02	43.34	-3.84	41.9	3
2790	26.869	24.582	2780.12	55.04	1.48	54.74	3
2820	29.867	24.781	2806.52	67.99	7.44	69	3

2850	32.866	24.946	2832.13	82.16	14	84.61	3
2880	35.865	25.087	2856.89	97.5	21.16	101.54	3
2910	38.864	25.208	2880.73	113.98	28.9	119.74	3
2940	41.863	25.315	2903.59	131.55	37.19	139.17	3
2970	44.863	25.41	2925.4	150.16	46.01	159.76	3
3000	47.862	25.496	2946.1	169.76	55.34	181.47	3
3030	50.861	25.573	2965.63	190.3	65.15	204.24	3
3060	53.861	25.645	2983.95	211.72	75.42	227.99	3
3090	56.86	25.711	3001	233.96	86.12	252.67	3
3120	59.86	25.772	3016.74	256.97	97.21	278.21	3
3150	62.859	25.831	3031.11	280.67	108.67	304.53	3
3180	65.859	25.886	3044.09	305	120.46	331.57	3
3210	68.859	25.938	3055.64	329.9	132.56	359.26	3
3240	71.858	25.989	3065.72	355.3	144.93	387.51	3
3270	74.858	26.037	3074.32	381.13	157.53	416.25	3
3300	77.858	26.085	3081.39	407.32	170.34	445.4	3
3330	80.857	26.131	3086.93	433.79	183.31	474.88	3
3360	83.857	26.177	3090.92	460.48	196.42	504.61	3
3390	86.856	26.222	3093.35	487.3	209.62	534.51	3
3420	89.856	26.266	3094.21	514.2	222.88	564.49	3
3421.97	90.053	26.269	3094.21	515.96	223.75	566.46	3
3450	90.053	26.269	3094.18	541.1	236.15	594.49	0
3480	90.053	26.269	3094.16	568	249.43	624.49	0
3510	90.053	26.269	3094.13	594.9	262.71	654.48	0
3540	90.053	26.269	3094.1	621.8	275.99	684.48	0
3570	90.053	26.269	3094.07	648.71	289.26	714.48	0
3600	90.053	26.269	3094.05	675.61	302.54	744.48	0
3630	90.053	26.269	3094.02	702.51	315.82	774.48	0
3660	90.053	26.269	3093.99	729.41	329.1	804.48	0
3690	90.053	26.269	3093.96	756.31	342.37	834.47	0
3720	90.053	26.269	3093.93	783.22	355.65	864.47	0
3750	90.053	26.269	3093.91	810.12	368.93	894.47	0
3780	90.053	26.269	3093.88	837.02	382.21	924.47	0
3810	90.053	26.269	3093.85	863.92	395.49	954.47	0
3840	90.053	26.269	3093.82	890.82	408.76	984.47	0
3870	90.053	26.269	3093.79	917.72	422.04	1014.46	0
3900	90.053	26.269	3093.77	944.63	435.32	1044.46	0
3930	90.053	26.269	3093.74	971.53	448.6	1074.46	0
3960	90.053	26.269	3093.71	998.43	461.87	1104.46	0
3990	90.053	26.269	3093.68	1025.33	475.15	1134.46	0
4020	90.053	26.269	3093.66	1052.23	488.43	1164.46	0
4050	90.053	26.269	3093.63	1079.13	501.71	1194.46	0
4080	90.053	26.269	3093.6	1106.04	514.98	1224.45	0
4110	90.053	26.269	3093.57	1132.94	528.26	1254.45	0
4140	90.053	26.269	3093.54	1159.84	541.54	1284.45	0
4170	90.053	26.269	3093.52	1186.74	554.82	1314.45	0

4200	90.053	26.269	3093.49	1213.64	568.1	1344.45	0
4230	90.053	26.269	3093.46	1240.54	581.37	1374.45	0
4260	90.053	26.269	3093.43	1267.45	594.65	1404.44	0
4290	90.053	26.269	3093.41	1294.35	607.93	1434.44	0
4320	90.053	26.269	3093.38	1321.25	621.21	1464.44	0
4350	90.053	26.269	3093.35	1348.15	634.48	1494.44	0
4380	90.053	26.269	3093.32	1375.05	647.76	1524.44	0
4410	90.053	26.269	3093.29	1401.95	661.04	1554.44	0
4440	90.053	26.269	3093.27	1428.86	674.32	1584.43	0
4470	90.053	26.269	3093.24	1455.76	687.59	1614.43	0
4500	90.053	26.269	3093.21	1482.66	700.87	1644.43	0
4530	90.053	26.269	3093.18	1509.56	714.15	1674.43	0
4560	90.053	26.269	3093.16	1536.46	727.43	1704.43	0
4590	90.053	26.269	3093.13	1563.36	740.71	1734.43	0
4620	90.053	26.269	3093.1	1590.27	753.98	1764.43	0
4650	90.053	26.269	3093.07	1617.17	767.26	1794.42	0
4680	90.053	26.269	3093.04	1644.07	780.54	1824.42	0
4710	90.053	26.269	3093.02	1670.97	793.82	1854.42	0
4740	90.053	26.269	3092.99	1697.87	807.09	1884.42	0
4770	90.053	26.269	3092.96	1724.78	820.37	1914.42	0
4800	90.053	26.269	3092.93	1751.68	833.65	1944.42	0
4830	90.053	26.269	3092.91	1778.58	846.93	1974.41	0
4860	90.053	26.269	3092.88	1805.48	860.2	2004.41	0
4889.86	90.053	26.269	3092.85	1832.26	873.42	2034.27	0

VII.17. **Trajectory of Well #4b (#17)**

Depth (m)	Inclination (°)	Azimuth (°)	TVD (m)	North (m)	East (m)	VS (m)	DLS $(°/30m)$
0	0	0	0	7.1	4.8	0	0
1700	0	0	1700	7.1	4.8	0	0
1710	1	24.052	1710	7.18	4.84	0.09	3
1740	4	24.052	1739.97	8.37	5.37	1.4	3
1770	7	24.052	1769.83	11	6.54	4.27	3
1800	10	24.052	1799.49	15.05	8.35	8.7	3
1830	13	24.052	1828.89	20.51	10.79	14.68	3
1860	16	24.052	1857.93	27.37	13.85	22.19	3
1890	19	24.052	1886.54	35.61	17.52	31.2	3
1920	22	24.052	1914.63	45.2	21.8	41.71	3
1950	25	24.052	1942.14	56.12	26.68	53.66	3
1980	28	24.052	1968.99	68.34	32.13	67.04	3
2010	31	24.052	1995.1	81.83	38.15	81.81	3
2040	34	24.052	2020.39	96.55	44.72	97.92	3
2070	37	24.052	2044.81	112.46	51.82	115.33	3
2100	40	24.052	2068.29	129.51	59.43	134	3
2130	43	24.052	2090.76	147.66	67.53	153.87	3
2160	46	24.052	2112.15	166.86	76.1	174.89	3
2190	49	24.052	2132.42	187.05	85.12	196.99	3
2220	52	24.052	2151.5	208.19	94.55	220.13	3
2250	55	24.052	2169.34	230.21	104.38	244.24	3
2280	58	24.052	2185.9	253.05	114.57	269.24	3
2310	61	24.052	2201.12	276.65	125.11	295.08	3
2340	64	24.052	2214.97	300.95	135.95	321.68	3
2351.98	65.198	24.052	2220.11	310.83	140.36	332.49	3
2370	65.198	24.052	2227.67	325.77	147.03	348.85	0
2400	65.198	24.052	2240.25	350.64	158.13	376.07	0
2430	65.198	24.052	2252.84	375.51	169.23	403.29	0
2460	65.198	24.052	2265.42	400.38	180.32	430.52	0
2490	65.198	24.052	2278.01	425.24	191.42	457.74	0
2520	65.198	24.052	2290.59	450.11	202.52	484.96	0
2550	65.198	24.052	2303.18	474.98	213.62	512.19	0
2580	65.198	24.052	2315.76	499.85	224.72	539.41	0
2610	65.198	24.052	2328.35	524.72	235.82	566.63	0
2640	65.198	24.052	2340.93	549.59	246.92	593.86	0
2670	65.198	24.052	2353.51	574.45	258.02	621.08	0
2700	65.198	24.052	2366.1	599.32	269.12	648.3	0
2730	65.198	24.052	2378.68	624.19	280.22	675.53	0
2760	65.198	24.052	2391.27	649.06	291.32	702.75	0
2790	65.198	24.052	2403.85	673.93	302.42	729.97	0
2820	65.198	24.052	2416.44	698.8	313.51	757.2	0
2850	65.198	24.052	2429.02	723.67	324.61	784.42	0

2880	65.198	24.052	2441.61	748.53	335.71	811.64	0
2910	65.198	24.052	2454.19	773.4	346.81	838.87	0
2940	65.198	24.052	2466.78	798.27	357.91	866.09	0
2970	65.198	24.052	2479.36	823.14	369.01	893.31	0
3000	65.198	24.052	2491.94	848.01	380.11	920.54	0
3030	65.198	24.052	2504.53	872.88	391.21	947.76	0
3060	65.198	24.052	2517.11	897.74	402.31	974.98	0
3090	65.198	24.052	2529.7	922.61	413.41	1002.21	0
3120	65.198	24.052	2542.28	947.48	424.51	1029.43	0
3150	65.198	24.052	2554.87	972.35	435.61	1056.65	0
3180	65.198	24.052	2567.45	997.22	446.7	1083.88	0
3210	65.198	24.052	2580.04	1022.09	457.8	1111.1	0
3240	65.198	24.052	2592.62	1046.95	468.9	1138.32	0
3270	65.198	24.052	2605.21	1071.82	480	1165.55	0
3300	65.198	24.052	2617.79	1096.69	491.1	1192.77	0
3330	65.198	24.052	2630.37	1121.56	502.2	1219.99	0
3360	65.198	24.052	2642.96	1146.43	513.3	1247.22	0
3390	65.198	24.052	2655.54	1171.3	524.4	1274.44	0
3420	65.198	24.052	2668.13	1196.16	535.5	1301.66	0
3450	65.198	24.052	2680.71	1221.03	546.6	1328.89	0
3480	65.198	24.052	2693.3	1245.9	557.7	1356.11	0
3510	65.198	24.052	2705.88	1270.77	568.79	1383.33	0
3540	65.198	24.052	2718.47	1295.64	579.89	1410.56	0
3570	65.198	24.052	2731.05	1320.51	590.99	1437.78	0
3600	65.198	24.052	2743.64	1345.38	602.09	1465	0
3630	65.198	24.052	2756.22	1370.24	613.19	1492.23	0
3660	65.198	24.052	2768.81	1395.11	624.29	1519.45	0
3690	65.198	24.052	2781.39	1419.98	635.39	1546.67	0
3720	65.198	24.052	2793.97	1444.85	646.49	1573.9	0
3750	65.198	24.052	2806.56	1469.72	657.59	1601.12	0
3780	65.198	24.052	2819.14	1494.59	668.69	1628.34	0
3810	65.198	24.052	2831.73	1519.45	679.79	1655.57	0
3840	65.198	24.052	2844.31	1544.32	690.89	1682.79	0
3870	65.198	24.052	2856.9	1569.19	701.98	1710.01	0
3900	65.198	24.052	2869.48	1594.06	713.08	1737.24	0
3930	65.198	24.052	2882.07	1618.93	724.18	1764.46	0
3960	65.198	24.052	2894.65	1643.8	735.28	1791.68	0
3990	65.198	24.052	2907.24	1668.66	746.38	1818.9	0
4020	65.198	24.052	2919.82	1693.53	757.48	1846.13	0
4050	65.198	24.052	2932.4	1718.4	768.58	1873.35	0
4080	65.198	24.052	2944.99	1743.27	779.68	1900.57	0
4110	65.198	24.052	2957.57	1768.14	790.78	1927.8	0
4140	65.198	24.052	2970.16	1793.01	801.88	1955.02	0
4170	65.198	24.052	2982.74	1817.88	812.98	1982.24	0
4200	65.198	24.052	2995.33	1842.74	824.07	2009.47	0
4230	65.198	24.052	3007.91	1867.61	835.17	2036.69	0

4260	65.198	24.052	3020.5	1892.48	846.27	2063.91	0
4264.91	65.198	24.052	3022.55	1896.55	848.09	2068.37	0
4290	67.682	23.666	3032.58	1917.58	857.39	2091.36	3
4320	70.654	23.223	3043.25	1943.3	868.54	2119.39	3
4350	73.626	22.795	3052.45	1969.58	879.7	2147.94	3
4380	76.599	22.381	3060.16	1996.35	890.84	2176.93	3
4410	79.573	21.976	3066.35	2023.53	901.92	2206.28	3
4440	82.547	21.579	3071.01	2051.05	912.91	2235.91	3
4470	85.522	21.188	3074.13	2078.83	923.79	2265.74	3
4500	88.497	20.8	3075.7	2106.79	934.52	2295.68	3
4505.3	89.022	20.731	3075.81	2111.75	936.4	2300.98	3
4530	89.022	20.731	3076.23	2134.85	945.14	2325.67	0
4560	89.022	20.731	3076.74	2162.9	955.76	2355.65	0
4590	89.022	20.731	3077.26	2190.95	966.38	2385.63	0
4620	89.022	20.731	3077.77	2219.01	976.99	2415.61	0
4650	89.022	20.731	3078.28	2247.06	987.61	2445.59	0
4680	89.022	20.731	3078.79	2275.11	998.23	2475.57	0
4710	89.022	20.731	3079.3	2303.17	1008.85	2505.55	0
4740	89.022	20.731	3079.81	2331.22	1019.47	2535.53	0
4770	89.022	20.731	3080.33	2359.27	1030.08	2565.51	0
4800	89.022	20.731	3080.84	2387.33	1040.7	2595.49	0
4830	89.022	20.731	3081.35	2415.38	1051.32	2625.47	0
4860	89.022	20.731	3081.86	2443.43	1061.94	2655.45	0
4890	89.022	20.731	3082.37	2471.49	1072.56	2685.43	0
4920	89.022	20.731	3082.89	2499.54	1083.17	2715.42	0
4950	89.022	20.731	3083.4	2527.59	1093.79	2745.4	0
4980	89.022	20.731	3083.91	2555.65	1104.41	2775.38	0
5010	89.022	20.731	3084.42	2583.7	1115.03	2805.36	0
5040	89.022	20.731	3084.93	2611.75	1125.65	2835.34	0
5070	89.022	20.731	3085.44	2639.81	1136.26	2865.32	0
5100	89.022	20.731	3085.96	2667.86	1146.88	2895.3	0
5130	89.022	20.731	3086.47	2695.91	1157.5	2925.28	0
5160	89.022	20.731	3086.98	2723.97	1168.12	2955.26	0
5190	89.022	20.731	3087.49	2752.02	1178.74	2985.24	0
5220	89.022	20.731	3088	2780.08	1189.35	3015.22	0
5250	89.022	20.731	3088.52	2808.13	1199.97	3045.2	0
5280	89.022	20.731	3089.03	2836.18	1210.59	3075.19	0
5310	89.022	20.731	3089.54	2864.24	1221.21	3105.17	0
5340	89.022	20.731	3090.05	2892.29	1231.83	3135.15	0
5370	89.022	20.731	3090.56	2920.34	1242.44	3165.13	0
5400	89.022	20.731	3091.07	2948.4	1253.06	3195.11	0
5430	89.022	20.731	3091.59	2976.45	1263.68	3225.09	0
5460	89.022	20.731	3092.1	3004.5	1274.3	3255.07	0
5490	89.022	20.731	3092.61	3032.56	1284.92	3285.05	0
5520	89.022	20.731	3093.12	3060.61	1295.53	3315.03	0
5550	89.022	20.731	3093.63	3088.66	1306.15	3345.01	0

5580	89.022	20.731	3094.15	3116.72	1316.77	3374.99	0
5610	89.022	20.731	3094.66	3144.77	1327.39	3404.97	0
5640	89.022	20.731	3095.17	3172.82	1338.01	3434.95	0
5670	89.022	20.731	3095.68	3200.88	1348.62	3464.94	0
5700	89.022	20.731	3096.19	3228.93	1359.24	3494.92	0
5730	89.022	20.731	3096.71	3256.98	1369.86	3524.9	0
5760	89.022	20.731	3097.22	3285.04	1380.48	3554.88	0
5790	89.022	20.731	3097.73	3313.09	1391.1	3584.86	0
5820	89.022	20.731	3098.24	3341.14	1401.71	3614.84	0
5850	89.022	20.731	3098.75	3369.2	1412.33	3644.82	0
5880	89.022	20.731	3099.26	3397.25	1422.95	3674.8	0
5910	89.022	20.731	3099.78	3425.3	1433.57	3704.78	0
5940	89.022	20.731	3100.29	3453.36	1444.19	3734.76	0
5970	89.022	20.731	3100.8	3481.41	1454.8	3764.74	0
6000	89.022	20.731	3101.31	3509.47	1465.42	3794.72	0
6030	89.022	20.731	3101.82	3537.52	1476.04	3824.7	0
6060	89.022	20.731	3102.34	3565.57	1486.66	3854.69	0
6090	89.022	20.731	3102.85	3593.63	1497.28	3884.67	0
6120	89.022	20.731	3103.36	3621.68	1507.89	3914.65	0
6150	89.022	20.731	3103.87	3649.73	1518.51	3944.63	0
6180	89.022	20.731	3104.38	3677.79	1529.13	3974.61	0
6210	89.022	20.731	3104.89	3705.84	1539.75	4004.59	0
6219.7	89.022	20.731	3105.06	3714.91	1543.18	4014.28	0

VII.18. **Trajectory of Well #4c (#18)**

Depth (m)	Inclination (°)	Azimuth (°)	TVD (m)	North (m)	East (m)	VS (m)	DLS $(°/30m)$
0	0	0	0	1	8.3	0	0
1700	0	0	1700	1	8.3	0	0
1707.29	0.729	120.025	1707.29	0.98	8.34	0.04	3
1710	0.729	120.025	1710	0.96	8.37	0.08	0
1740	0.729	120.025	1740	0.77	8.7	0.44	0
1770	0.729	120.025	1769.99	0.58	9.03	0.81	0
1800	0.729	120.025	1799.99	0.39	9.36	1.17	0
1830	0.729	120.025	1829.99	0.2	9.69	1.54	0
1860	0.729	120.025	1859.99	0	10.02	1.91	0
1890	0.729	120.025	1889.99	-0.19	10.35	2.27	0
1920	0.729	120.025	1919.98	-0.38	10.68	2.64	0
1950	0.729	120.025	1949.98	-0.57	11.01	3	0
1980	0.729	120.025	1979.98	-0.76	11.34	3.37	0
2010	0.729	120.025	2009.98	-0.95	11.67	3.73	0
2040	0.729	120.025	2039.97	-1.14	12	4.1	0
2070	0.729	120.025	2069.97	-1.33	12.33	4.47	0
2100	0.729	120.025	2099.97	-1.52	12.66	4.83	0
2130	0.729	120.025	2129.97	-1.71	13	5.2	0
2160	0.729	120.025	2159.96	-1.9	13.33	5.56	0
2190	0.729	120.025	2189.96	-2.1	13.66	5.93	0
2220	0.729	120.025	2219.96	-2.29	13.99	6.29	0
2250	0.729	120.025	2249.96	-2.48	14.32	6.66	0
2280	0.729	120.025	2279.95	-2.67	14.65	7.02	0
2310	0.729	120.025	2309.95	-2.86	14.98	7.39	0
2340	0.729	120.025	2339.95	-3.05	15.31	7.76	0
2370	0.729	120.025	2369.95	-3.24	15.64	8.12	0
2400	0.729	120.025	2399.94	-3.43	15.97	8.49	0
2430	0.729	120.025	2429.94	-3.62	16.3	8.85	0
2460	0.729	120.025	2459.94	-3.81	16.63	9.22	0
2490	0.729	120.025	2489.94	-4	16.96	9.58	0
2520	0.729	120.025	2519.93	-4.2	17.29	9.95	0
2550	0.729	120.025	2549.93	-4.39	17.62	10.32	0
2580	0.729	120.025	2579.93	-4.58	17.95	10.68	0
2610	0.729	120.025	2609.93	-4.77	18.28	11.05	0
2640	0.729	120.025	2639.92	-4.96	18.61	11.41	0
2670	0.729	120.025	2669.92	-5.15	18.94	11.78	0
2700	0.729	120.025	2699.92	-5.34	19.27	12.14	0
2730	0.729	120.025	2729.92	-5.53	19.6	12.51	0
2760	0.729	120.025	2759.91	-5.72	19.93	12.87	0
2790	0.729	120.025	2789.91	-5.91	20.26	13.24	0
2820	0.729	120.025	2819.91	-6.11	20.59	13.61	0
2850	0.729	120.025	2849.91	-6.3	20.92	13.97	0

2880	0.729	120.025	2879.9	-6.49	21.25	14.34	0
2910	0.729	120.025	2909.9	-6.68	21.58	14.7	0
2924.04	0.729	120.025	2923.94	-6.77	21.74	14.87	0
2940	2.288	104.852	2939.9	-6.9	22.14	15.29	3
2970	5.279	100.954	2969.83	-7.32	24.07	17.27	3
3000	8.276	99.873	2999.61	-7.95	27.55	20.8	3
3030	11.275	99.365	3029.17	-8.8	32.57	25.88	3
3060	14.274	99.068	3058.43	-9.86	39.12	32.5	3
3090	17.274	98.873	3087.3	-11.13	47.18	40.63	3
3103.05	18.579	98.807	3099.71	-11.74	51.15	44.63	3
3120	18.579	98.807	3115.78	-12.57	56.48	50.02	0
3150	18.579	98.807	3144.22	-14.03	65.93	59.54	0
3180	18.579	98.807	3172.65	-15.5	75.37	69.07	0
3199.63	18.579	98.807	3191.26	-16.45	81.55	75.31	0

VII.19. **Trajectory of Well #4d (#19)**

Depth (m)	Inclination (°)	Azimuth (°)	TVD (m)	North (m)	East (m)	VS (m)	DLS $(°/30m)$
0	0	0	0	-7.1	-4.8	0	0
1700	0	0	1700	-7.1	-4.8	0	0
1710	1	110.008	1710	-7.13	-4.72	0.05	3
1740	4	110.008	1739.97	-7.58	-3.49	0.85	3
1770	7	110.008	1769.83	-8.56	-0.79	2.61	3
1800	10	110.008	1799.49	-10.08	3.38	5.31	3
1830	13	110.008	1828.89	-12.12	9	8.96	3
1860	16	110.008	1857.93	-14.69	16.06	13.55	3
1890	19	110.008	1886.54	-17.78	24.53	19.06	3
1920	22	110.008	1914.63	-21.37	34.4	25.47	3
1950	25	110.008	1942.14	-25.47	45.64	32.77	3
1980	28	110.008	1968.99	-30.05	58.22	40.94	3
2010	31	110.008	1995.1	-35.1	72.1	49.96	3
2040	34	110.008	2020.39	-40.62	87.24	59.8	3
2070	37	110.008	2044.81	-46.58	103.61	70.43	3
2100	40	110.008	2068.29	-52.96	121.16	81.83	3
2130	43	110.008	2090.76	-59.76	139.83	93.97	3
2160	46	110.008	2112.15	-66.96	159.59	106.8	3
2190	49	110.008	2132.42	-74.53	180.37	120.3	3
2195.72	49.572	110.008	2136.15	-76.01	184.44	122.95	3
2220	49.572	110.008	2151.89	-82.33	201.81	134.23	0
2250	49.572	110.008	2171.35	-90.15	223.27	148.18	0
2280	49.572	110.008	2190.8	-97.96	244.73	162.12	0
2310	49.572	110.008	2210.26	-105.77	266.19	176.06	0
2340	49.572	110.008	2229.71	-113.59	287.64	190	0
2370	49.572	110.008	2249.17	-121.4	309.1	203.94	0
2400	49.572	110.008	2268.62	-129.21	330.56	217.88	0
2430	49.572	110.008	2288.08	-137.03	352.02	231.82	0
2460	49.572	110.008	2307.53	-144.84	373.48	245.77	0
2490	49.572	110.008	2326.99	-152.65	394.94	259.71	0
2520	49.572	110.008	2346.44	-160.47	416.39	273.65	0
2550	49.572	110.008	2365.9	-168.28	437.85	287.59	0
2580	49.572	110.008	2385.35	-176.1	459.31	301.53	0
2610	49.572	110.008	2404.81	-183.91	480.77	315.47	0
2640	49.572	110.008	2424.26	-191.72	502.23	329.41	0
2670	49.572	110.008	2443.71	-199.54	523.69	343.36	0
2700	49.572	110.008	2463.17	-207.35	545.14	357.3	0
2730	49.572	110.008	2482.62	-215.16	566.6	371.24	0
2760	49.572	110.008	2502.08	-222.98	588.06	385.18	0
2790	49.572	110.008	2521.53	-230.79	609.52	399.12	0
2820	49.572	110.008	2540.99	-238.6	630.98	413.06	0
2850	49.572	110.008	2560.44	-246.42	652.44	427	0

2880	49.572	110.008	2579.9	-254.23	673.89	440.95	0
2910	49.572	110.008	2599.35	-262.04	695.35	454.89	0
2940	49.572	110.008	2618.81	-269.86	716.81	468.83	0
2970	49.572	110.008	2638.26	-277.67	738.27	482.77	0
3000	49.572	110.008	2657.72	-285.49	759.73	496.71	0
3030	49.572	110.008	2677.17	-293.3	781.19	510.65	0
3060	49.572	110.008	2696.63	-301.11	802.64	524.59	0
3090	49.572	110.008	2716.08	-308.93	824.1	538.54	0
3120	49.572	110.008	2735.54	-316.74	845.56	552.48	0
3150	49.572	110.008	2754.99	-324.55	867.02	566.42	0
3180	49.572	110.008	2774.45	-332.37	888.48	580.36	0
3194.41	49.572	110.008	2783.79	-336.12	898.78	587.06	0
3210	49.787	107.983	2793.88	-339.99	910.02	594.48	3
3240	50.299	104.126	2813.15	-346.34	932.12	609.74	3
3270	50.937	100.333	2832.19	-351.25	954.77	626.24	3
3300	51.695	96.614	2850.94	-354.7	977.93	643.96	3
3330	52.568	92.978	2869.36	-356.67	1001.52	662.83	3
3360	53.55	89.431	2887.39	-357.17	1025.48	682.8	3
3390	54.634	85.977	2904.99	-356.19	1049.76	703.83	3
3420	55.814	82.619	2922.11	-353.74	1074.27	725.84	3
3450	57.082	79.356	2938.69	-349.82	1098.96	748.79	3
3480	58.433	76.189	2954.7	-344.44	1123.75	772.61	3
3510	59.859	73.115	2970.09	-337.62	1148.58	797.24	3
3540	61.356	70.13	2984.81	-329.38	1173.38	822.59	3
3570	62.915	67.231	2998.83	-319.73	1198.08	848.62	3
3600	64.533	64.413	3012.12	-308.71	1222.61	875.24	3
3630	66.203	61.671	3024.62	-296.35	1246.91	902.39	3
3660	67.92	58.999	3036.32	-282.67	1270.91	929.98	3
3690	69.679	56.393	3047.17	-267.72	1294.55	957.95	3
3720	71.476	53.846	3057.14	-251.54	1317.75	986.21	3
3750	73.307	51.352	3066.22	-234.17	1340.46	1014.69	3
3780	75.166	48.906	3074.37	-215.67	1362.62	1043.31	3
3810	77.052	46.502	3081.57	-196.07	1384.15	1071.99	3
3840	78.959	44.134	3087.81	-175.43	1405.01	1100.66	3
3870	80.884	41.797	3093.06	-153.82	1425.14	1129.23	3
3900	82.823	39.485	3097.31	-131.29	1444.48	1157.62	3
3930	84.775	37.192	3100.55	-107.9	1462.98	1185.77	3
3960	86.734	34.914	3102.77	-83.71	1480.58	1213.59	3
3990	88.699	32.645	3103.97	-58.8	1497.25	1241	3
3998.51	89.257	32.002	3104.12	-51.61	1501.8	1248.7	3
4020	89.257	32.002	3104.4	-33.39	1513.18	1268.06	0
4050	89.257	32.002	3104.79	-7.95	1529.08	1295.11	0
4080	89.257	32.002	3105.18	17.49	1544.98	1322.16	0
4110	89.257	32.002	3105.57	42.93	1560.88	1349.2	0
4140	89.257	32.002	3105.95	68.37	1576.77	1376.25	0
4170	89.257	32.002	3106.34	93.81	1592.67	1403.29	0

4200	89.257	32.002	3106.73	119.25	1608.57	1430.34	0
4230	89.257	32.002	3107.12	144.68	1624.46	1457.39	0
4260	89.257	32.002	3107.51	170.12	1640.36	1484.43	0
4290	89.257	32.002	3107.9	195.56	1656.26	1511.48	0
4320	89.257	32.002	3108.29	221	1672.16	1538.52	0
4350	89.257	32.002	3108.68	246.44	1688.05	1565.57	0
4380	89.257	32.002	3109.07	271.88	1703.95	1592.61	0
4410	89.257	32.002	3109.46	297.32	1719.85	1619.66	0
4440	89.257	32.002	3109.85	322.76	1735.74	1646.71	0
4470	89.257	32.002	3110.23	348.19	1751.64	1673.75	0
4500	89.257	32.002	3110.62	373.63	1767.54	1700.8	0
4530	89.257	32.002	3111.01	399.07	1783.44	1727.84	0
4560	89.257	32.002	3111.4	424.51	1799.33	1754.89	0
4590	89.257	32.002	3111.79	449.95	1815.23	1781.94	0
4620	89.257	32.002	3112.18	475.39	1831.13	1808.98	0
4650	89.257	32.002	3112.57	500.83	1847.03	1836.03	0
4680	89.257	32.002	3112.96	526.26	1862.92	1863.07	0
4710	89.257	32.002	3113.35	551.7	1878.82	1890.12	0
4740	89.257	32.002	3113.74	577.14	1894.72	1917.16	0
4770	89.257	32.002	3114.12	602.58	1910.61	1944.21	0
4800	89.257	32.002	3114.51	628.02	1926.51	1971.26	0
4830	89.257	32.002	3114.9	653.46	1942.41	1998.3	0
4860	89.257	32.002	3115.29	678.9	1958.31	2025.35	0
4890	89.257	32.002	3115.68	704.34	1974.2	2052.39	0
4920	89.257	32.002	3116.07	729.77	1990.1	2079.44	0
4950	89.257	32.002	3116.46	755.21	2006	2106.49	0
4980	89.257	32.002	3116.85	780.65	2021.89	2133.53	0
5010	89.257	32.002	3117.24	806.09	2037.79	2160.58	0
5040	89.257	32.002	3117.63	831.53	2053.69	2187.62	0
5070	89.257	32.002	3118.02	856.97	2069.59	2214.67	0
5100	89.257	32.002	3118.4	882.41	2085.48	2241.71	0
5130	89.257	32.002	3118.79	907.85	2101.38	2268.76	0
5160	89.257	32.002	3119.18	933.28	2117.28	2295.81	0
5190	89.257	32.002	3119.57	958.72	2133.18	2322.85	0
5220	89.257	32.002	3119.96	984.16	2149.07	2349.9	0
5250	89.257	32.002	3120.35	1009.6	2164.97	2376.94	0
5280	89.257	32.002	3120.74	1035.04	2180.87	2403.99	0
5310	89.257	32.002	3121.13	1060.48	2196.76	2431.04	0
5340	89.257	32.002	3121.52	1085.92	2212.66	2458.08	0
5370	89.257	32.002	3121.91	1111.35	2228.56	2485.13	0
5400	89.257	32.002	3122.3	1136.79	2244.46	2512.17	0
5430	89.257	32.002	3122.68	1162.23	2260.35	2539.22	0
5460	89.257	32.002	3123.07	1187.67	2276.25	2566.27	0
5490	89.257	32.002	3123.46	1213.11	2292.15	2593.31	0
5520	89.257	32.002	3123.85	1238.55	2308.04	2620.36	0
5550	89.257	32.002	3124.24	1263.99	2323.94	2647.4	0

5580	89.257	32.002	3124.63	1289.43	2339.84	2674.45	0
5610	89.257	32.002	3125.02	1314.86	2355.74	2701.49	0
5640	89.257	32.002	3125.41	1340.3	2371.63	2728.54	0
5670	89.257	32.002	3125.8	1365.74	2387.53	2755.59	0
5700	89.257	32.002	3126.19	1391.18	2403.43	2782.63	0
5730	89.257	32.002	3126.57	1416.62	2419.32	2809.68	0
5760	89.257	32.002	3126.96	1442.06	2435.22	2836.72	0
5790	89.257	32.002	3127.35	1467.5	2451.12	2863.77	0
5820	89.257	32.002	3127.74	1492.94	2467.02	2890.82	0
5850	89.257	32.002	3128.13	1518.37	2482.91	2917.86	0
5880	89.257	32.002	3128.52	1543.81	2498.81	2944.91	0
5910	89.257	32.002	3128.91	1569.25	2514.71	2971.95	0
5940	89.257	32.002	3129.3	1594.69	2530.61	2999	0
5950.18	89.257	32.002	3129.43	1603.32	2536	3008.17	0

VII.20. **Template Position**

Template	North	East
#1	0	0
#2	1678	1198
#3	4702	2276
#4	4246	17222